2011

The Characterization of PG0228 in Porphyromonas gingivalis W83

Courtney Schlenker
Virginia Commonwealth University

THE CHARACTERIZATION OF PG0228 IN *PORPHYROMONAS GINGIVALIS* W83

A thesis submitted in partial fulfillment of the requirements for the degree of Master of Science in Physiology and Biophysics at Virginia Commonwealth University.

by

COURTNEY DANIELLE SCHLENKER
Bachelor of Science in Biology, University of Toledo, 2007

Director: JANINA P. LEWIS, PH.D.
ASSOCIATE PROFESSOR, PHILIPS INSTITUTE OF OCMB
SCHOOL OF DENTISTRY

Virginia Commonwealth University
Richmond, Virginia
May, 2011

ACKNOWLEDGEMENTS

Most importantly, I would like to thank Dr. Lewis for this exciting project and giving me the opportunity to work in her lab. Her mentorship and constant support have made pursuing a Masters degree a challenging yet rewarding process. No matter how busy she was, she always managed to find the time to address any concerns or questions I might have had. In addition to Dr. Lewis, I would like to thank the other members of my committee, Dr. Rife and Dr. Qiao, for their insight and guidance on this project. A special thank you goes to Cecilia Anaya-Bergman for her mentorship during my research rotation last year. I would especially like to thank Sai Yanamandra, Dr. Karl Thompson, and Dr. Tiana Wyant for their time, patience, guidance, and advice this past year and a half. Finally, I must thank the rest of the lab including Kandice Klepper, Anuya Paranjape, Tyrone King, Evys Collazo, Cheyanne Warren, and Huan Mo for their support and friendship.

Lastly, I would like to thank my parents and family for giving me the unconditional love, support, and confidence to go out and chase my dreams. You have been there to guide me through life's many roadblocks, and through your example, you have shown me the power of hard work and dedication.

TABLE OF CONTENTS

LIST OF TABLES

LIST OF FIGURES

LIST OF ABBREVIATIONS

Abbreviation	Definition
α	alpha
β	beta
Δ	delta
Δ0228	PGΔ0228
σ	sigma
°C	degree Celsius
µg	microgram
µL	microliter
BLAST	Basic Local Alignment Search Tool
BHI	brain heart infusion
cDNA	complementary DNA
DNA	deoxyribonucleic acid
dNTP	deoxyribonucleotide triphosphate
E. coli	*Escherichia coli*
FBS	fetal bovine serum
HN4	human oral epithelial cell line derived from SCC of tongue
LB	Luria Bertani broth
M	molar
min	minute

mL	milliliter
MOI	multiplicity of infection
NCBI	National Center for Biotechnology Information
OD	optical density
PBS	Phosphate-buffered saline
PCR	Polymerase Chain Reaction
qRT-PCR	Quantitative Real-time Polymerase Chain Reaction
RNA	ribonucleic acid
SCC	squamous cell carcinoma
SDS	sodium dodecyl sufate
WT	wild type

ABSTRACT

THE CHARACTERIZATION OF PG0228 IN *PORPHYROMONAS GINGIVALIS* W83

By Courtney Danielle Schlenker
Bachelor of Science in Biology, University of Toledo, 2007

A thesis submitted in partial fulfillment of the requirements for the degree of Master of Science in Physiology and Biophysics at Virginia Commonwealth University.

Virginia Commonwealth University, 2011

Major Director: JANINA P. LEWIS, PH.D.
ASSOCIATE PROFESSOR, PHILIPS INSTITUTE OF OCMB
SCHOOL OF DENTISTRY

Periodontitis affects 10 to 15 percent of most adult populations and can contribute to numerous systemic diseases. *Porphyromonas gingivalis*, a gram-negative anaerobic bacterium, is a recognized prime causative agent in periodontitis. Studies have shown a number of small non-coding RNAs (sRNAs) have been related to bacterial virulence. Many of these sRNAs require the facilitation of the bacterial Sm-like protein, Hfq, for optimum function. Hfq is a RNA chaperone involved in RNA stability, sRNA function, and polyadenylation. Mutants lacking in Hfq often show pleiotropic phenotypes, although the extent and severity of *hfq* null phenotypes is often species-specific. Hfq has been encoded by nearly half of eubacteria, including pathogens. Based on a standard BLAST search, *hfq* has not been detected in *P. gingivalis*. It is highly likely, however, that the bacterium possesses an Hfq homologue due to its importance as an overall RNA cofactor. The *P. gingivalis* hypothetical protein, PG0228, possesses the Sm-like protein motif, thus we believe it is an excellent Hfq candidate. Our goal

was to characterize PG0228 so we can gain a better insight into the function of this hypothetical protein and determine if it indeed behaves like Hfq. Microarray analysis, growth studies, and a survival study were done on a Δ0228 mutant to determine the biological role of the protein encoded by PG0228. PG0228 was also tagged *in vivo* in order to determine if the protein binds to RNA. Our results show *P. gingivalis* deficient in PG0228 show significant similarities to other bacterium deficient in *hfq*. The Δ0228 strain showed significant sensitivity to host defense mechanisms and an overall gene regulation in 15% of the genome. In addition, the mutant is viable but produces a lower final cell density. Thus, we believe PG0228 is an excellent Hfq candidate, and suggest further studies will show PG0228 is an Hfq homologue.

Chapter 1: INTRODUCTION

1.1 Periodontal Disease

Periodontal diseases can contribute to systemic diseases including myocardial infarctions, diabetes mellitus, adverse birth effects, nonhemorrhagic strokes, and atherosclerosis[8;40;66;77;108]. Numerous studies show the gram-negative anaerobic bacterium, *Porphyromonas gingivalis* is extremely important in initiating and progressing advanced periodontal diseases. By fully understanding this bacterium and how it behaves, we can better treat periodontal disease by lowering levels of *P. gingivalis* inside the oral cavity.

Periodontal disease is a group of infectious diseases affecting the structures surrounding teeth. There are two stages of periodontal disease: gingivitis and periodontitis. Gingivitis, which precedes periodontitis, is inflammation of gingival tissue resulting from accumulations of plaque composed primarily of bacteria along the gum lining. Gums bleed easily during tooth brushing or other stimulation. However, gingivitis is reversible with proper oral hygiene practices. If left untreated, gingivitis can lead to periodontitis, the advanced stage of periodontal disease. Periodontitis breaks down the supporting structures surrounding teeth, including periodontal ligaments and alveolar bone, leading to tooth loss[15].

Periodontitis affects 10 to 15 percent of most adult populations[30]. The loss of connective tissue surrounding the tooth increases pocket depth, a hallmark of periodontitis. As

a result, the gingival tissue pulls away from the tooth enabling anaerobic bacteria to colonize in the sub-gingival regions[105]. This causes a larger problem because bacteria in the sub-gingival regions are not accessible by routine dental maintenance. The current treatment for periodontitis is complete removal of the bacteria followed by treatment with antibiotics. Problems with the current therapy include antibiotic resistance and recurrent infections[50]. Therefore, it is important we find new ways to treat the infections to more permanently rid the sub-gingival area of these aggressive bacteria.

In severe cases of periodontitis, a highly permeable epithelial lining is the only defense between virulent bacteria and the host's underlying connective tissue and blood vessels. Once in the blood stream, bacterial toxins and inflammatory mediators are carried to other parts of the body. Recent studies have shown there is significant evidence an association between periodontal infections and systemic diseases or conditions exists (see review,[28]). It is suggested the periodontal pockets become a gateway for inflammatory mediators such as cytokines tumour necrosis factor-alpha (TNF-α) and interferon-gamma (IFN-γ) to enter circulation, therefore linking periodontal infections with cardiovascular diseases, diabetes mellitus, adverse birth outcomes, and pulmonary infections [33].

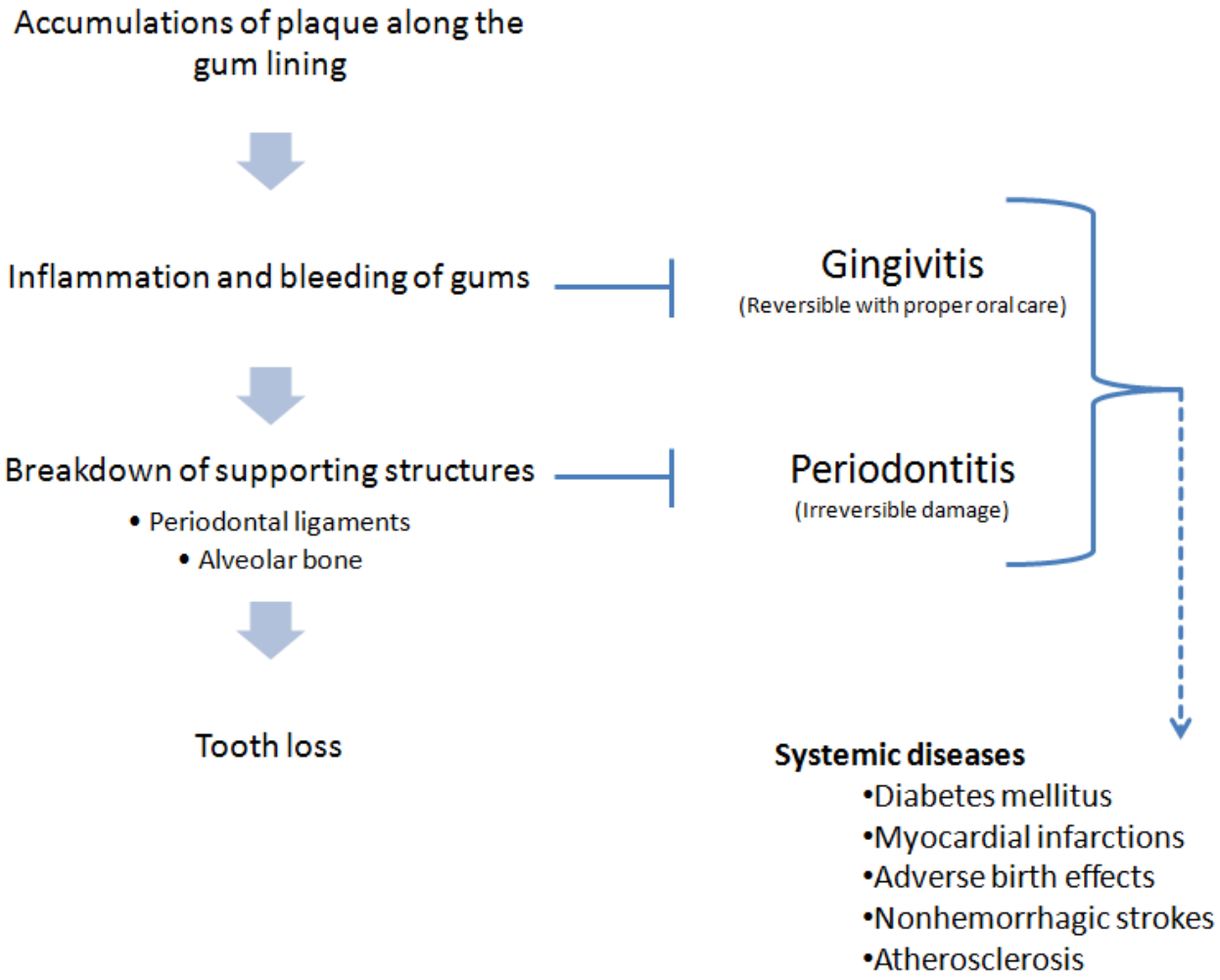

Figure 1. Periodontal Diseases. This flow chart represents the stages of periodontitis and examples of the systemic diseases which it is linked to.

1.2. Oral Microflora

Just like other places within the digestive tract, the oral cavity houses natural microflora. Various bioinformatic approaches show there are over 700 species of bacteria living in the oral cavity[71]. These bacteria usually have beneficial properties for the host. However, without proper oral hygiene, these biofilms can accumulate to levels beyond homeostasis. Oral microbial deposits along with extracellular components keeping microbial cells together are commonly referred to as dental plaques. High level accumulations of dental plaque is responsible for dental caries, periodontal disease, and peri-implantitis (inflammation affecting tissue surrounding dental implants)[13;55].

Bacteria were first suspected to play an important role in gingivitis and periodontitis starting in the 1960s (for review,[6]). Then, it was discovered that certain bacteria in plaque are more important causative agents of periodontal infections. It is not simply the number of plaques in the mouth but what constitutes the bacterial community. Bacterial species *Porphyromonas gingivalis, Tannerella forsythia, Treponema denticola, Campylobacter rectus, Micromonas micros, Streptococcus intermedius, Eubacterium nodatum, Aggregatibacter actinomycetemcomitans,* and *Prevotella intermedia* were found to be important in causing periodontitis[6]. The three members of the red complex are Gram negative anaerobic bacteria. Each expresses several virulence factors allowing it to set off the host immune response[11]. It is essentially this host immune response that results in host tissue damage seen with periodontitis. Studies have shown, the proportions of *P. gingivalis, T. denticola,* and *T. forsythia* from sites of periodontal disease were significantly higher than normal tissue samples and

therefore indicating these bacterial species are associated with local development of periodontitis[60]. Currently, treatment approaches for severe periodontitis includes the removal of these bacteria along with antibiotic treatment. Recurrent infections are a huge problem with current treatment strategies because of the bacterium's ability to become resistant to antibiotics[50]. Better suited approaches need to be developed to reduce the virulence potential of *Porphyromonas gingivalis*. This can only be done once we fully understand this pathogenic bacterium.

1.3. *Porphyromonas gingivalis*

Porphyromonas gingivalis is a black-pigmented, anaerobic, gram-negative bacterium that is a prime causative agent in periodontitis[24;50;109]. *P. gingivalis* is classified in the genus *Porphyromonas*, family *Porphyromonadacae*, order *Bacteroidales*, and class *Bacteroides*. It is closely related to *Bacteroides fragilis*, but distantly related to *E. coli*. For this reason, the traditional *E. coli* model gives limited information about *P. gingivalis*.

Along with diseased sites*, P. gingivalis* exists in healthy sites in the oral cavity such as the tongue, palate, and supragingival tissue[20;76]. However, the amount of *P. gingivalis* is increased in diseased and subgingival areas[63]. Several studies have stated *P. gingivalis* produces many virulence factors. These factors modulate the host immune system and cleave or degrade host cell proteins and surface receptors. This suggests that there is a delicate balance between the bacterium and the oral mucosa allowing the organism to commensally co-exist with its host (see review,[109]).

Pathogenic *P. gingivalis* can adhere to, penetrate, and replicate in its host. The host's first line of defense is epithelial tissue. Epithelial cells have the ability to recognize and eliminate infections before causing harm to the host. However, *P. gingivalis* has developed ways to successfully remain viable within epithelial cells and cause severe problems. Studies show the colonization of bacteria such as *P. gingivalis* in epithelium causes the gingival tissue to secrete inflammatory cytokines and antimicrobial peptides setting off host immune response[41]. Furthermore, *P. gingivalis* can replicate within the epithelium at high levels. However, despite the number of intracellular bacteria, *Porphyromonas gingivalis* are able to inhibit gingival epithelial cell apoptosis[110].

Colonizing *P. gingivalis* is significantly stressed when exposed to the host environment. The bacteria must regulate its gene expression of virulent genes to survive in torturous host conditions. Sensing and responding to changes in pH, temperature, oxygen exposure, osmolarity, and redox potential allows for optimal growth and survival in host tissue[29]. It is crucial virulence genes are turned on and off during infection by gene regulation. Understanding gene regulation and expression in *Porphyromonas gingivalis* will provide better information on periodontal disease pathogens.

1.4. Gene Regulation in *Porphyromonas gingivalis*

The complete genome sequence of *P. gingivalis* strain W83 has been identified by the Institute for Genomic Research[68]. Less is known, however, about its gene regulation. Studies have shown there is expression of oxidative stress genes controlled by OxyR, a regulatory protein, shortly after host infection[43]. RprY regulates genes involved in transport

or oxidative stress[22]. Another gene, designated regT, is suggested to be involved in regulating activity of major proteases at higher temperatures, called gingipains, which are important in oxidative stress[99]. vimE (virulence-modulating gene E) is involved in modulating the protease activity[100]. Despite these suggested modulators, gene and protein regulation and activation in *Porphyromonas gingivalis* remains poorly understood. It is extremely unlikely these few regulators are the only ones present in *P. gingivalis*.

1.5. Regulatory small RNAs (sRNAs)

Strands of RNA look similar to DNA at first glance. However, functionally, these nucleic acids are very different. RNA consists of a uracil instead of thymine and has a hydroxyl group at the 2' position of the aldopentose. DNA is double stranded leaving little room for conformation changes. On the other hand, most RNA is single stranded allowing it to fold. The ability for RNA to fold back on itself produces diverse structures which allow RNA to carry out several important cellular functions.

Regulatory bacterial small ribonucleic acids (sRNAs), also known as non-coding RNAs, are not translated into proteins. They are found in both prokaryotes and eukaryotes [7] but small RNAs are not ribosomal, transfer, or messenger RNAs. It is accepted most sRNAs are vital post-transcriptional regulators of gene expression in response to environmental changes and may be involved in numerous cellular processes including cell development, growth, differentiation, and death by turning genes on and off[1;16;46].

Pathogenic prokaryotic sRNAs have recently become a hot topic because some have been related to bacterial virulence. It is suggested less energy is expelled by the cell using

sRNAs compared to synthesizing bulky regulatory proteins in response to environmental stress[4]. Because these RNAs are small and untranslated, they are more cost effective which allows for a fast response to external stimuli and fast recovery once the external stimulus is removed[82].

In the past, gene regulation research has focused on transcriptional regulation and protein-protein interactions. However, small RNAs regulate gene expression at the post transcriptional level by base pairing with mRNA transcripts. This binding of sRNA with mRNA influences translation or mRNA stability therefore upregulating or downregulating gene expression[72].

Small RNAs have been extensively studied in species like *Escherichia coli*. These molecules range from 50-400 nucleotides long and many are evolutionary conserved. So far, there have been about 80 known sRNAs identified just in *E. coli.* For example, OxyS RNA acts as a global regulator and is activated in response to oxidative stress in *E. coli*. By an antisense mechanism, OxyS regulates the expression of as many as 40 genes, including the rpoS σ subunit of RNA polymerase and fhlA. OxyS regulates fhlA by pairing with a short segment of the Shine-Dalgarno sequence blocking ribosome binding[5]. DsrA is another example of a sRNA discovered in *E. coli*. DsrA regulates two transcriptional regulators: HN-S, a histone-like protein that silences several bacterial genes, and RpoS σ, the stationary phase sigma factor of RNA polymerase[4]. These are just two examples of sRNA and already there are two levels of regulation for just RpoS σ. The sRNA can regulate one or many target genes. Plus, the mRNA targets can be regulated by several sRNAs creating extensive overlap, further complicating the

global regulation. However, the molecular functions of many of these sRNAs are still not known[82]. Plus, even though sRNAs in *E. coli* have been extensively studied, little is known about sRNAs among distant species, specifically *Porphyromonas gingivalis*[72].

Binding sRNA with their mRNA targets influences translation or mRNA stability. The antisense sRNA regulators are either *cis* or *trans*-acting. The RNA-encoding gene overlaps with the target gene in *cis* regulators. There is only one target gene and there is complete complementarity between the regulator and target. On the other hand, trans-acting regulators are found at loci distant to their target genes. *Trans* regulators are not completely complementary and regulate by imperfect duplexes. The imperfect complementation of trans-acting sRNAs with specific mRNAs allows these sRNAs to regulate multiple targets[4]. Plus, extensive research has revealed there is a crucial third party to this equation, proteins. Specific proteins, notably Hfq, interact with the sRNAs acting as a catalyst, induce sRNA changes in conformation, or are sequestered by the sNRA to inhibit protein action.

1.6. Sm Family of RNA-Associated Proteins

The Sm protein family consists of Sm and Sm-like proteins that bind to RNA in bacteria, Archaea, and eukaryotes. These proteins assemble in heteromorphic or homomorphic six or seven member ring complexes. The Sm family is characterized by the Sm motif which allows the protein to bind to its neighboring subunits to form a central pore. The central pore binds to short uracil-rich stretches of RNA[95].

Sm proteins were first discovered in the 1960s. A patient, Stephanie Smith, diagnosed with systemic lupus erythematosus (SLE), produced antibodies to a set of proteins in the

nucleus. The proteins were given the name, Sm, in her honor. It was later discovered these eukaryotic proteins formed protein-RNA complexes and called them small nuclear ribonucleoproteins (snRNPs), which are involved in a variety of RNA-processing functions. In prokaryotes, structure studies reveal that Hfq possesses the Sm-motif found previously only in eukaryotes and archaea. In prokaryotes, however, Hfq forms a homo-hexameric ring unlike the heptameric Sm rings found in eukaryotes and archaea[95].

1.7. Hfq protein

Sm-like proteins are important in RNA processing, splicing, and messenger RNA decay. One Sm-like protein, Hfq, has been identified in bacteria and bears a striking resemblance to Sm-like proteins both structurally and functionally[61;78]. Hfq is an RNA chaperone involved RNA stability, small RNA function and polyadenylation[48]. Hfq (also known as HF-I) was originally identified as a host factor required for the replication of the bacteriophage Qβ-RNA in the 1960s[31;32;81]. Following its discovery, decades of research focused on the protein's binding features[21;79]. At this time, it was suspected this highly conserved protein must hold an important role in cellular function. Why else would bacteria conserve a protein if its sole purpose is to allow for viral infection? It wasn't until the early 1990s, Hfq received significant attention when it was discovered that it acts as a key global regulator of gene expression[65;97]. New functions of this fascinating regulator are being identified all the time but it could be years until we fully understand its limits.

The Hfq gene is highly conserved among bacteria but has been extensively researched in *E. coli* [90] and was first discovered as a gene regulator when geneticists disrupted the gene in

E. coli. The *hfq* null mutant showed pleiotropic phenotypes, including decreased yields, increased cell size, osmosensitivity, and increased sensitivity to UV light[97]. Interestingly, some of these phenotypes caused by the *hfq* null mutant were the same as defects caused by *rpoS* (gene encodes stationary phase sigma factor, σ^S) mutations. The *E. coli* σ^S activates genes involved in stress-protective functions including resistance against oxidative stress, UV irradiation, and hyperosmolarity[42]. It was then found that Hfq was involved in the regulation of expression of σ^S subunit of RNA polymerase and therefore all σ^S-independent genes in *E. coli* and *Salmonella typhimurium*[65]. The *E. coli* Hfq binds the sRNAs transcribed by genes *rprA, dsrA*, and *oxyS*. All three of these sRNAs regulate the translation of *rpoS* gene, which encodes the σ^S subunit, thus having indirect control of σ^S translation.

However, some pleiotropic phenotypes caused by the *hfq* null mutant could not be explained by a lack of *rpoS* expression indicating Hfq does more than regulate translation of *rpoS* gene. Further experiments showed that Hfq's interaction with other RNAs, thus allowing these small RNAs to interact with their targets[59;61]. For instance, Hfq represses the translation of *E. coli ompA* gene by interfering with ribosomal binding, resulting in degradation of ompA messenger RNA[61]. It was also shown Hfq is involved in poly(A) tail metabolism by stimulating polyadenylation and is essential for growth at temperatures of 45°C and above[9;39;96].

Hfq is considered to act as a global gene regulator, its primary function facilitating the interaction of sRNAs with their target mRNAs. Inactivation of Hfq reduces the translation of stress σ^S factor, induces the σ^E-dependent envelope stress response in *Salmonella enterica* and

E. coli, and reduces expression of the σ^{32} mediated cytoplasmic stress response[26;37;94]. There have also been reports Hfq interacts with tRNAs[14]. Since then, several more sRNAs have been shown to associate with Hfq or need Hfq for transcriptional control of its target mRNAs[104]. For example, DsrA and RyhB require Hfq for their stabilization[56;83]. Hfq binding protects DsrA and RyhB from cleavage by RNase E, which is an endonuclease involved in mRNA decay and tRNA processing. Hfq may bind to other riboregulators as well because Hfq may bind to the same sites as RNase E (see review,[98]).

Hfq also directly facilitates the interaction between sRNA and their RNA target as it does with OxyS and Spot 42[61]. As previously stated, OxyS RNA is transcribed in response to oxidative stress. Importantly, Hfq increases the efficiency of OxyS by increasing the interaction between OxyS and its target mRNAs by directly facilitating OxyS but Hfq does not affect OxyS stability. Meaning, Hfq does not stabilize OxyS but Hfq is extremely important for OxyS to do its job. OxyS downregulates the translation of rpoS and fhlA and therefore translation of rpoS and fhlA would be upregulated without Hfq regulation. Moreover, the upregulation of rpoS and fhlA could not be restored by mutating OxyS[111]. Spot 42 regulates gene expression of the galactose operon by antisense mechanism on galK. Hfq also binds to galK but Hfq does not change the structure of Spot 42 RNA. It is suggested Hfq and Spot 42 RNA both bind to target RNA, galK, producing a complex including RNA-RNA and RNA-protein interactions[62]. The third gene in the galactose operon, galK, is targeted by Spot 42 RNA repressing translation. In the presence of Hfq, there is a 150 fold increase in the interaction between Spot 42 and galK compared to the absence of Hfq.

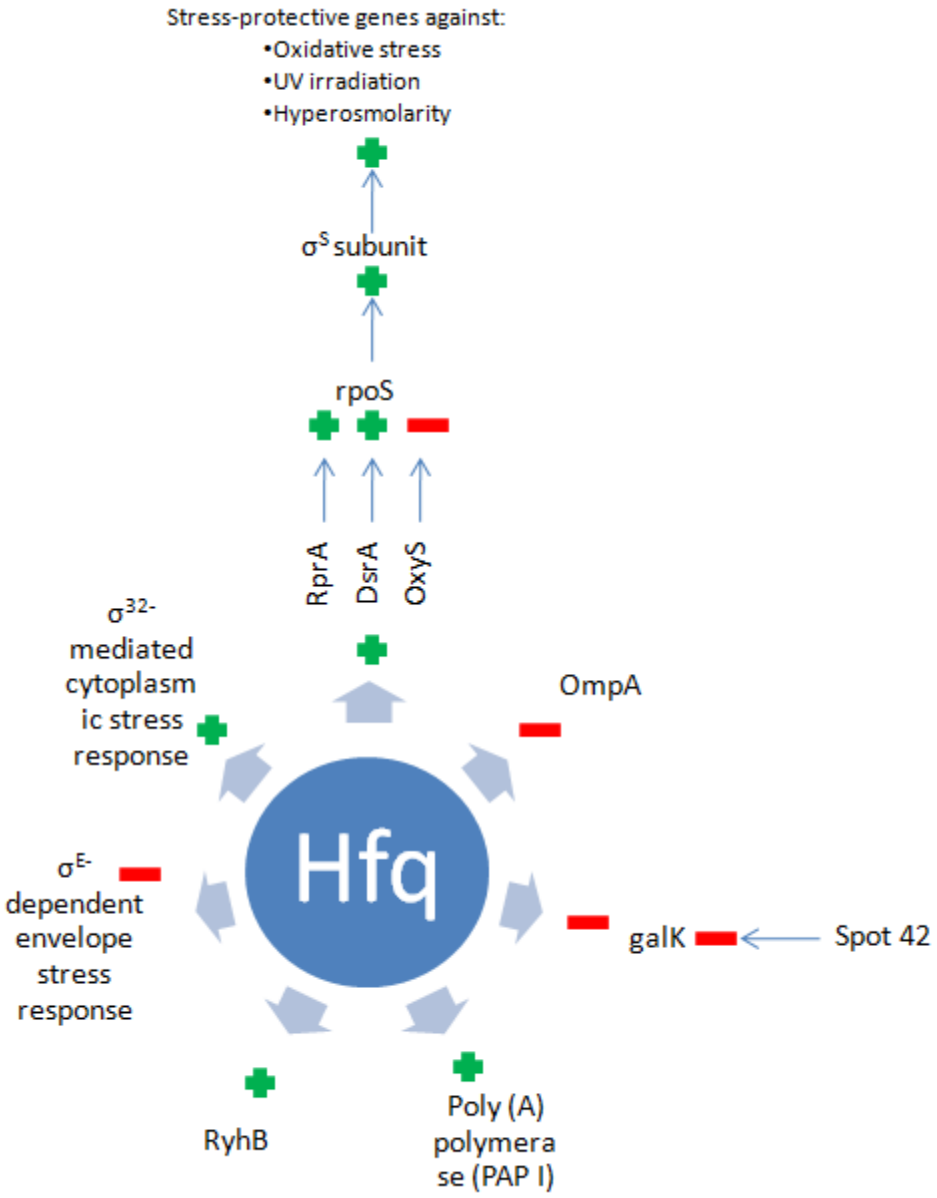

Figure 2. Examples of Hfq regulation in *E. coli*

The expression of Hfq is regulated by transcriptional and post-transcriptional control (no evidence for post-translational control). Its internal promoters ensure Hfq is expressed during stress conditions (see review,[98]). During stress conditions, there is a greater incidence of misfolded proteins intracellularly, therefore becoming detrimental to the bacteria's health. Experiments also demonstrate Hfq has the ability to modulate the rate of its own expression. Modulation is done by decreasing the stability of its mRNA. This suggests there is a negative feedback mechanism decreasing expression when Hfq accumulates[102]. The expression rate of Hfq during stress responses has competing results. Azam et al showed there are a large number of Hfq molecules per cell expressed during log phase reaching 50,000-60,000. This number decreases by half during transition to stationary phase (phase when growth and death rate are equal)[2]. However, studies have shown Hfq is elevated during transition to stationary phase and times of slow growth in comparison to log phase[103].

The function of Hfq may also be regulated by its interaction with other proteins. Hfq interacts with several proteins including RNases, helicases, Rho-factor, ribosomal proteins, RNA polymerase in the presence of S1 protein, and poly(A)polymerase (PAP I)[17;64;89]. Hfq stimulates the synthesis of poly(A) tails by protecting the poly(A) tails from degradation by exoribonucleolytic degradation[73]. Plus, studies have shown the majority of Hfq associated with translational machinery inside the cell but a small percentage is present associated with the nucleoid. Hfq has been identified as a DNA binding protein that affects negative supercoiling[93].

Like it is with most proteins, the function of Hfq is related to its structure. As stated, Hfq can associate with a variety of RNAs by binding to their A/U-rich sequences and is largely nonpolar[78]. Hfq forms a homo-hexameric ring with each subunit consisting of a five-stranded antiparallel β-sheet with an N-terminal α-helix[78]. It is interesting to note, even though there is little sequence homology between Hfq and Sm/Lsm monomers, their structures are quite similar. RNA binds in a circular shape inside the pore of the Hfq hexameric protein. The sequence recognized by Sm proteins is 5'-AUUUUUG-3' and it binds to six binding pockets within Hfq's pore (excluding the 3'G). Although there have been specific sequences identified for Hfq targets ompA, DsrA, OxyS, and Spot 42, no single motif has been identified. There are two proposed mechanisms of how Hfq-RNA interactions allow for Hfq to act as a facilitator of RNA. First, the target site of single-stranded RNA is unwound when interacting with the pore of Hfq, most likely destabilizing surrounding nucleotides on the RNA strand. This would allow for these surrounding RNA nucleotides to create new RNA-RNA interactions. Second, there are six identical binding pockets within the Hfq pore which would suggest Hfq can bind to more than one RNA at a time. This would jumpstart interactions between sRNAs and their target mRNAs if both bound to the Hfq facilitator (See review,[98]).

(a)

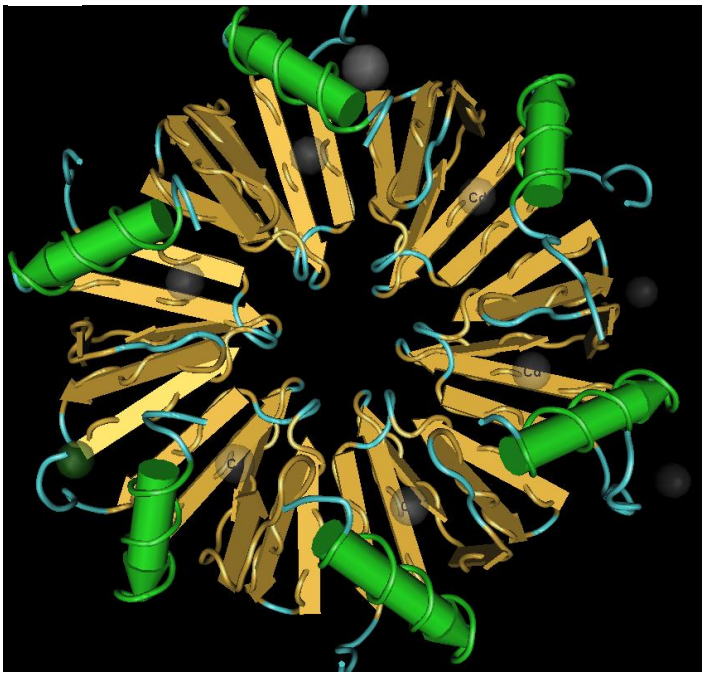

(b)

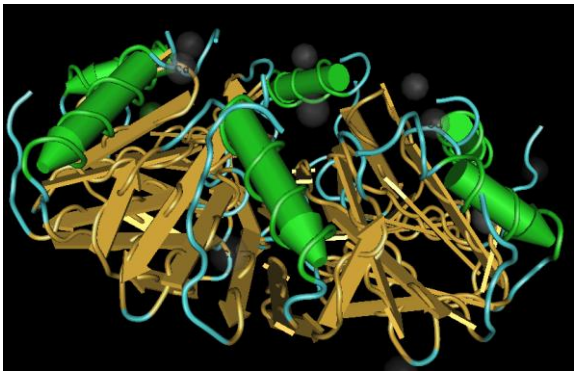

(c)

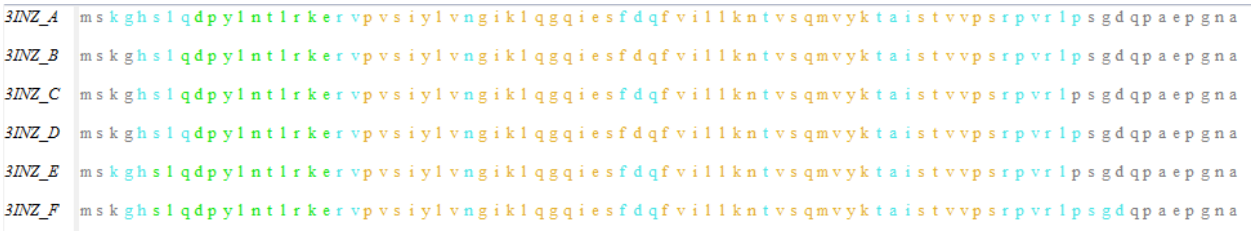

Figure 3. Structure Summary of Hfq From *Pseudomonas aeruginosa*. Structures from the **(a)** front and **(b)** side are shown. The sequence and alignment **(c)** of all six sequences are also shown. Information has been taken from NCBI (http://www.ncbi.nlm.nih.gov/Structure).

Given the numerous studies on Hfq, one can infer Hfq acts an important cofactor for regulatory RNAs; for a review, see[98]. Hfq interacts with many trans-encoded RNAs. As stated, these regulatory RNAs do not have complementary interactions with their targets thus allowing them to recognize many target strands. Hfq enables these sRNAs to more efficiently act on targets by changing the RNA's structure, affect stability, and facilitate complex formation. This is most likely the reason Hfq acts in such a species-specific manner, making it is hard to predict the exact genes Hfq will regulate within each bacterial species.

Hfq is continually being discovered in a wide range of bacteria. So, far, Hfq candidates have been identified in at least half of all sequenced bacterial genomes[18]. Among bacterial species, the protein varies in length from 70-100 amino acids but the Sm motif is located in the N-terminal in all cases implying the C terminal is not important for the function of the protein. Interestingly, the species *Novosphingobium aromaticivorans* encodes tandem Hfq sequences (193 amino acids) that form dimers instead of homo-hexamers. Plus, duplicated copies of Hfq are found in species *Bacillus anthracis* and *Ralstonia metallidurans*[90]. Even though Hfq is highly conserved among bacteria, *Porphyromonas gingivalis* does not appear to have Hfq. Based on BLAST searches, there is no open reading frame encoding Hfq in *P. gingivalis*, Cyanobacteria, green sulphur bacteria, some proteobacteria, several Gram-positive bacteria, and *Chlamydia*[18]. It is unlikely this information means there are no Hfq orthologues in these bacteria. Several *trans* encoded sRNAs are highly conserved among bacteria and numerous studies show Hfq is imperative to their function. Plus, the level of sequence homology is varied considerably within the Sm/Lsm family, including a low sequence homology between species-specific Hfq proteins. The motif consists of four to seven highly conserved amino acids and a

pattern of hydrophobic and hydrophilic residues. Also, studies have shown different residues can bind to RNA. For instance, one of the Hfq proteins in *Bacillus anthracis* and *Ralstonia metallidurans* contains a Lys-His sequence that binds to RNA while the other Hfq protein in these bacteria both contain a Lys-Gln or Lys-Arg conserved sequence. Even though both of these sequences on Hfq bind RNA, a standard BLAST search would not reveal both Hfq proteins[98]. As stated, new Hfq candidates are being discovered with new combinations of sequences that still form perfect conservation of the Sm motif similar to those of the *S. aureus* and *E. coli* Hfq structures that were first discovered. This further suggests the amino acid sequence of Hfq can differ extensively between bacterial species making it impossible to determine certain species don't have Hfq based solely on a BLAST search. Because of this information, we believe *Porphyromonas gingivalis* protein PG0228 is an excellent Hfq candidate. PG0228 does not have sequence homology with "traditional" Hfq. However, structure analysis shows this conserved hypothetical protein has a Sm-like motif, one of the few things Hfq proteins from different bacteria have in common. By characterizing PG0228 in this study, we will be able to determine if it indeed behaves like Hfq.

Gram stain	Phyla	Species with Hfq	Species without Hfq
Gram-positive	Firmicutes	*Bacillus anthracis, B. cereus, B. licheniformis, B. thuringiensis, Clostridium botulinum, C. difficile, Listeria monocytogenes, Staphylococcus aureus*	*Mesoplasma florum, Streptococcus pneumoniae, S. pyogenes, S. suis, Ureaplasma parvum*
	Actinobacteria		*Clavibacter michiganensi, Corynebacterium* spp. *Leifsonia xyli, Mycobacterium* spp.
Gram-negative	α-proteobacteria	*Agrobacterium tumefaciens, Bartonella bacilliformis, Brucella abortus, Granulibacter bethesdensis, Ochrobactrum anthropi*	*Rickettsia rickettsii*
	β-proteobacteria	*Acidovorax avenae, Bordetella pertussis, Burkholderia mallei, Chromobacterium violaceum, Laribacter hongkongensis, Neisseria gonorrhoeae, N. meningitidis, Ralstonia solanacearum*	
	γ-proteobacteria	*Acinetobacter baumannii, Actinobacillus pleuropneumoniae, Citrobacter koseri, Dickeya dadantii, Edwardsiella tarda, Erwinia carotovora, Escherichia coli* spp., *E. fergusonii, Francisella tularensis, Haemophilus influenzae, Klebsiella pneumoniae, Legionella pneumophila, Pasteurella multocida, Pseudomonas aeruginosa, P. syringae, Salmonella* spp., *Serratia proteamaculans, Shewanella oneidensis, Shigella* spp., *Vibrio cholerae, Xanthomonas campestris, Xylella fastidiosa, Yersinia* spp.	*Coxiella burneti*
	δ-proteobacteria		*Lawsonia intracellularis*
	ε-proteobacteria		*Campylobacter jejuni, Helicobacter pylori*
	Bacteroidetes/ Chlorobi		*Bacteroides fragilis, Porphyromonas gingivalis*
	Chlamydiae/ Verrucomicrobia		*Chlamydia trachomatis, Chlamydophila abortus, C. pneumoniae*
	Cyanobacteria		*Microcystis aeruginosa*
	Fusobacteria		*Fusobacterium nucleatum*
	Spirochaetes	*Leptospira borgpetersenii*	*Borrelia burgdorferi***, *Brachyspira hyodysenteriae, Treponema pallidum*

Figure 4a. Presence or absence of an *hfq* gene in completed genomes of bacterial pathogens. Data were obtained from NCBIGenome database in July 2009. Table has been taken from Chao et al. [18].

Summary of phenotypes of *hfq* mutants of pathogenic bacteria.

Gram stain	Pathogen	Growth defect*	Impaired motility	Increased sensitivity to									Impaired biofilm formation	Reduced virulence**	Ref.
				Starvation	Ethanol	Oxidative stress	Acid stress	High osmolarity	Detergent	Antimicropeptide/ antibiotic	Iron limitation	Heat stress			
G–	*B. abortus*	+		+		+	+							+	[4]
	B. cepacia	–	+	+		+		+				+		+	[13]
	EHEC	+	+				+								[14•,35•]
	UPEC	–	+			+	+			+			+		[15]
	F. tularensis	+						+	+			+		+	[16,30]
	L. pneumophila	+									+			–	[17]
	M. catarrhalis	+				+		+					Increased		[18]
	N. meningitidis	+		+		+		+	+	+				+	[19,21]
	N. gonorrhoeae	+	–											–	[20]
	P. aeruginosa	+	+	+		+								+	[22]
	S. flexneri													+	[34]
	S. sonnei													+	[31]
	S. typhimurium	+	+											+	[12,23•, 28•]
	S. enteritidis	+	–				+			+		+		+	[29]
	V. cholerae	+												+	[24]
	V. parahaemolyticus	+													[42]
	Y. pestis	+		+		+		–		+		+		+	[25]
G+	*L. monocytogenes*	–		+	+	–	–	+	+	–		–		+	[26]
	S. aureus	–				–		–				–			[27]

* (+)/(–) represents agree/disagree to the observations; blank means that phenotype was not-tested.

** Δ*hfq* mutants of *B. abortus*: decreased survival rate in murine primary macrophages and decreased spleen colonization of mice; *B. cepacia*: reduced colonization and lethality in *C. elegans* infection model; UPEC: reduced ability to colonize and persist in kidney and bladder in mice; *F. tularensis*: impaired in multiplication in murine macrophage cell lines and in mice, and decreased mortality in mice; *L. pneumophila*: showed only slight replication defect in macrophages, and no significant defect in amoebae infection; *N. meningitidis*: decreased bacterial counts in whole blood, in serum (*ex vivo* model) and in infant rats; *N. gonorrhoeae*: infected epithelial cells exhibit only moderate reduction of IL-8 secretion and JNK activation; *P. aeruginosa*: decreased mortality in mice; *S. flexneri*: impaired invasion to Henle cells line; *S. sonnei*: guinea pigs showed less severe symptoms and faster recovery after infection; *S. typhimurium*: reduced invasion and intracellular replication in HeLa cells, impaired replication in murine macrophage cell lines, decreased bacterial counts in spleen in mice, and less lethality in mice infection; *S. entiritidis*: decreased survival in serum and lethality in mice infection; *V. cholerae*: out-competed by wild-type and impaired colonization in mice; *Y. pestis*: impaired intracellular survival rate in murine macrophage cell line, out-competed by wild-type in mice, decreased mortality and less bacterial counts in mice; *L. monocytogenes*: less bacterial counts in spleen and liver of infected mice.

Figure 4b. Summary of Phenotypes of *hfq* Mutants of Pathogenic Bacteria. Table has been taken from Chao et al. [18].

Chapter 2: MATERIALS AND METHODS

2.1. Project Aims

1. Determine the biological role of the protein encoded by PG0228.
    a. PGΔ0228 mutant (abbreviated Δ0228) is generated by fusion PCR techniques. Areas downstream and upstream of PG0228 on the chromosome are amplified using *P. gingivalis* W83 strain genomic DNA and general PCR methods. Then, *ermF* cassette is inserted in between the two amplified segments therefore deleting the PG0228 from the W83 DNA segment. The DNA segment is ligated into a plasmid vector and then inserted into the W83 genome by a double cross-over into the chromosome thus replacing *PG0228* with *ermF*. The 0228 null mutant is verified by PCR amplification, enzyme digestion, and sequencing.
    b. A growth curve is done to assess the growth of the Δ0228 mutant compared to the wild type. Both the growth rates and overall densities of the two strains are compared.
    c. Then, changes in transcription profile are studied using microarray analysis. Both W83 and Δ0228 are grown under the same conditions together. Their RNA is isolated and reverse transcribed into cDNA and labeled. The cDNAs from both strains are mixed and hybridized onto microarray slides containing probes for all

ORF present on the W83 genome. Microarray slides are scanned and analyzed to identify the genes upregulated and downregulated in the Δ0228 mutant.

d. Changes in host invasion rates and survival can be measured by a survival study. Epithelial cells are infected with wild type and Δ0228 *Porphyromonas gingivalis* for 30 minutes. Bacteria sticking on the surface of epithelial cells are washed off and then killed with an antibiotic while internalized bacteria remain unaffected. Epithelial cells are then lysed and their contents are plated onto Blood agar plates in anaerobic conditions. The viable intracellular bacteria grow a certain number of colonies, therefore indicating if PG0228 has influence on bacterial survival during host invasion.

2. Determine if the protein binds to RNA

   a. The 0228-*tagged* fusion mutant (0228-HaLo) is also generated by fusion PCR techniques. PG0228 is inserted into a Halo plasmid vector containing "tag". Erm cassette (*ermF-ermAM*) is then inserted. DNA segment containing gene, tag, and erm is amplified by general PCR along with a segment downstream of PG0228. The two segments are ligated by Fusion PCR methods. The DNA construct is then ligated into a plasmid vector and inserted into the W83 genome by a double cross-over into the chromosome. The 0228-HaLo strain is verified by PCR amplification and sequencing.

   b. 0228-HaLo strain is treated with formaldehyde and immunoprecipitation is carried out to study RNA-protein interactions *in vivo*. The cross-linked 0228/RNA is immunoprecipitated using the HaLoTag Resin. The RNA bound to PG0228 is

then sequenced, therefore indicating if PG0228 is a RNA binding protein and if so, the identities of these bound RNAs.

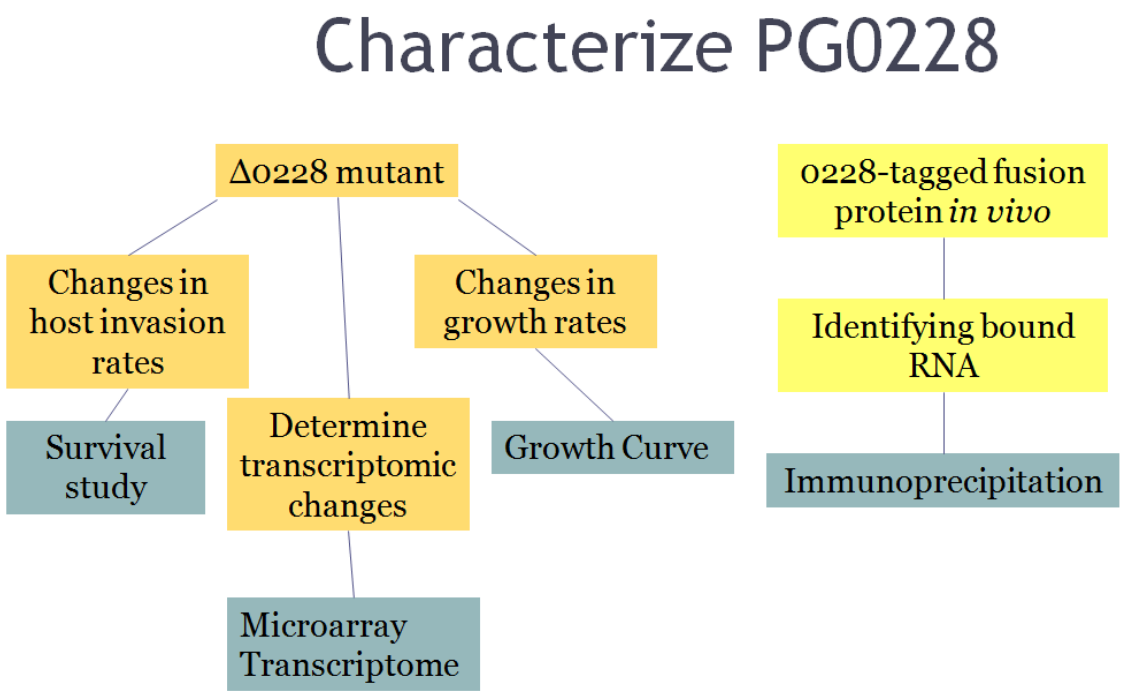

Figure 5. Project Aims. This is a flow chart identifying the focus of this study.

AIM 1: Determine the biological role of the protein encoded by PG0228

AIM 2: Determine if the protein binds to RNA

2.2. Bacterial Strains and Plasmids

Porphyromonas gingivalis W83 strain was used as the wild type for this study. This strain is known to contain a compliment of known virulent factors. Strain W83 (also known as strain HG66) was sequenced by The Institute for Genomic Research (TIGR) and general properties can be found at the Los Almos National Laboratory Bioinformatics (ORALGEN) (http://www.oralgen.lanl.gov). The genomic DNA sequence includes 2, 343,479 base pairs with a G+C content of 49%.

For cloning purposes, the pCR2.1-TOPO Vector (Figure 6) or pFC20K T7 SP6 Flexi Vector (Figure 7) was mixed with the desired PCR product for ligation. All transformations were performed using One Shot TOP10 Chemically Competent *Escherichia coli*.

2.3. Growth Conditions and Media

All *P. gingivalis* strains were grown on blood agar plates (TSA II, 5% Sheep Blood) (BBL, Cockeysville, MD) containing 0.5-1% clindamycin. The liquid cultures were grown in BHI (brain heart infusion, Difco Laboratories, Detroit, MI) media supplemented with hemin (2µg/mL) (Sigma-Aldrich, St. Louis, MO) added. *P. gingivalis* was grown in anaerobic conditions in an atmosphere composed of 10 % Hydrogen, 10% Carbon dioxide, and 80% of Nitrogen at 37° Celsius.

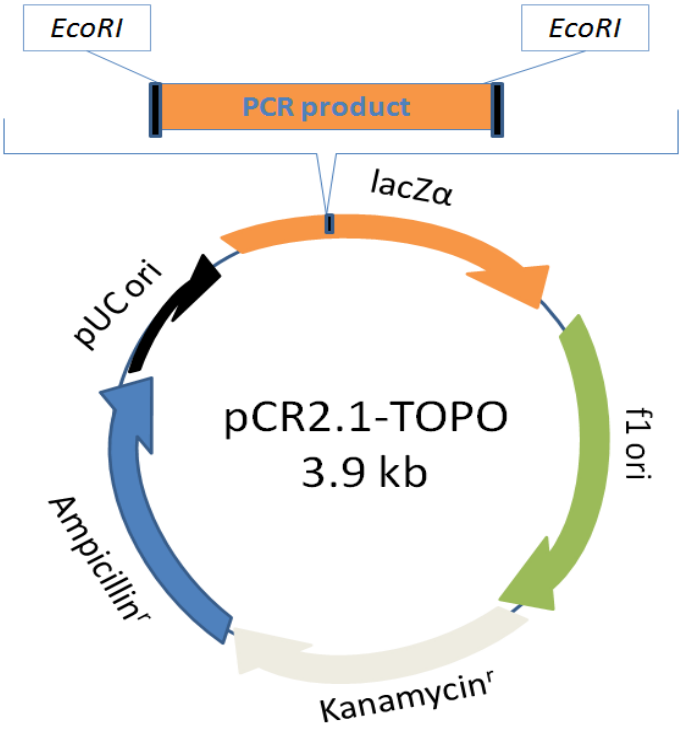

Figure 6. pCR2.1 TOPO Vector. Vector used to introduce mutant PCR fragment into TOP 10 *E. coli* chemically competent cells. The vector equals 3.9 kb and includes 3'-T overhangs for ligation PCR products using *Taq* Polymerase. *Eco*RI sites flank the PCR product insertion site for easy excision of inserts. The vector also contains kanamycin and ampicillin resistance genes for selection in *E. coli*.

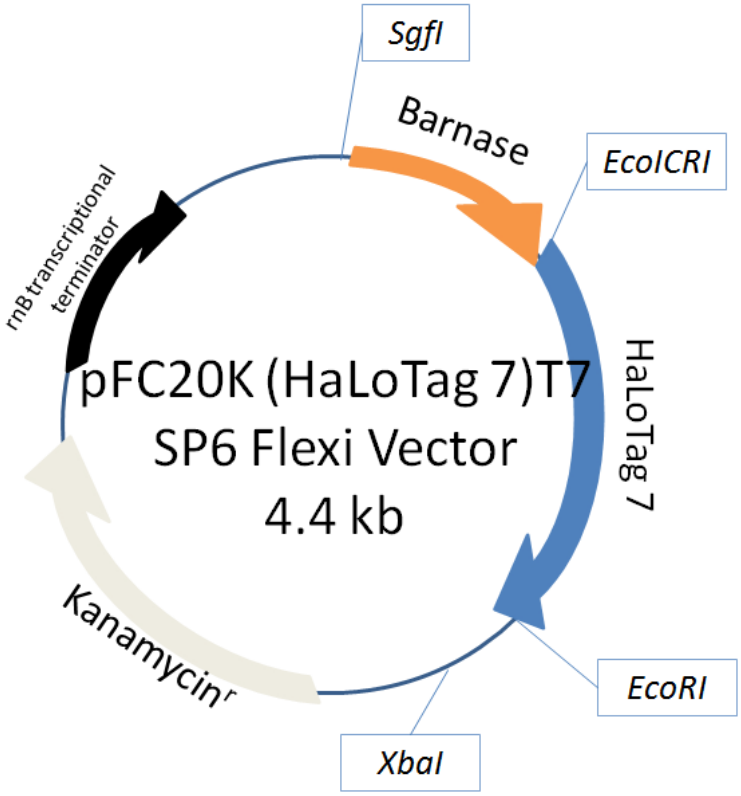

Figure 7. pFC20K (HaLoTag 7) T7 SP6 Flexi Vector. The HaLoTag was used to introduce 0228 with HaLoTag and *ermF-ermAM* into TOP 10 *E. coli* chemically competent cells. The vector itself is 4.4 kb. The insertion of the PCR product (0228) is added between the *Sgf*I and *Eco*ICRI sites. The vector can only be introduced to *E. coli* once the lethal barnase gene is replaced with the PCR gene of interest. The vector also contains a kanamycin-resistance gene for selection purposes.

Table 1. Primer Sequences.

Segment	Name	Primer Sequence	Tm (°C)
Mut1	Mut1F	5’ GTC CCG AAA GAC GGA GAA T 3’	55.2
	Mut1R	5’ CCC CCG GGG GCC CCC CTG TCG AAG C 3’	75.4
Mut2	Mut2F	5’ GGG GGG GGG GGG GGG TAG TCA TGG 3’	74.1
	Mut2R	5’ TTG AGG AAC TCT CCG CTT GT 3’	56.2
Ext	ExtF	5’ GGG GGG GGG GGG GGG ATC GCT GGC 3’	73.5
	ExtR	5’ CTC TTC GGC ATC AGG AGT TC 3’	55.3
ermF	ErmF1	5’ CGA TAG CTT CCG CTA TTG CT 3’	54.8
	ErmR2	5’ CCC CCC CCC CCC CCC TTT TAC GTT TC 3’	73.2
PG0228	CF2	5’ GAC TGC AGC TAG TCT AGA GCT CCC GA 3’	66.2
	CR2	5’ GAA TCA GAT CGC AGC TGC AGG TCG C 3’	69.1
ermF-ermAM	RP-Erm	5’ GTC CAC CAT GGG AAG CTG TCA GTA GT 3’	63.2
	FP-Erm	5’ GTC GAC ATA TGC CGA TAG CTT CCG CT 3’	64.0

2.4. Generation of *P. gingivalis* Mutant Strains

Two mutant strains, labeled Δ0228 and 0228-HaLo, were constructed for the purpose of this study in order to characterize gene PG0228. The Δ0228 strain was obtained for the purpose of characterizing a genetic knockout of PG0228 compared to wild type strain, W83. The 0228-HaLo was created to see if protein PG0228 is an RNA binding protein. Each mutant strain was verified by gel electrophoresis, PCR, restriction enzyme digestion, and sequencing.

Fusion PCR techniques [91] can be used to replace genes, tag genes, or replace promoters by introducing the proper selective cassette, thus, was the major method used to generate both mutants. For each round of PCR amplification, W83 genomic DNA was used as the DNA template and Platinum *Taq* HiFidelity Polymerase (Invitrogen, Carlsbad, California) was the enzyme chosen. All PCR purifications of PCR products were done using the MinElute PCR Purification kit from QIAGEN (Valencia, CA) or the GeneJET PCR Purification Kit from Fermentas (Glen Burnie, MD). Both worked equally well for all experiments.

2.5. Generation of Δ0228 Mutant *Porphyromonas gingivalis* Strain

P. gingivalis genomic DNA was used to amplify flanking DNA fragments (labeled Mut1 and Mut2 for reference). Primers Mut1F and Mut1R (see Table 1 for primer sequences) were used to amplify fragment Mut1 and primers Mut2F and Mut2R were used to amplify Mut2. The vector, pV2198 carries the 2kb *ermF-ermAM* antibiotic resistant gene cassette[27], therefore, was the template DNA used to amplify erm cassette. The first 1kb of this cassette containing clindamycin resistance was amplified, labeled *ermF*, using primers ErmF1 and ErmR2.

The Platinum *Taq* DNA Polymerase High Fidelity protocol was followed with a sample size of 25µL. Each PCR sample contained 2.5 µL of 10X High Fidelity PCR Buffer, 0.5µL of 10mM dNTP mixture, 2µL of 50mM $MgSO_4$, approximately 100ng of Genomic DNA, 0.2µL of Platinum *Taq* HiFidelity polymerase, and autoclaved, distilled water. The tubes were then capped and centrifuged for a short time to mix all the contents. The thermal cycler was run for 30 cycles. The first cycle heated the sample to 94°C for 2 minutes. Cycles 2-30 included denaturing the sample at 94°C, annealing the strands at 55°C, and extending strands for 2 minutes at 68°C.

Next, 5µL of the PCR products were run on a 1% agarose gel electrophoresis using 1X TAE buffer. For visualization of DNA strands, the gel was stained with ethidium bromide. The desired PCR products were then purified using the MinElute PCR Purification kit from QIAGEN.

The purified flanking DNA fragments from the first round of general PCR were annealed together through fusion PCR techniques [91] using Mut1, *ermF*, and Mut2 fragments as template DNA. Fragment Mut1 sits upstream of *ermF* and Mut2 sits downstream of *ermF* totaling a length of 2.1kb. The original primers Mut1F and Mut2R were used for amplification of the desired fusion PCR product.

The Platinum *Taq* DNA Polymerase High Fidelity protocol was followed with a sample size of 25µL. Each PCR sample contained 2.5µL of 10X High Fidelity PCR Buffer, 0.5µL of 10mM dNTP mixture, 2µL of 50mM $MgSO_4$, approximately 100ng of Genomic DNA, 0.4µL of Platinum *Taq* HiFidelity, and autoclaved, distilled water. The tubes were then capped and centrifuged for a short time to mix all the contents. The thermal cycler was run for 35 cycles. Cycle 1 heated the sample to 94°C for 2 minutes. Cycles 2-35 denatured the sample at 94°C, annealed at 57°C, and

had an extension time of four and a half minutes with a temperature of 68°C. The size of the PCR product was confirmed on a 1% agarose gel, and purified.

Transformation and Cloning

Once the desired PCR fragment was produced, the product was cloned into the pCR2.1-TOPO Vector (Figure 6) according to the manufacturer's protocol (Invitrogen). First, a reaction containing PCR products, vector, salt, and sterile water were combined and incubated for five minutes at room temperature. The reaction was then placed on ice until transformation. The TOPO cloning reaction was added to One Shot TOP10 Chemically Competent *Escherichia coli* and gently mixed. Then, the mixture was placed on ice and incubated for 30 minutes. The cells were heat-shocked at 42°C for 30 seconds and transferred back on ice. S.O.C. medium was added in sterile conditions. The culture was grown at 37°C in a shaker for one hour. The transformation was then spread onto a pre-warmed selective LB plate supplemented with X-gal and kanamycin (50µg/mL) and grown overnight at 37 °C.

Positive white colonies were cultured in LB media overnight at 37°C in a shaker. Plasmids were isolated from the *E.coli* using QIAprep Spin Miniprep kit and digested with *Eco*RI enzyme. The digestion incubated at 37°C for approximately 2 hrs and then separated on a 1% agarose gel in 1X TAE buffer. Correct PCR plasmids were verified by sequencing done by DNA Core (MCV-VCU Nucleic Acids Research Facilities, Richmond, VA).

Electroporation of DNA into *P. gingivalis*

Transformation of the desired PCR products was done using electroporation into *P. gingivalis* to obtain the Δ0228 mutant strain. A 10µL sample of construct DNA was added to 100µL of EP competent cells. A control containing only EP cells was also used. These samples were incubated on ice for around five minutes. The samples were electroporated for several seconds at 2.5 volts. The low range registered 400 and high range registered 800. Immediately, 500µL of BHI + hemin was added to the mixtures within the anaerobic chamber to grow overnight. The cultures were then plated on blood agar plates with 1% clindamycin to grow for up to one week. Colonies obtained on the plates were characterized for the presence of correct organization of the genetic locus as described below.

Colonies on the blood agar plate were labeled and inoculated on two new blood agar plates; one plate contained 1% clindamycin antibiotic and one plate contained no clindamycin. The plate containing the antibiotic was left inside the anaerobic incubator. The plate with no antibiotic was taken out of anaerobic conditions and was incubated at 37°C to check for aerobic bacterial contamination. The positive colonies from the electroporation were also cultured into 8mL of BHI + hemin to grow overnight. 3mL of the culture was saved at -80°C in DMSO and 5mL was used for genomic DNA isolation.

Genomic DNA isolation

The 5mL of culture was spun down at 6000rpm for ten minutes to form a pellet. The supernatant was extracted. The genomic DNA was isolated using Puregene DNA Purification System (Gentra Systems, Minneapolis, MN) according to manufacturer's protocol. Then, 3mL of

lysis solution was added to pellet and mixed until cells are suspended. The cells were lysed at 80°C for 5 min and 15µL of RNase solution (product from Sigma-Aldrich, St. Louis, MO) was added to the suspension. It was mixed by inversion, and then incubated for 15-60min at 37°C. Then, 1mL of protein precipitation solution was added to the lysate after solution cooled back to room temperature. Mixture was then vortexed at high speed for 20 seconds to mix solution with cell lysate.

Protein and cell fragments were separated from DNA by centrifuging at 6000rpm for 13 minutes. The supernatant containing DNA was extracted and put into clean 15mL tube containing 3mL of 100% isopropanol. Contents were mixed by inverting and then centrifuged at 2000rpm for 3 minutes. This caused DNA to form a small white pellet. Supernatant was removed and drained on clean absorbent paper. Next, 3mL of 70% ethanol was added to wash the DNA. The sample was again centrifuged for 1min at 2000rpm. Ethanol was removed and drained on clean absorbent paper. Then, 500µL of DNA hydration solution was added and incubated for 1hr at 65°C and overnight at room temperature.

The isolated genomic DNA was run through a PCR to check for correct band size. The PCR was run with an annealing temperature of 57°C and extension time of 4 minutes using AccuPrime *Taq* DNA Polymerase (Invitrogen). The size of the PCR product was confirmed on a 1% agarose gel and then purified. The PCR samples were verified by sequencing done by DNA Core (MCV-VCU Nucleic Acids Research Facilities, Richmond, VA).

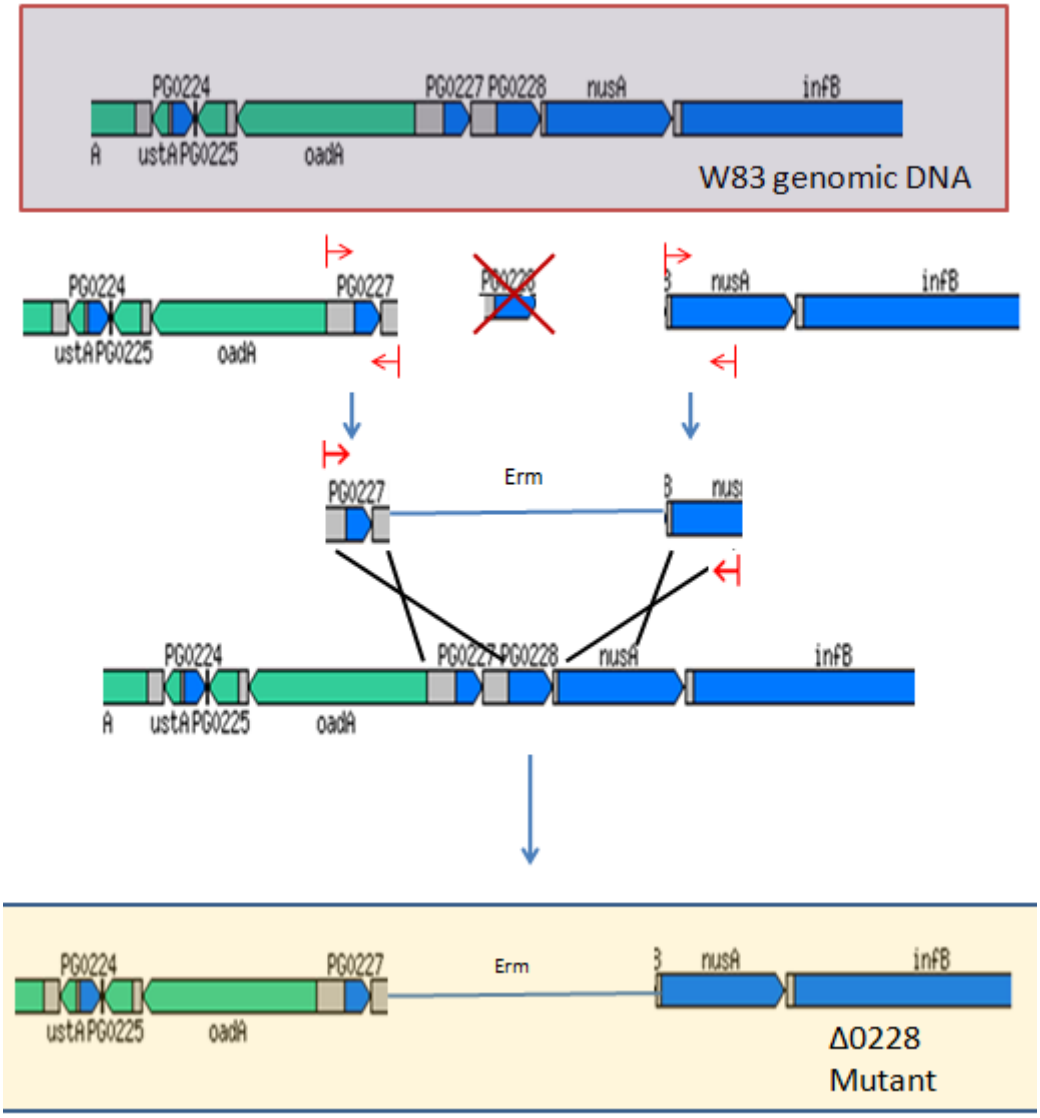

Figure 8. Schematic Diagram of Δ0228 Strain Generation. Upstream and downstream regions of PG0228 were amplified. *ermF* cassette is inserted using fusion PCR. Desired fragment is integrated into the W83 genome by electroporation. The map of PG0228 genomic locus is adapted from Oralgen (http://www.oralgen.lanl.gov).

2.6. Generation of 0228-HaLo *Porphyromonas gingivalis* Strain

The 0228-HaLo mutant was created in order to determine whether or not the protein PG0228 indeed binds to RNA. 0228-HaLo does not contain any genetic deletions and behaves as wild type. 0228-HaLo contains an additional manufacturer-engineered HaLoTag (1Kb) (Promega, Madison, WI) downstream of PG0228 and an insert of the *ermF* cassette (1Kb) for mutant selection. The HaLoTag was added for specific protein selection by HaloLink Resin (also engineered by Promega) according to manufacturer's protocol during immunoprecipitation.

First, the primers CF2 and CR2 (see Table 1 for sequences) were used to amplify PG0228 using general PCR. Specific primers were selected based on manufacturer's suggestions. Specific primers for PG0228 were intended to produce 3' overhangs for easy insertion into our desired vector, pFC20K (HaLoTag 7) T7 SP6 Flexi Vector between *SgfI* and *EcoICRI* restriction sites (Figure 2.2). The size of this PCR product was confirmed on a 1% agarose gel. After pFC20K was digested with *SgfI* and *EcoICRI*, PG0228 was inserted between *SgfI* and *EcoICRI* sites.

To insert the *ermF-ermAM* cassette into pFC20K between *Eco*RI and *Xba*I, pV2198 was digested with *Eco*RI and *Xba*I. The digestion mixture incubated at 37 °C for 2 hours and was confirmed on a 1% agarose gel. The 2.1kb band *ermF-ermAM* was extracted under UV light from the pV2198 digestion and purified using the MinElute Gel Extraction Kit (QIAGEN) protocol. Six volumes of QG buffer per volume of gel were added. The surrounding gel was dissolved with an incubation of 50°C for 10 minutes, mixing every 2 minutes. One volume of isopropanol was added to the mixture, mixed, and placed into a MinElute column. The column

was centrifuged for 1 minute at 14,000rpm and the flow through was discarded. Next, 500µL of buffer QG was added. The column was again centrifuged for 1 minute and flow through was discarded. Next, 750µL of Buffer PE was added to wash, then centrifuged, and flow through was discarded. The column was centrifuged for 2 minutes to empty out the residual buffer. The column was placed in a new tube and 10µL of EB Buffer was added. The mixture was left for one minute and then centrifuged for one minute. This time the flow through was kept because it contained the *ermF-ermAM* fragment.

The plasmid pFC20K T7 SP6 Flexi Vector (Promega Corporation, Madison, WI) contains the HaLoTag and was also digested. Digestion of plasmid pFC20K T7 SP6 with *Eco*RI and *Xba*I allowed *ermF-ermAM* antibiotic resistant gene to be inserted into the pFC20K vector downstream of the HaLoTag fusion protein.

The DNA plasmid pFC20K T7 was then transformed into One Shot TOP10 Chemically Competent *Escherichia coli* according to the Invitrogen protocol (as described above). Positive white colonies were cultured in LB media overnight at 37°C shaking. Plasmids were then isolated from the *E.coli* using QIAprep Spin Miniprep kit (QIAGEN).

Next, a general PCR was run to amplify the DNA of interest. CF2 and ermR2 primers (see Table 1 for primer sequences) were used to amplify PG0228, HaLoTag, and *ermF* (*ermF* is only the first 1kb of the 2.1kb *ermF-ermAM* cassette containing clindamycin resistance). The PCR was run at an annealing temperature of 55°C, extension time of 3 minutes, and an enzyme temperature of 68°C. The size of the PCR product was confirmed on a 1% agarose gel and then purified.

The gene downstream was then added to the PCR fragment to ensure a double crossover. First, a general PCR was run to amplify the gene downstream of PG0228, PG0229 (*nusA*). Both ExtF/ExtR primers (see Table 1 for sequences) were used for the PCR. The PCR was run at an annealing temperature of 55°C, an extension time of 2 minutes, and at an enzyme temperature of 68°C. The size of the PCR product was confirmed on a 1% agarose gel and then purified.

A fusion PCR was then run to anneal the fragments together[91]. The fusion PCR included primers CF2 and ExtR, an annealing temperature of 58°C, and an extension time of 5 minutes at 68°C. The fragment was confirmed on a 1% agarose gel. The product was cloned into the pCR2.1-TOPO vector according to the protocol (Invitrogen). The TOPO cloning reaction was then added to One Shot TOP10 Chemically Competent *Escherichia coli*. Positive colonies were cultured overnight and plasmids were isolated by mini prep. Correct PCR plasmids were verified by sequencing done by Retrogen Inc. (San Diego, CA).

The Fusion PCR products were also electroporated into *P. gingivalis* using the protocol described previously. A fraction of the LB culture was frozen at -80°C and another fraction harvested for genomic DNA isolation. The isolated genomic DNA was run through a PCR to check for correct band size. The PCR was run with an annealing temperature of 58°C and extension time of 3 minutes using Platinum *Taq* HiFidelity polymerase. The size of the PCR product was confirmed on a 1% agarose gel electrophoresis using 1X TAE buffer.

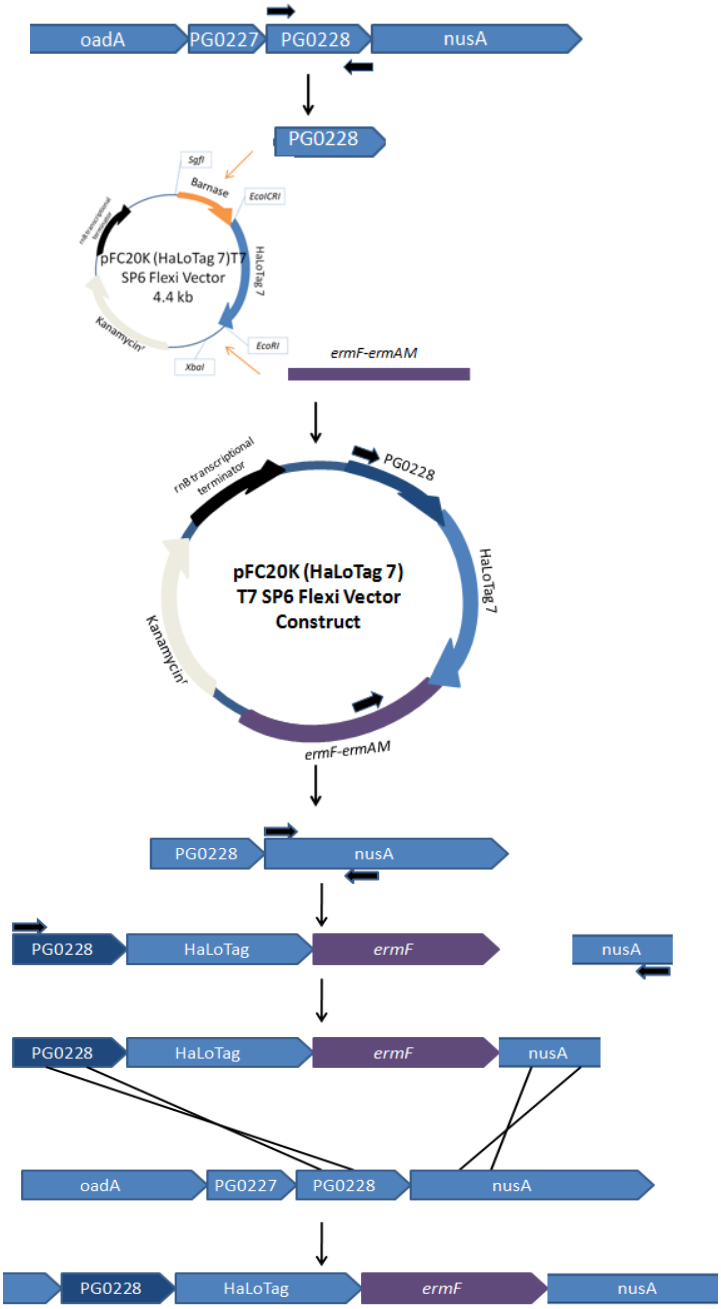

Figure 9. Schematic Diagram of 0228-HaLo Strain Generation. PG0228 and *ermF-ermAM* are inserted into pFC20K. PG0228, HaLoTag, and *ermF* are amplified along with the 5' of *nusA*. Both strands are annealed together by fusion PCR. The desired fragment is transformed into W83 genome by electroporation.

2.7. Growth Curve of Δ0228 Mutant

A growth curve was done to assess the growth of the mutant compared to the wild type. Each culture was left to grow overnight. Quantitative results were obtained by checking optical density at 660nm. Each sample was diluted to an optical density (OD_{660nm}) of 0.1 in a total of 7mL of BHI + hemin media. Both W83 and Δ0228 were grown in triplicates. The growth was measured for 24hrs in 4hr increments (8hrs for the 16-24hr time block).

2.8. Microarray Analysis of Δ0228 Mutant

RNA Isolation

Overnight cultures of W83 and Δ0228 were diluted to an OD_{660nm} of 0.2 and grown to an OD_{660nm} of 0.5. First, 5mL cultures were collected by centrifugation for 15 minutes @4°C, and spun at 6000rpm. Cells were then saved in -80°C freezer. Total RNA was isolated from pelleted cultures (protocol from Karl M. Thompson, Ph.D.). Pellets were resuspended in 500µL of 1X lysis buffer and placed on ice. An equal volume of hot acid phenol-chloroform was added to samples. Then, samples were placed on a heat block at 65°C for 10 minutes. Solution was mixed by inversion every two minutes during heating process. Samples were spun for 10 minutes at 10,000rpm. The supernatant was transferred to a new Eppendorf tube, and then mixed with an equal volume of acid phenol-chloroform. This step was repeated until there was no interface visible.

The sample was then mixed with two volumes of ice cold 100% ethanol and precipitated at -80°C overnight. The mixture was spun at 14,000rpm for 30 minutes at 4°C. Supernatant was

discarded and pellet was washed with ice cold 70% ethanol. Residual ethanol was removed. The RNA pellet was resuspended in RNase free water and saved at -80°C.

cDNA Generation

Then, cDNA was generated using the Fairplay III Microarray Labeling Kit (Stratagene Co.). The RNA concentration was determined with the NanoDrop Spectrophotometer by Thermo Fischer Scientific. 3µL of Random primers were added to 10ug of W83 and Δ0228 RNA samples. The volume of the samples was brought up to 15µL with RNase free water. Samples were then incubated at 70°C for 10 minutes. Samples were cooled to room temperature. 2.2µL of 10X Affinity Script RT buffer, 1µL 20X dNTP mix, 1.5µL 0.1M DTT, 0.5µL RNAse block, 2µL Affinity Script HCRT, and 2µL Superscript III (Invitrogen) Reverse Transcriptase were added. The mixture was incubated overnight at 42°C. The next day, 10µL of 1N NaOH was added. The mixture was incubated for 10 minutes at 70°C. Samples were cooled to room temperature. 10µL of 1M HCl was added to neutralize the reaction. The DNA was isolated using MinElute PCR Purification kit from QIAGEN. During wash step, fresh TIGR was buffer was used instead of buffer supplied by QIAGEN. The TIGR wash buffer consists of 125µL KPO_4 (pH 8.5), 3.8mL MilliQ H_20, and 21.0mL of 100% ethanol per 25mL. The samples were eluted twice into 10µL of Sodium bicarbonate (pH 9.3) making the final volume 20µL for both W83 and Δ0228. Now cDNAs were ready for labeling.

The samples were labeled for hybridization using cyanide-labeled probes (GE Healthcare). Wild type (W83) was labeled with Cy-3 dye and the mutant (Δ0228) with Cy-5 dye. The samples were placed in the dark to protect the light sensitive dyes. Samples were incubated for one and

a half hours at room temperature. Next, 5µL of 4M Hydroxylamine was added to stop the reaction. The cDNA was isolated using the QIAGEN MinElute PCR Purification kit in the dark. 1µL of 0.1M DTT was added to each sample. Samples were saved at -20°C for pre-hybridization.

Hybridization

First, 350mL of Pre-hybridization buffer (87.5mL 20X SSC, 3.5mL 10% Sodium Dodecyl Sulfate, 3.5g BSA powder, and 259mL MilliQ water) was prepared then filtered with a 0.22µm Mini-Miser Filter. The buffer was pre-heated in water bath at 42°C for 30-40 minutes. The pre-hybridization buffer was poured over microarray slides (containing the *P. gingivalis* genome) and incubated at 42°C for at least 2 hours. Then, the pre-hybridization buffer was removed and washed with MilliQ Water by gently shaking.

Three different pre-hybridization buffers were prepared. The pre-hybridized microarray slides were washed in each buffer. Buffer 1 consisted of 100mL of 20X SSC and 20mL 10% SDS. Buffer 2 consisted of 100mL 20X SSC. Buffer 3 consisted of 10mL of 20X SSC and 25µL of 100mM DTT. Each buffer was brought up to a 1 Liter volume with MilliQ water and placed in a water bath at exactly 55°C until needed. The pre-hybridized microarray slides were placed in a clean glass container and approximately 500mL of Buffer 1 was added. The container was wrapped up with an absorbent cloth and placed on a shaker for 15minutes at room temperature. This step was repeated with new Buffer 1. This process was repeated with Buffer 2 (10 min. incubation) and then with Buffer 3 (5 min. incubation). After washing, the slides were centrifuged at 1000rpm for 30 seconds to dry. If the slides contained any streaks or spots they were rewashed.

For microarray hybridization, both labeled W83 and labeled Δ0228 were combined (in the dark) and purified using the QIAGEN MinElute purification kit. The DNA was then spun in a speedvac centrifuge for approximately 10 minutes to form a DNA pellet.

A hybridization buffer was made consisting of 400µL formamide, 250µL 20X SSC, 10µL 10% SDS, 1µL 0.1M DTT, 60µL of salmon sperm, and 339µL of MilliQ water. The hybridization buffer was added using a 1mL syringe through a 0.45µM filter. Then, 50µL of the filtered hybridization buffer was added to the hybridized sample containing both W83 and Δ0228. The mixture was centrifuged for 30 seconds, vortexed, and heated at 95°C for 5 minutes. This last step was repeated. These labeled probes were now ready to hybridize to the pre-hybridized microarray slides.

Next, 24mm x 60mm microscope glass cover slips were gently placed of the area on the slide containing the probes. Care was taken to make sure there were no air bubbles. 50µL of sample containing labeled W83 and Δ0228 was added to the edge of the microarray slide. The samples covered the entire slide by capillary action. The slides were then placed into the hybridization chamber overnight at 42°C.

The microarray slides were then washed with 3 post-hybridization buffers. Buffer 1 contained 100mL 20X SSC, 20mL 10% SDS, and 25µL of 100mM DTT. Buffer 2 contained 100mL 20X SSC and 25µL 100mM DTT. Buffer 3 contained 10mL 20X SSC. Each buffer mixture was brought to a final volume of 1 liter by adding MilliQ water. The buffers were preheated to 55°C. The slides were washed in Buffer 1 and shaken until the cover slide fell off. The slides stayed in this buffer for 10 minutes. The slides were transferred to new Buffer 1 for an incubation time

of 10 minutes. The slides were washed in Buffer 2 for 10 minutes twice. Then, the slides were washed in Buffer 3 for 10 minutes twice. Then the slides were centrifuged for 30 seconds to dry the slides. At this point, the slides were ready to be analyzed by scanning.

Microarray Analysis

The Axon 4200 Scanner Program GenePix pro v6 was used to scan and analyze the hybridization signals from the microarray slides. The slides were placed in the scanner and first previewed to adjust wavelength and brightness conditions to optimize data. Actual data scanning followed. The signal intensities from each probe (gene) were analyzed using ArrayAssist software (Stratagene Co. La Jolla, CA). Each array contained 5 probes for each gene representing the entire *P. gingivalis* genome.

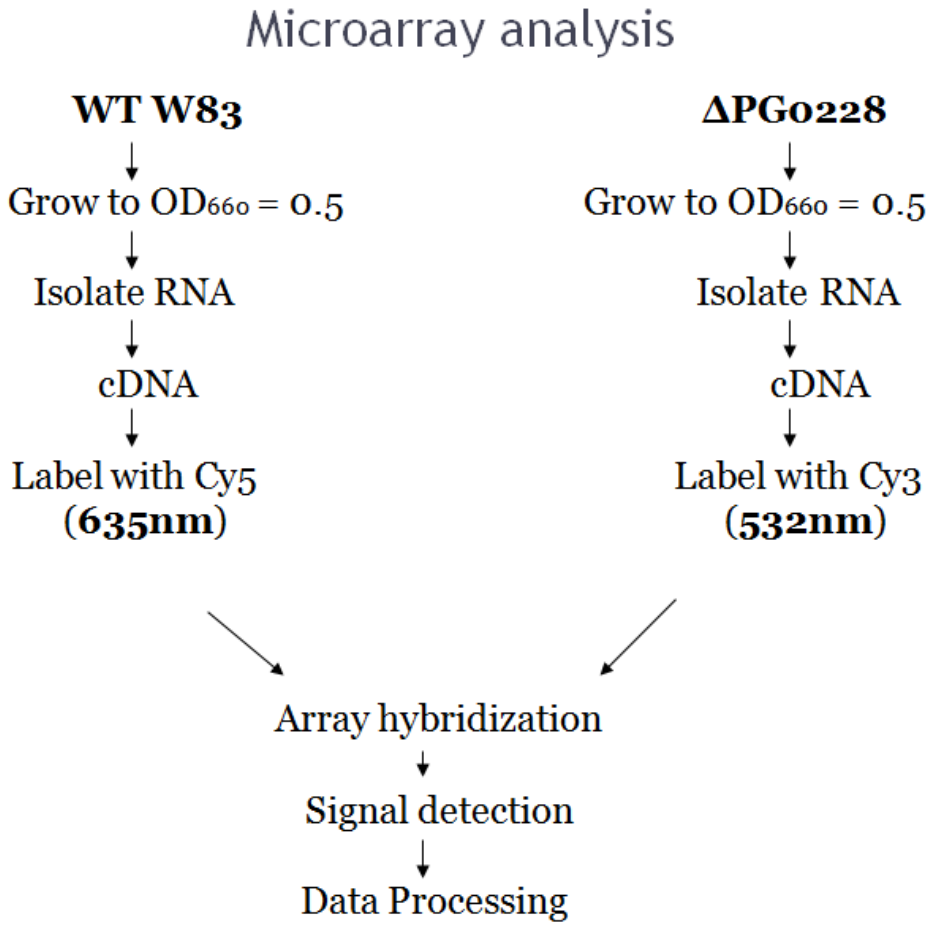

Figure 10. Schematic Diagram of Microarray Analysis.

2.9. Survival of Δ0228 Mutant Strain with Eukaryotic Cells

A survival was done with Δ0228 to analyze any changes in sensitivity to host defense mechanisms compared to its wild type (W83). Overnight cultures of Δ0228 and W83 were diluted to an OD_{660nm} 0.2. The cultures were grown to an OD_{660nm} of about 0.5 to ensure cells were in log phase. HN4 cells were also grown in a 6 well plate to a density of 4×10^5 epithelial cells/well. Both *P. gingivalis* cultures and the HN4 cells were washed twice with PBS. Each bacterial strain was resuspended in their appropriate volume of antibiotic-free HN4 media.

Three wells containing HN4 cells were infected with W83 cells and 3 wells containing HN4 cells were infected with Δ0228 cells. The HN4 cells were infected at a 100:1 MOI (bacteria:host cell ratio). This meant 4×10^7 bacteria had to be added to each appropriate well. The HN4 cells were infected inside the anaerobic chamber at 37°C for 30 minutes. The wells were then washed 3X with PBS media inside the anaerobic chamber to wash away the bacteria on the HN4 cell surface. A media containing 440µg/mL metronidozole and 300µg/mL gentamycin was added to each well. These antibiotics were used to kill the bacteria left on the surface of the HN4 cells. This was done to ensure we were left with only *P. gingivalis* bacteria that invaded the HN4 cells. The cells were incubated with the antibiotics at 37°C for 60 minutes inside the anaerobic chamber. The cells were again washed three times with PBS.

One mL of BHI supplemented with 1% saponin was added to each well. This mixture was incubated for 15 minutes at 37°C in the anaerobic chamber. Each well was then scratched using a cell scraper to ensure all cells were lysed. The contents of each well were added to separate tubes of 3mL BHI media. 200µL of this sample was then diluted into a tube containing

2mL of BHI media. Therefore, the resulting dilutions were 1:4 and 1:10. 200µL of each sample was inoculated on to a blood agar plate totaling 12 plates (6W83/6Δ0228).

2.10. Immunoprecipitation with 0228-HaLo Tagged Strain

A reversible cross-linking combined with immunoprecipitation was done with 0228-HaLo strain to study RNA-protein interactions *in vivo.* This method is based on the chromatin immunoprecipitation (ChIP) assay used to study DNA-protein interactions. Cross-linking with formaldehyde allows rapid preservation of interactions between the target protein and RNA. The cells are then lysed. A resin based ligand, the HaloLink Resin, covalently interacts with the 0228-HaLo protein and is precipitated out. The cross-links are reversed using glycine and the RNA bound to the protein is isolated. Then, a library of RNA is generated and sequenced for identification.

The method used for this study is based on the HaloCHIP System protocol (Promega). Both wild type (W83) and mutant (0228-HaLo) *Porphyromonas gingivalis* strains are used for this study. 30mL cultures were diluted to and OD_{660nm} 0.2 and grown to and OD of 0.7. A 1% concentration of formaldehyde was added to cultures and incubated at room temperature with gentle shaking for 20 minutes. The crosslinking was stopped by adding a 125mM concentration of glycine. Samples were then incubated for 10 minutes at room temperature. Then, cultures were spun at 6000rpm for 10 minutes at 4°C to harvest. The supernatant was discarded and the pellet was washed twice with ice cold PBS (pH 7.5). Pellets were stored at -80°C until immunoprecipitation. Next, 4mL of fresh ice cold lysis buffer (50mM Tris HCl-pH7.5, 150mM NaCl, 0.1% Sodium deoxycholate, 1% Triton X-100) was added and incubated on ice for 5

minutes. The crosslinked complexes are then sonicated to help solubilize them using a sonicator and spun at 14000g for 5 minutes at 4°C. Supernatant is collected.

Next, the HaloLink Resin is prepared according to company's protocol (Promega). Then, 500µL of HaloLink Resin is centrifuged at 800g for 2 minutes and supernatant is discarded. Immediately, 1mL of resin equilibration buffer (1X TE buffer-pH 8.0, 0.1% IGEPAL) is added to the resin and mixed by inverting several times. The sample is then centrifuged at 800g for 2 minutes and supernatant is removed. This process is repeated two more times. It is very important to keep the beads moist until sonicated samples are added.

The supernatant from sonication spin is collected and added to the equilibrated HaloLink Resin. Samples are incubated for 3hrs with shaking at room temperature. After incubation, samples are spun at 800g for 2 minutes and supernatant is removed. Then, 5mL of lysis buffer is added to the resin, mixed, and spun again at 800g. Supernatant is removed and nuclease free water is added, centrifuged, and removed, twice. 1mL of high salt was buffer (50mM Tris HCl-pH7.5, 700mM NaCl, 1% Triton X-100, 0.1% Sodium deoxycholate, and 5mM EDTA) is added, mixed, and incubated for 5 minutes. Samples are then centrifuged and supernatant is discarded. Next, 1mL of LiCl wash buffer (100mM Tris HCl-pH 8.0, 500mM LiCl, 1% IGEPAL, and 1% Sodium deoxycholate) is added, mixed, centrifuged, and supernatant discarded. A 1mL sample of nuclease free water is added, mixed, centrifuged, and supernatant discarded. Then, 1mL of nuclease free water is added, mixed, incubated for 5 minutes, centrifuged, and supernatant discarded. Next, 500µL of reversal buffer (10mM Tris HCl-pH 8.0, 1mm EDTA, and 300mM NaCl) is added, mixed by pipetting, and incubated for 45 minutes at

70°C to reverse the cross-linking done by formaldehyde. After spinning, the supernatant is collected followed by RNA isolation using RNA isolation protocol previously described. Pellet of RNA is suspended in 10µL of RNase free water followed by a DNase treatment from Ambion Inc.

Next, a RNA library is generated using ScriptSeq mRNA-Seq Library Preparation kit according to manufacturer's directions (Epicentre Biotechnologies, Madison, WI). Both a 1µL StarScript Reverse Transcriptase Buffer and 1µL of cDNA Synthesis Primer is added to the 10µL RNA sample. Mixture was incubated at 85°C for five minutes and placed on ice in order to fragment the RNA. Next, cDNA was generated by adding the cDNA synthesis master mix (1.5µL StarScript Reverse Transcriptase Buffer, 1µL dNTP PreMix, 0.5µL RiboGuard RNase inhibitor, and 0.5µL StarScript Reverse Transcriptase to each sample. Samples were placed in the thermocycler at 25°C for 5 minutes, 45°C for 20 minutes, then 1µL of Finishing Solution was added and samples were incubated at 37°C for 10 minutes, and 95°C for 3 minutes. Samples were then placed on ice until the 3' tagging of cDNA. Terminal Tagging Master Mix (1µ Terminal Tagging Oligo, 0.5µL DTT, and 0.5µL DNA Polymerase) was added to each sample and mixed. Samples were heated at 37°C for 15 minutes, 95° for 3 minutes, then 1µL of Finishing Solution was added and samples were incubated at 37°C for 10 minutes, and 95°C for 3 minutes before being placed on ice. The di-tagged cDNA was then purified using the MinElut PCR Purification Kit (QIAGEN) and eluted into 20µL of EB buffer. Next, the samples are amplified by PCR. PCR mix (4.5µL nuclease free water, 25µL FailSafe PCR PreMix E, 1µL Forward Primer, 1µL RNA-Seq Barcode Primer, and 0.5µL FailSafe PCR Enzyme) is added to cDNA and placed in the thermocycler for 12 cycles. Excess PCR primers are removed by adding 1µL of Exonuclease I to each reaction and incubated

at 37°C for 15 minutes. Reactions are again purified using the QIAGEN MinElute PCR Purification Kit and sent in for sequencing.

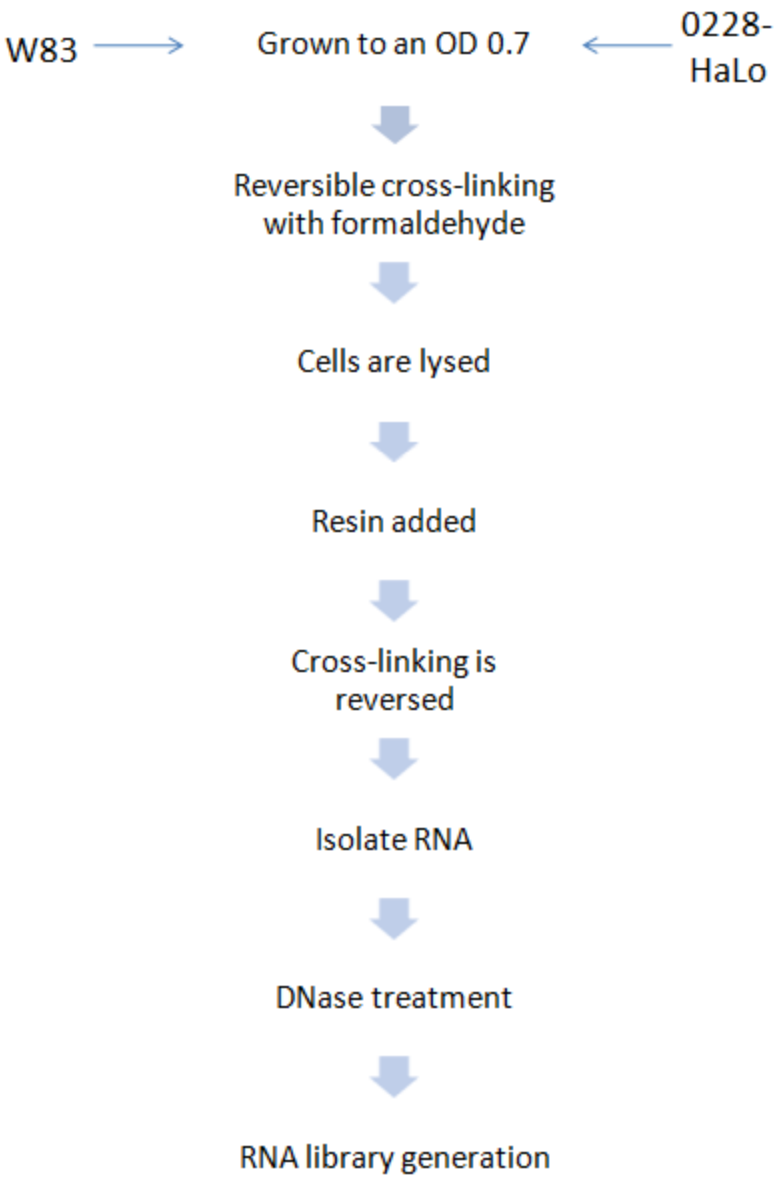

Figure 11. Broad Overview of Immunoprecipitation Using 0228-HaLo. This study was done to see if the PG0228 protein (1) binds to RNA and (2) the identities of these bound RNAs.

2.11 Bioinformatics

The amino acid sequence of PG0228 (PG0253, according to NCBI and TIGR designations) was taken from ORALGEN and inserted into BLAST protein sequence alignment program (http://blast.ncbi.nlm.nih.gov/Blast.cgi)[3]. Then, the 152 amino acids sequence was then searched for similarities against the NCBI database. A taxonomy report was established by using the Taxonomy Report tool within BLAST. Also, a tree was established by using the Distance Tree of Results tool within BLAST.

Chapter 3: RESULTS

3.1. Sequence Alignment with PG0228

According to BLAST protein sequence alignment[3], PG0228 contains a conserved Sm like family domain and it partially aligns with DUF150 (Figure 1seq.). Details about the Sm like family can be found within the introduction under Sm Family of RNA-Associated Proteins. DUF150 is designated as uncharacterized BCR, within YhbC family COG0779. The taxonomy report shows significant homology between PG0228 and proteins within Bacteroidetes phylum (Figure 1seq.). Most proteins within this group are hypothetical proteins and therefore their function has not been determined. Sequence alignment also exists with a ribosome maturation factor RimP for 7 species. A tree view of sequence alignment was also established showing the distance between the species encoding the similar protein within the CFB group of bacteria (Figure 2seq.). There was also alignment to an unnamed protein product and sea anemones.

(a)

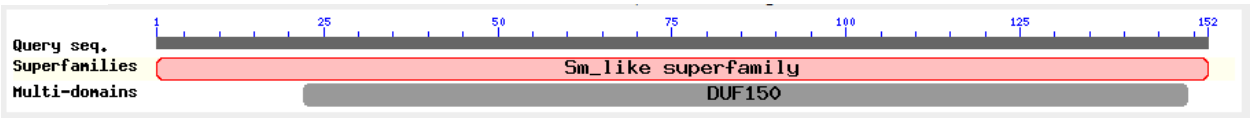

(b)

cellular organisms
. Bacteroidetes [CFB group bacteria]
. . Bacteroidales [CFB group bacteria]
. . . Porphyromonadaceae [CFB group bacteria]
. . . . Porphyromonas [CFB group bacteria]
. . . . . Porphyromonas gingivalis [CFB group bacteria]

. . . . . Porphyromonas gingivalis W83 ----------	306	2 hits	[CFB group bacteria]	hypothetical protein PG0253 [Porphyromonas gingivalis W83]
. . . . . Porphyromonas gingivalis	306	1 hit	[CFB group bacteria]	hypothetical protein PG0253 [Porphyromonas gingivalis W83]
. . . . . Porphyromonas gingivalis ATCC 33277	305	3 hits	[CFB group bacteria]	hypothetical protein PGN 0353 [Porphyromonas gingivalis ATC
. . . . . Porphyromonas endodontalis ATCC 35406 -----	89	2 hits	[CFB group bacteria]	conserved hypothetical protein [Porphyromonas endodontalis
. . . . . Porphyromonas uenonis 60-3	68	2 hits	[CFB group bacteria]	conserved hypothetical protein [Porphyromonas uenonis 60-3]
. . . . . Porphyromonas asaccharolytica PR426713P-I .	67	2 hits	[CFB group bacteria]	conserved hypothetical protein [Porphyromonas asaccharolyti
. . . . Parabacteroides johnsonii DSM 18315 ---------	138	2 hits	[CFB group bacteria]	hypothetical protein PRABACTJOHN 04179 [Parabacteroides joh
. . . . Parabacteroides merdae ATCC 43184	136	2 hits	[CFB group bacteria]	hypothetical protein PARMER 01586 [Parabacteroides merdae A
. . . . Paludibacter propionicigenes WB4	130	2 hits	[CFB group bacteria]	hypothetical protein Palpr 2899 [Paludibacter propionicigen
. . . . Parabacteroides sp. D13	126	2 hits	[CFB group bacteria]	conserved hypothetical protein [Parabacteroides sp. D13] >g
. . . . Parabacteroides distasonis ATCC 8503	125	3 hits	[CFB group bacteria]	hypothetical protein BDI 3532 [Parabacteroides distasonis A
. . . . Odoribacter splanchnicus DSM 20712	93	2 hits	[CFB group bacteria]	Ribosome maturation factor rimP [Odoribacter splanchnicus D
. . . Bacteroides coprocola DSM 17136 ----------	130	2 hits	[CFB group bacteria]	hypothetical protein BACCOP 00455 [Bacteroides coprocola DS
. . . Bacteroides vulgatus ATCC 8482	127	3 hits	[CFB group bacteria]	hypothetical protein BVU 1353 [Bacteroides vulgatus ATCC 84
. . . Bacteroides dorei DSM 17855	127	2 hits	[CFB group bacteria]	hypothetical protein BVU 1353 [Bacteroides vulgatus ATCC 84
. . . Bacteroides sp. 9 1 42FAA	127	2 hits	[CFB group bacteria]	hypothetical protein BVU 1353 [Bacteroides vulgatus ATCC 84
. . . Bacteroides dorei 5 1 36/D4	127	2 hits	[CFB group bacteria]	hypothetical protein BVU 1353 [Bacteroides vulgatus ATCC 84
. . . Bacteroides sp. 4 3 47FAA	127	2 hits	[CFB group bacteria]	hypothetical protein BVU 1353 [Bacteroides vulgatus ATCC 84
. . . Bacteroides sp. 3 1 33FAA	127	2 hits	[CFB group bacteria]	hypothetical protein BVU 1353 [Bacteroides vulgatus ATCC 84
. . . Bacteroides vulgatus PC510	127	2 hits	[CFB group bacteria]	hypothetical protein BVU 1353 [Bacteroides vulgatus ATCC 84
. . . Bacteroides sp. 3 1 40A	127	2 hits	[CFB group bacteria]	hypothetical protein BVU 1353 [Bacteroides vulgatus ATCC 84
. . . Bacteroides sp. 20 3	126	2 hits	[CFB group bacteria]	conserved hypothetical protein [Parabacteroides sp. D13] >g
. . . Bacteroides plebeius DSM 17135	125	2 hits	[CFB group bacteria]	hypothetical protein BACPLE 03630 [Bacteroides plebeius DSM
. . . Bacteroides sp. 2 1 7	125	1 hit	[CFB group bacteria]	hypothetical protein BDI 3532 [Parabacteroides distasonis A
. . . Bacteroides salanitronis DSM 18170	125	2 hits	[CFB group bacteria]	Ribosome maturation factor rimP [Bacteroides salanitronis D
. . . Bacteroides sp. 2 1 33B	125	2 hits	[CFB group bacteria]	UPF0090 protein [Bacteroides sp. 2 1 33B] >gi|262295479|gb|
. . . Bacteroides sp. 3 1 19	125	2 hits	[CFB group bacteria]	conserved hypothetical protein [Bacteroides sp. 3 1 19] >gi
. . . Bacteroides uniformis ATCC 8492	124	2 hits	[CFB group bacteria]	hypothetical protein BACUNI 00272 [Bacteroides uniformis AT
. . . Bacteroides sp. D20	124	2 hits	[CFB group bacteria]	hypothetical protein BACUNI 00272 [Bacteroides uniformis AT
. . . Bacteroides sp. 4 1 36	124	2 hits	[CFB group bacteria]	hypothetical protein BACUNI 00272 [Bacteroides uniformis AT
. . . Bacteroides stercoris ATCC 43183	124	2 hits	[CFB group bacteria]	hypothetical protein BACSTE 02505 [Bacteroides stercoris AT
. . . Bacteroides fragilis YCH46	124	2 hits	[CFB group bacteria]	hypothetical protein BF0261 [Bacteroides fragilis YCH46] >g
. . . Bacteroides fragilis NCTC 9343	124	3 hits	[CFB group bacteria]	hypothetical protein BF0261 [Bacteroides fragilis YCH46] >g
. . . Bacteroides sp. 3 2 5	124	2 hits	[CFB group bacteria]	hypothetical protein BF0261 [Bacteroides fragilis YCH46] >g
. . . Bacteroides sp. 2 1 16	124	2 hits	[CFB group bacteria]	hypothetical protein BF0261 [Bacteroides fragilis YCH46] >g
. . . Bacteroides fragilis	124	1 hit	[CFB group bacteria]	hypothetical protein BF0261 [Bacteroides fragilis YCH46] >g
. . . Bacteroides fragilis 638R	124	1 hit	[CFB group bacteria]	hypothetical protein BF0261 [Bacteroides fragilis YCH46] >g
. . . Bacteroides fragilis 3 1 12	124	3 hits	[CFB group bacteria]	hypothetical protein Bfra3 13350 [Bacteroides fragilis 3 1
. . . Bacteroides intestinalis DSM 17393	124	2 hits	[CFB group bacteria]	hypothetical protein BACINT 01424 [Bacteroides intestinalis
. . . Bacteroides eggerthii DSM 20697	124	2 hits	[CFB group bacteria]	hypothetical protein BACEGG 03444 [Bacteroides eggerthii DS
. . . Bacteroides eggerthii 1 2 48FAA	124	2 hits	[CFB group bacteria]	hypothetical protein BACEGG 03444 [Bacteroides eggerthii DS
. . . Bacteroides cellulosilyticus DSM 14838	123	2 hits	[CFB group bacteria]	hypothetical protein BACCELL 01541 [Bacteroides cellulosily
. . . Bacteroides clarus YIT 12056	122	2 hits	[CFB group bacteria]	hypothetical protein HMPREF9445 00063 [Bacteroides clarus Y
. . . Prevotella tannerae ATCC 51259	122	2 hits	[CFB group bacteria]	conserved hypothetical protein [Prevotella tannerae ATCC 51
. . . Bacteroides sp. D22	120	2 hits	[CFB group bacteria]	conserved hypothetical protein [Bacteroides sp. D22] >gi|29
. . . Bacteroides finegoldii DSM 17565	120	2 hits	[CFB group bacteria]	conserved hypothetical protein [Bacteroides finegoldii DSM
. . . Bacteroides helcogenes P 36-108	119	2 hits	[CFB group bacteria]	hypothetical protein Bache 0520 [Bacteroides helcogenes P 3
. . . Bacteroides sp. D1	119	2 hits	[CFB group bacteria]	conserved hypothetical protein [Bacteroides sp. D1] >gi|262
. . . Bacteroides sp. 2 1 22	119	2 hits	[CFB group bacteria]	conserved hypothetical protein [Bacteroides sp. D1] >gi|262
. . . Bacteroides ovatus SD CC 2a	119	2 hits	[CFB group bacteria]	conserved hypothetical protein [Bacteroides sp. D1] >gi|262
. . . Bacteroides xylanisolvens SD CC 1b	119	2 hits	[CFB group bacteria]	conserved hypothetical protein [Bacteroides sp. D1] >gi|262

Figure 1seq. (a) Amino acid alignment of PG0228 (152aa) showing its conserved domains with the Sm like family. **(b) Taxonomy BLAST report of PG0228 protein sequence**. Species with similar protein sequences are listed according to NCBI.

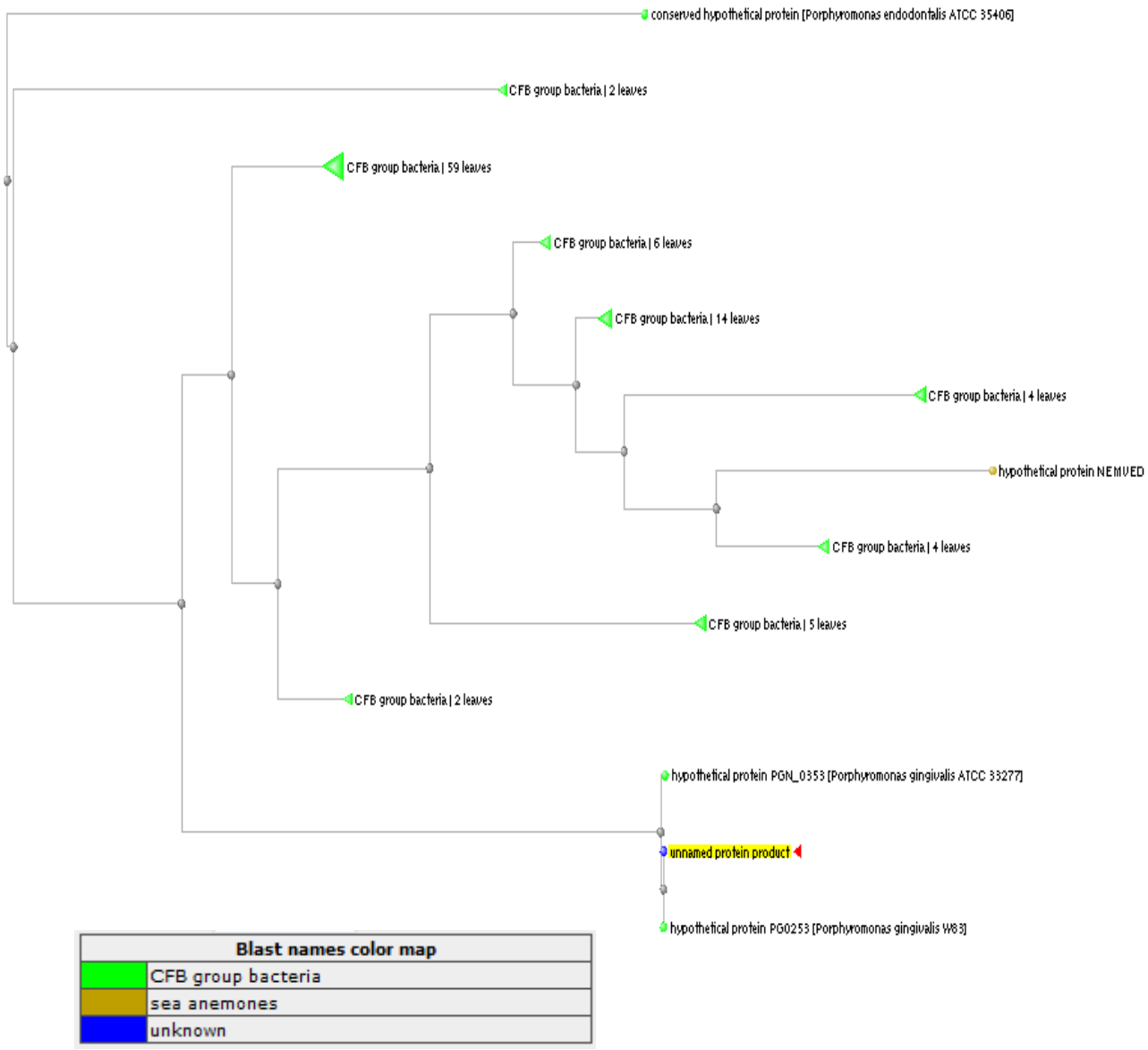

Figure 2seq. Amino Acid Alignment of PG0228 in Distance Tree Formation.

3.2. Generation of Δ0228 Mutant Strain

The Δ0228 mutant strain contains a deletion of gene PG0228 (LANL gene ID) along with insert of *ermF* cassette marker (1Kb). *ErmF* is an antibiotic resistance gene cassette marker for erythromycin and clindamycin[27]. A PCR amplification of genomic *P. gingivalis* fragments was done. Three separate PCRs were set up to amplify each flanking DNA fragment. Samples were then run on a 1% agarose gel to confirm fragment length using a 1kb Plus DNA ladder (Figure 12). Mut1 amplification shows a length of 250bp and Mut2 amplification has a length of 750bp. pVA2198, containing *ermF*, was used as a template to amplify the *ermF* clindamycin resistance cassette. The *ermF* cassette equaled a length of 1.1kb on the 1% agarose gel. Next, the purified flanking DNA fragments from this general PCR were annealed together through fusion PCR techniques using Mut1, *ermF*, and Mut2 as a DNA template. The purified DNA construct was run on a 1% agarose gel resulting in a length of 2.1kb, therefore indicating the three individual fragments annealed together in the fusion PCR.

The desired PCR fragment was cloned into the pCR2.1-TOPO vector (Invitrogen) that carries both an ampicillin (bases 2129-2989) and kanamycin (bases 1317-2111) antibiotic resistance-encoding gene. Between the M13 forward primer (bases 389-404) and reverse primer (bases 205-221) the desired PCR fusion product was inserted. It is also important to note the 3.9kb vector contained the *lacZ* gene. The ligation mixture was then used to introduce the desired PCR fragment into TOP 10 *E. coli* chemically competent cells. After the transformation, the mixture was spread on an LB plate supplemented with X-gal and kanamycin to grow overnight. Transformed *E. coli* containing plasmid with kanamycin resistance gene

were capable of growing on the supplemented LB plate despite the presence of the antibiotic. Both blue and white colonies appeared on the plate after the incubation period. Only white colonies were candidates for successful ligations. *E. coli* containing a functional β-galactosidase enzyme metabolizes the galactose sugar (X-gal) forming an intermediate which is spontatneously oxidized to a bright blue pigment. White colonies contain vector with foreign DNA inserted within the lacZ gene which disrupts the β-galactosidase enzyme, indicated by their lack of bright blue pigment.

Plasmids were isolated from 3 white *E. coli* colonies (designated A, B, and C) and digested with the *Eco*RI enzyme. *Eco*RI restriction enzyme sites were located on both sides of PCR fragment insertion and will result in two DNA fragments at 3.9kb and 2.1kb if insertion is correct. Digestions of all three candidates were run on an agarose gel (Figure 13). Plasmid digestion of colony A shows 4 fragments on the gel equaling 1.4kb, 2.1kb, 3.9kb, and approximately 6kb. Colonies in lane B and C each show one fragment on the agarose gel, equaling a length of 3.9kb. 3.9kb is the length of the TOPO vector alone, therefore B and C do not contain the insert. A, however, contains fragments 2.1kb and 3.9kb in length, therefore further screening tests were done. Sample A and W83 genomic DNA were amplified by PCR with the original MutF1 and MutR2 primers (Figure 14). W83 genomic DNA was used as a control which resulted in a length of 1.5kb which is the length predicted of wild type. An agarose gel confirmed the DNA fragment insert equals a length of 2.1kb so the isolated construct was sent in for plasmid sequencing. The isolated pCR2.1-TOPO vector containing the PCR fusion insert was sequenced using standard M13 forward and reverse primers by DNA Core

(MCV-VCU Nucleic Acids Research Facilities, Richmond, VA). Each result contained the correct ordered sequence of Mut1-ermF-Mut2.

PCR fusion product was electroporated into *P. gingivalis* to obtain the Δ0228 mutant strain. After an incubation of 7 days inside the anaerobic chamber, 8 *P. gingivalis* colonies were selected for mutant selection and plated onto both clindamycin and blood agar plates. Genomic DNA was isolated from each sample and mutant DNA was amplified with the original MutF1 and MutR2 primers (Figure 15). Wild type W83 genomic DNA was used as a control to select for mutants. Agarose gel confirmed samples 1, 2, 3, 4, 5, 7, and 8 were identical with a band length of 2.1kb and most likely Δ0228 mutants. Genomic DNA amplification of wild type resulted in a length of 1.5kb. Genomic DNA from sample 6 did not appear on the agarose gel. PCR products from mutants 1, 3, 5, and 8 were confirmed by sequencing done by DNA Core (MCV-VCU Nucleic Acids Research Facilities, Richmond, VA). Each contained the correct ordered sequence of Mut1-*ermF*-Mut2. The sequence of the determined genomic DNA can be found in Appendix.

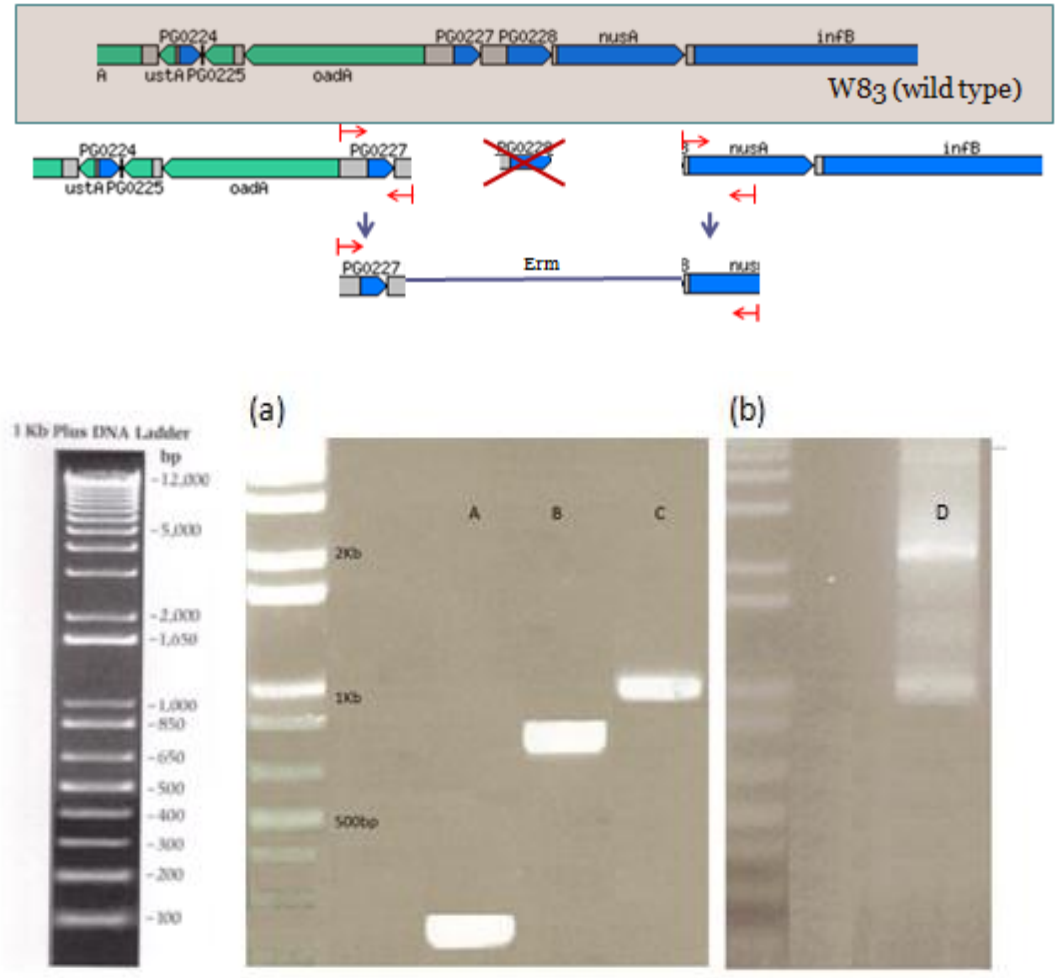

Figure 12. Generation of Δ0228 Mutant DNA Fragment. (a) General PCR to amplify each flanking DNA fragment. Mut1 (A) was amplified using primers Mut1F/Mut1R. Mut2 (B) was amplified using primers Mut2F/Mut2R, and *ermF* (C) , for mutant selection, was amplified using primers ErmF1/ErmR2. *P. gingivalis* genomic DNA was used as a template for Mut1 and Mut2. Plasmid pV2198 was used as a template for *ermF*. **(b)** These purified DNA segments were annealed together by a second round of PCR. Mut1, *ermF*, and Mut2 were used as templates in a Fusion PCR and run on a 1% agarose gel for confirmation.

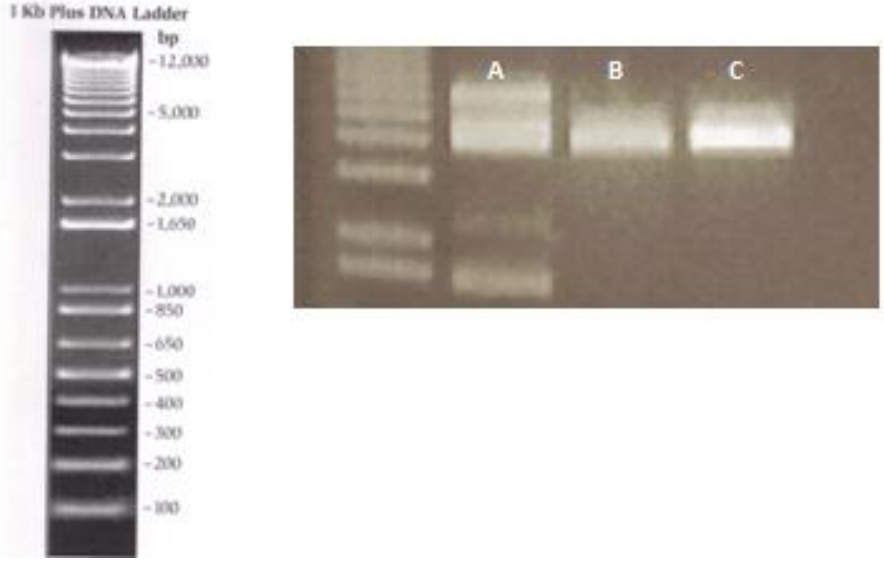

Figure 13. Plasmid screening with *Eco*RI digestion. Plasmids were isolated from 3 *E. coli* colonies grown on LB plates supplemented with kanamycin and x-gal. A, B, C plasmids isolated from 3 colonies, pCR2.1 TOPO TA + insert screening. B and C show one band indicating vector contains no insert. Only A contains the DNA insert (2.1kb) band and vector band (3.9kb). IKb marker is included in lane on the left side of the gel, the sizes of corresponding bands are shown in image of 1Kb ladder.

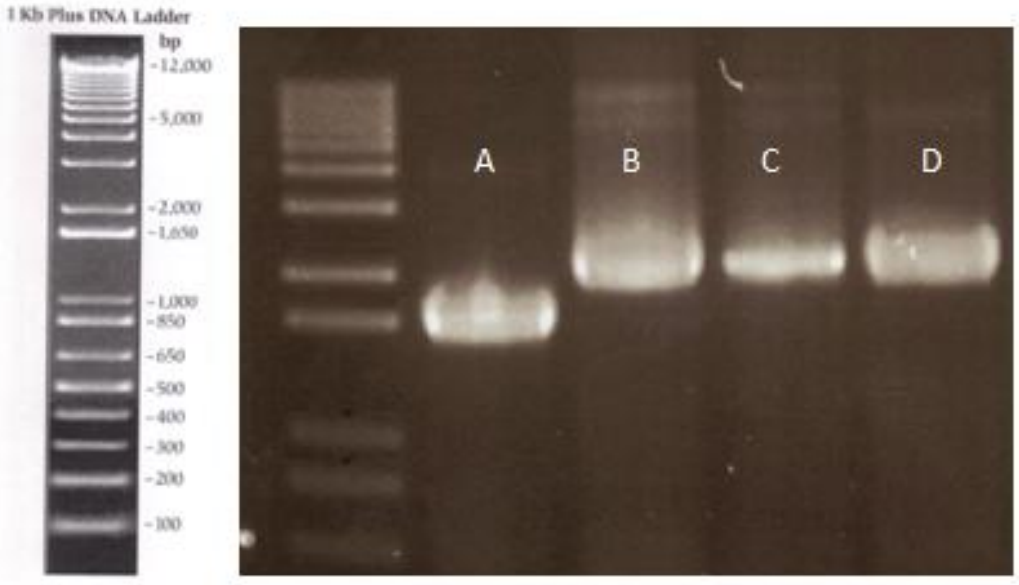

Figure 14. PCR amplification to check for mutant DNA fragment. Isolated plasmids (B, C, D) and *P. gingivalis* genomic DNA (A) were amplified using original fusion primers MutF1 and MutR2 and run on an agarose gel. The isolated plasmids (B, C, D) contain fragments equaling around 2.1kb while the W83 control (A) contains a fragment of 1.5kb in length predicted of wild type. Plasmid constructs were therefore sent in for sequencing.

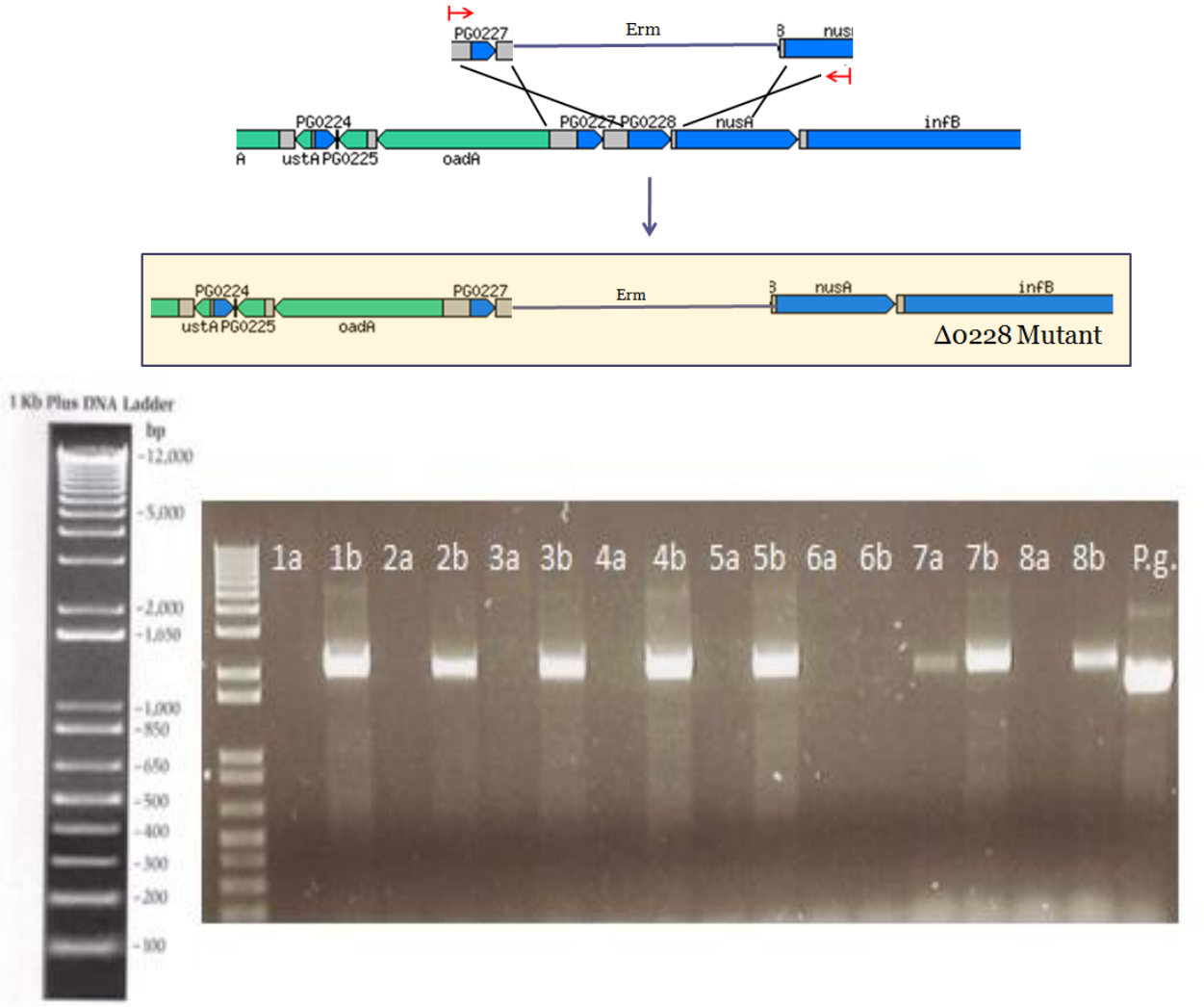

Figure 15. Δ0228 Mutant Selection by Amplification of Genomic DNA. Verified mutant DNA fragment was electroporated into *Porphyromonas gingivalis* to obtain Δ0228 mutant strain. Eight *P. gingivalis* colonies were selected for mutant screening. Lanes labelled "a" are concentrated samples. Lanes labelled "b" contain a lower concentration of 50ng/µL. Genomic DNA was isolated from each sample and amplified with the original primers MutF1 and MutR2. W83 genomic DNA *(P.g)* was used as a control to select for mutants. Samples 1, 2, 3, 4, 5, 7, and 8 are potential mutants because primers amplified the predicted 2.1kb fragment. Identical primers amplified 1.5kb fragments in the *P.g* control. Samples 1,3, 5, and 8 were sent for sequencing.

3.3. Generation of 0228-HaLo tagged *Porphyromonas gingivalis* Strain

The 0228-HaLo tagged strain was created in order to show if protein PG0228 indeed binds to RNA. The strain does not have any genetic deletions and behaves like wild type W83 but includes an additional HaLoTag downstream of PG0228 and ermF for mutant selection. The primers CF2/CR2 were used to amplify PG0228 from W83 genomic DNA. An agarose gel confirmed the band length of the amplification is approximately 500bp (Figure 16). For cloning purposes, PG0228 and *ermF-ermAM* were inserted into our desired vector, pFC20K (HaLoTag 7) T7 SP6 Flexi Vector. The HaLoTag vector measures a length of 4417 base pairs, includes a region for PCR insertion between nucleotides 71-78, and contains an open reading frame for HaLoTag (507-1397). Specific primers were selected based on manufacturer's suggestions (Promega, Madison, WI). Specific primers for PG0228 were intended to produce 3' overhangs for easy insertion between *SgfI* and *EcoICRI* restriction sites (Figure 16). Cutting the vector with *SgfI* and *EcoICRI* excises the lethal barnase gene from the vector, thus allowing propagation in *E. coli*. The 2.1kb *ermF-ermAM* was inserted with manufacturer suggested restriction enzymes (Promega, Madison, WI) *Eco*RI and *Xba*I downstream of tagging region between nucleotides 1398-1509. Enzymes were compared and chosen based on specificity of digestion. A list of acceptable enzymes needed to cut the Halo vector once but not cut our gene of interest (http://tools.neb.com/NEBcutter2/index.php). The plasmid vectors, HaLoTag and pV2198, which contains *ermF-ermAM*, were digested with *Eco*RI and *Xba*I for *ermF-ermAM* insertion (Figure 17).

The HaLoTag vector containing PG0228 and *ermF-ermAM* was introduced to One Shot TOP10 chemically competent *E. coli*. Eight positive white colonies went through additional screening by PCR using primers FP-Erm/RP-Erm. Figure 18 includes an agarose gel containing the PCR products from the 8 colonies. Samples 1, 2, 3, and 4 show bands 2.1kb in length indicating these pFC20K plasmids include the 2.1kb *ermF-ermAM* insert.

The mutant construct containing PG0228, HaloTag, and *ermF* was amplified by PCR using primers CF2/ermR2. It is important to note the ermR2 primer amplifies only the first 1kb of *ermF-ermAM* cassette containing clindamycin resistance only. DNA agarose gel analysis of amplification shows band length of 2.5kb (Figure 19). This length would agree with our prediction and therefore we then proceeded with the addition of the 5' segment of PG0228's downstream gene, *nusA*. The 5' segment (600bp) of *nusA* was added to ensure a double cross-over into W83 genomic DNA. Figure 3.8 shows the amplification of the *nusA* segment from W83 genomic DNA using primers ExtF/ExtR. In order to anneal the mutant construct with the nusA extension, fusion PCR methods were used. An agarose gel (Figure 20) revealed a band at 3kb indicating the 2 flanking fragments annealed together.

The desired PCR fragment was cloned into the pCR2.1-TOPO vector and transformed into One Shot TOP10 chemically competent *E. coli*. Plasmids were isolated from 7 white colonies and verified by sequencing done by Retrogen Inc. (San Diego, CA). Each contained the correct ordered sequence of PG0228-HaLo-*ermF*-nusA. The sequence of the determined genomic DNA can be found in Appendix.

Electroporation into *P. gingivalis* was done to obtain the 0228-*tagged* fusion mutant strain. After an incubation of 7 days inside the anaerobic chamber, 4 *P. gingivalis* colonies were selected for mutant selection and plated onto both clindamycin and blood agar plates. Genomic DNA was isolated from each sample and mutant DNA was amplified with FP-Erm/ExtR primers (Figure 21). Wild type W83 genomic DNA and the sequenced plasmid were used as a control to select for mutants. Agarose gel revealed both the amplified sequenced plasmid, acting as the positive control, and mutant genomic DNA showed bands at 1.6kb, confirming the generation of the desired 0228-*tagged* fusion mutant strain. No amplification was found using FP-Erm/ExtR primers on wild type W83.

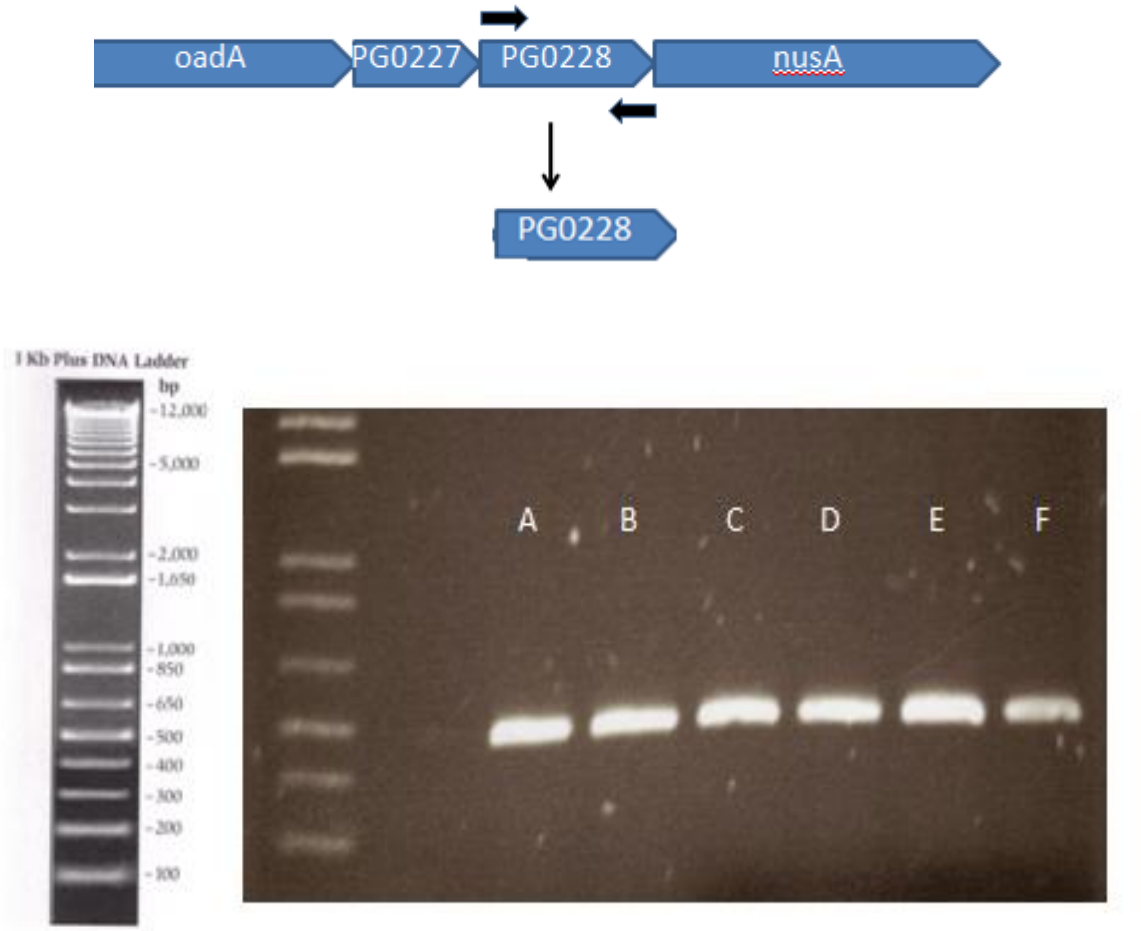

Figure 16. Amplification of PG0228. Agarose gel representing the amplification of the 456bp PG0228 (Lanes A-F) using specific primers CF2 and CR2 for direct HaLoTag plasmid insertion. The fragment is then inserted into the desired 4.4kb vector, pFC20K (HaLoTag 7) T7 SP6 Flexi Vector. to add the specific 1kb C-terminal tag to the protein. PG0228 is inserted into the HaLoTag vector between the *Sgf*I and *EcoICR*I restriction sites.

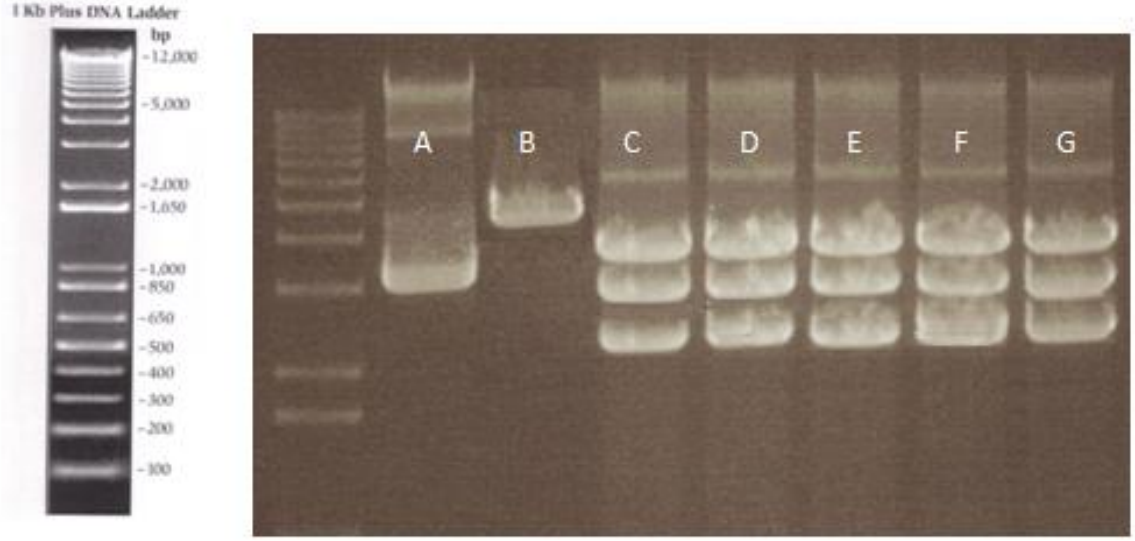

Figure 17. Digestion of pFC20K and pV2198 with *Eco*RI and *Xba*I. Undigested pFC20K (HaLoTag 7) T7 SP6 Flexi Vector is found in Lane A. Both pFC20K (B) and PV2198(C-G) are digested with *EcoR*I and *Xba*I in order to insert the 2.1kb *ermF-ermAM* into the pFC20K vector. PV2198 is digested into 3 fragments . The bottom fragment contains *ermF-ermAM*. The 2.1kb *ermF-ermAM* is inserted into pFC20K downstream of tagging regions between nucleotides 1398-1509.

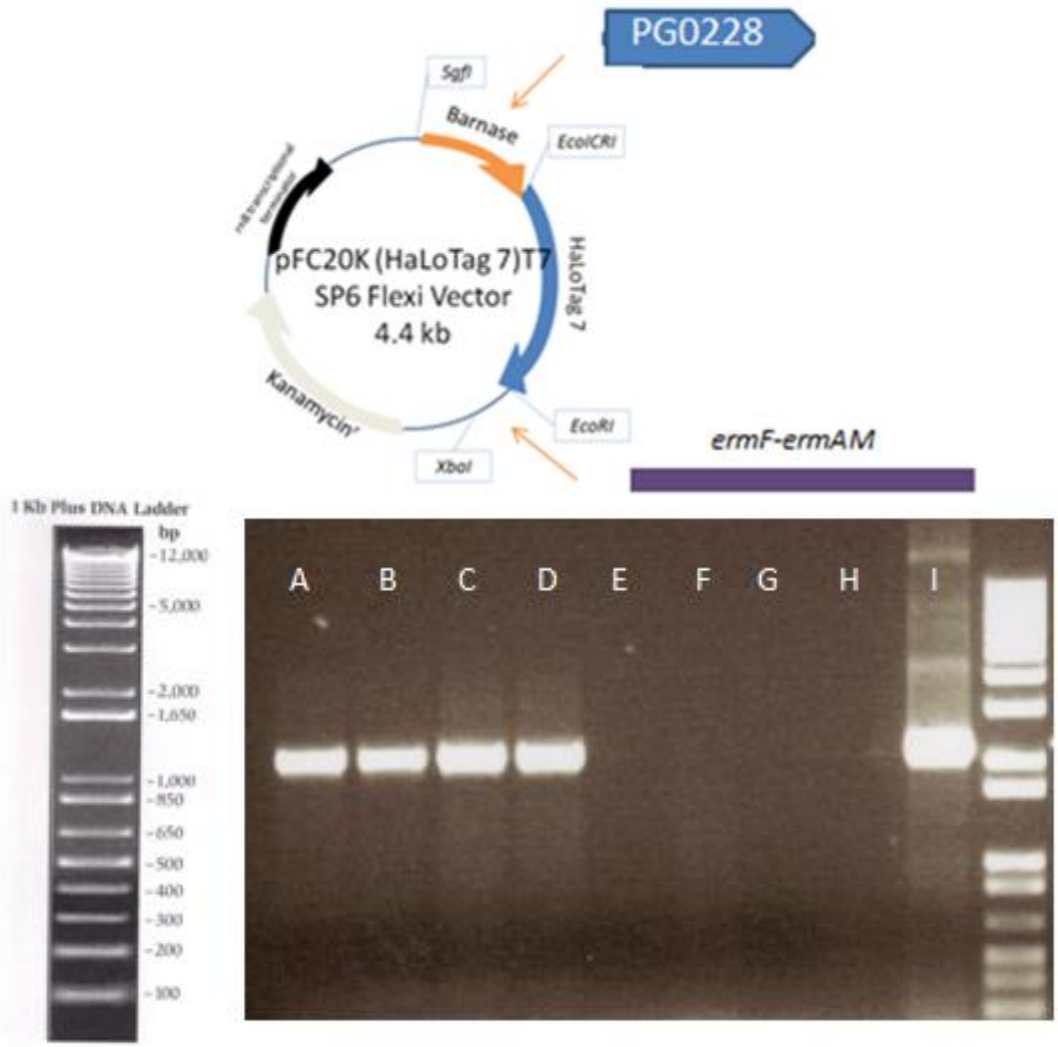

Figure 18. Transformation Colony Screening. Agarose gel confirming the insertion of *ermF-ermAM* into vector by PCR using primers FP-Erm/RP-Erm. pFC20K plasmids were isolated from *E. coli* colonies grown on LB plates supplemented with kanamycin and x-gal. Four colonies(A-D) show the transformation of DNA construct including *ermF-ermAM* 2.1kb insert. Lane I contains pV2198 also amplified with primers FP-Erm/RP-Erm as a control.

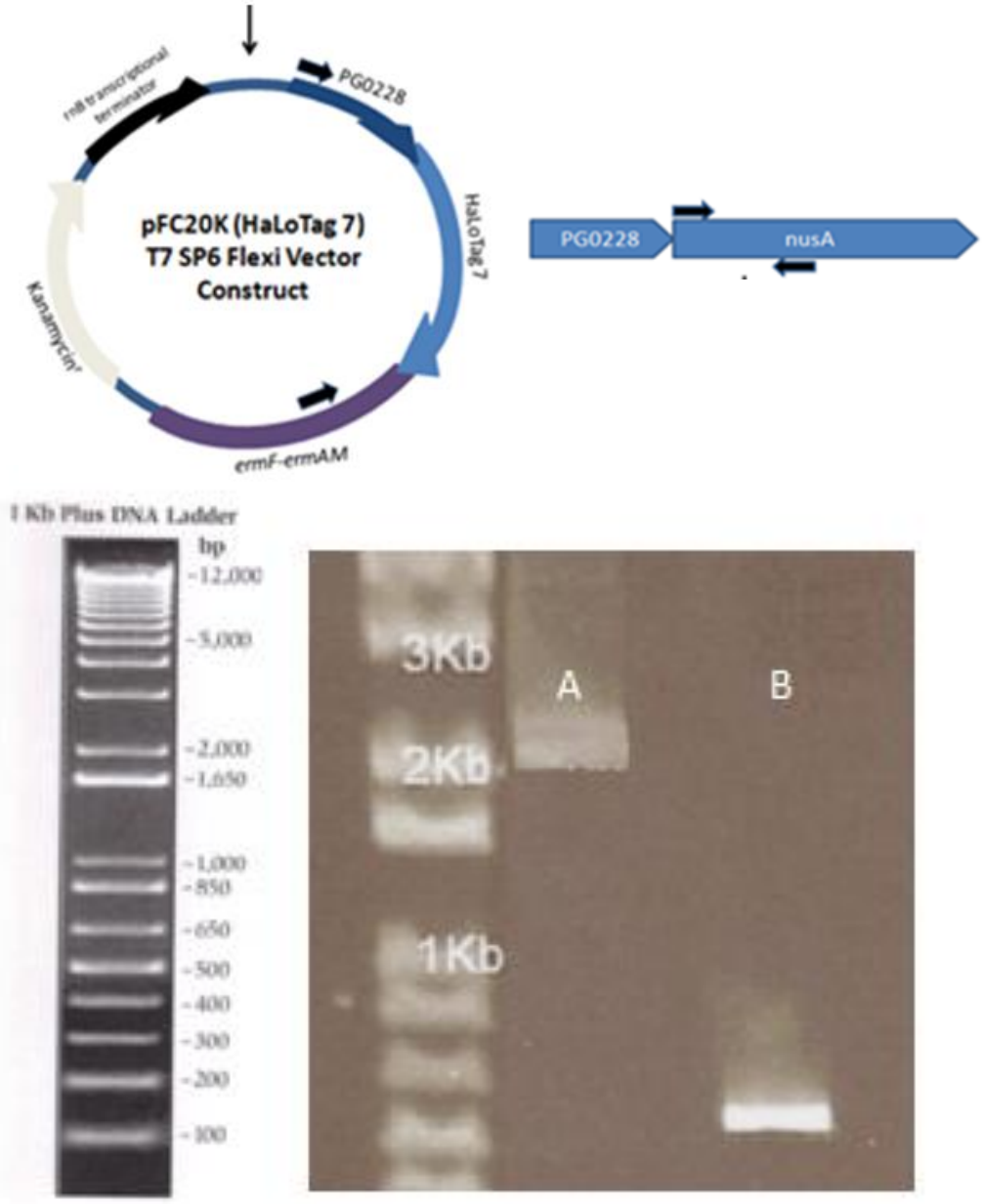

Figure 19. Amplification of the Mutant Construct Containing PG0228, HaLoTag, and *ermF* (A) and 5'*nusA* Extension (B). The mutant construct containing PG0228, HaLoTag, and *ermF* (2.5kb) was amplified using primers CF2/ermR2. The *nusA* extension (600bp) was amplified using primers ExtF/ExtR. Only *ermF* was amplified from *ermF-ermAM* cassette because fusion PCR methods tend to have a higher incidence of nonspecific amplification with longer DNA fragments.

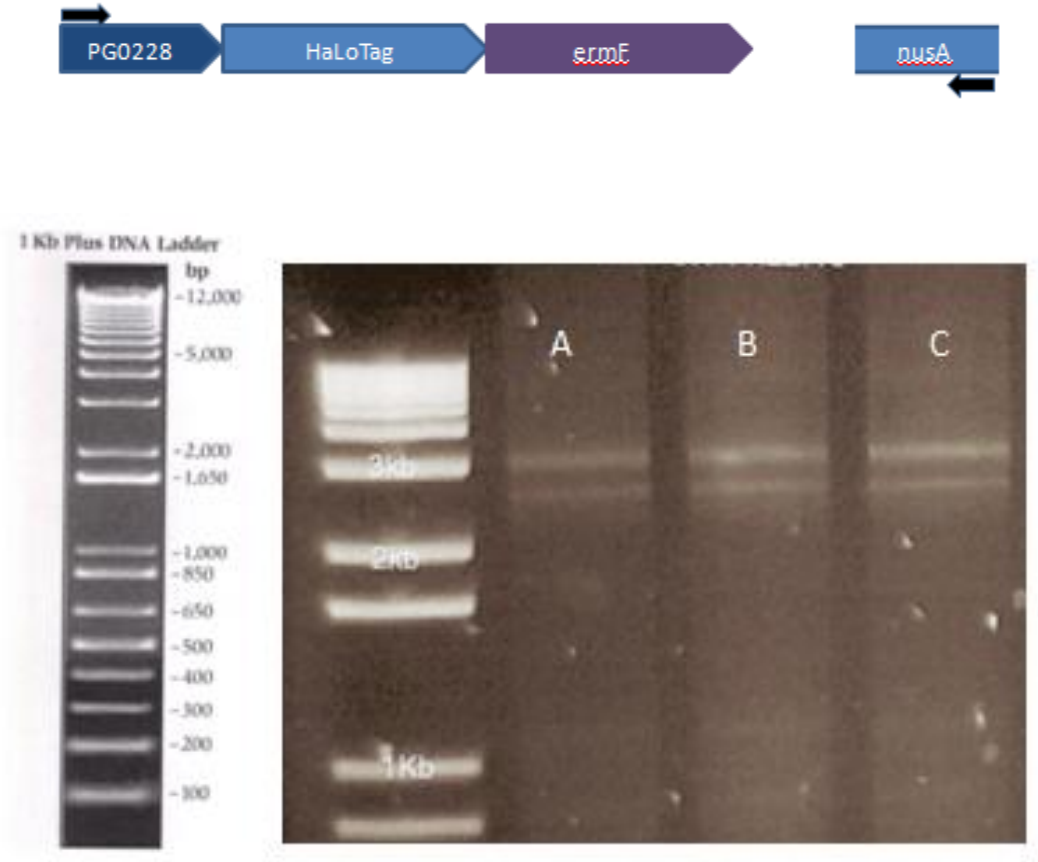

Figure 20. Annealing 0228-HaLo Construct to *nusA* Extension Using Fusion PCR methods. An agarose gel shows the amplification of a 3kb band using the primers CF/ExtR. The 5' segment (600bp) of *nusA* was added to ensure a double cross-over into W83 genomic DNA. Individually, the mutant construct containing PG0228, HaLoTag, and *ermF* equals a length of 2.5kb, while the *nusA* extension measures a length of 600 base pairs. When annealed together, the final product, 0228-HaLo DNA fragment, measures a length of around 3.1kb. This 0228-HaLo DNA fragment is then electroporated into *P. gingivalis* to obtain the 0228-HaLo strain.

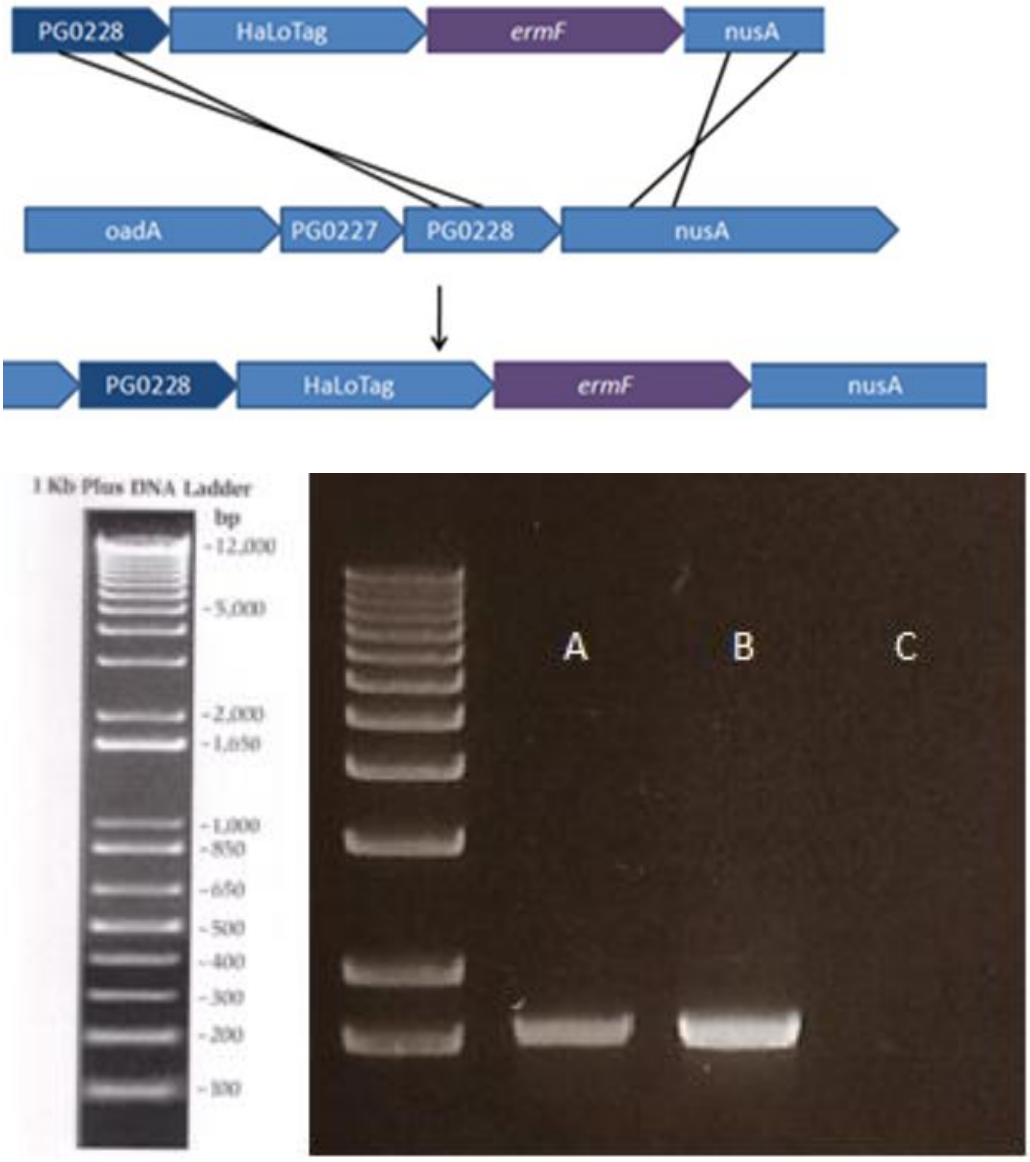

Figure 21. PCR Confirmation of 0228-HaLo Strain. Electroporation into *P. gingivalis* was done to obtain the 0228-HaLo strain. *P. gingivalis* colonies were selected for mutant selection and plated onto both clindamycin and blood agar plates and their genomic DNA isolated. 0228-HaLo strain (A), pCR2.1-TOPO vector containing 0228-HaLo mutant DNA fragment (B), and W83 genomic DNA were amplified using primers FP-Erm/ExtR. Wild type W83 and sequenced plasmid were used as a control to select for mutants. Both the mutant strain (A) and plasmid (B) contain the 1.5kb amplification of *ermF*-5' *nusA,* however, no amplification was found using FP-Erm/ExtR primers on W83 because W83 does not contain *ermF*.

3.4. Evaluation of Δ0228 Growth Compared to Wild Type W83

A growth study was done to assess the growth of the Δ0228 mutant strain compared to the W83 wild type. Overnight cultures of both strains were diluted to an optical density of 0.1 in BHI + hemin media. Both W83 and Δ0228 were grown in triplicates. The growth was measured for 24hrs in 4hr increments (8hrs for the 16-24hr time block).

Table 2 contains OD recordings for WT and Δ0228. Six time points were taken from both triplicates equaling 36 data points. There were no optical densities taken at the 20hr incubation time point. According to these data, the growth rate of Δ0228 strain is comparable to W83 for the first 8-10 hrs of incubation which is the log phase of bacterial growth for these strains. The mutant bacteria, however, enters stationary phase, indicated by the loss of slope on the graph, at an earlier time point than W83. The overall density of the mutant strain peaks at 12hrs with an OD of 0.831 average for the triplicate while W83 has not yet shown entrance into stationary phase at 24hrs. At 24hrs after dilution, the average optical density of Δ0228 strain is 0.775. The average optical density of W83 is higher at 1.184 24hrs after dilution. The growth study was repeated with data measured in 2hr and 5hr increments. The data from both studies mirror data points given in this study with 4hr increments and thus confirms that the observation is biologically consistent.

Table 2.

(a) Optical Density of Δ0228 Compared to W83 at Specific Incubation Periods.

	0hrs	4hrs	8hrs	12hrs	16hrs	20hrs	24hrs
W83 (1)	0.098	0.32	0.561	1.007	1.158	N/A	1.247
W83 (2)	0.095	0.321	0.552	0.983	1.149	N/A	1.185
W83 (3)	0.133	0.331	0.551	0.964	1.161	N/A	1.121
Δ0228 (1)	0.135	0.517	0.719	0.825	0.821	N/A	0.768
Δ0228 (2)	0.131	0.519	0.695	0.844	0.823	N/A	0.791
Δ0228 (3)	0.108	0.489	0.701	0.824	0.822	N/A	0.766

(b) Average Optical Density of Triplicate.

W83	0.109	0.324	0.555	0.985	1.156	N/A	1.184
Δ0228	0.125	0.508	0.705	0.831	0.822	N/A	0.775

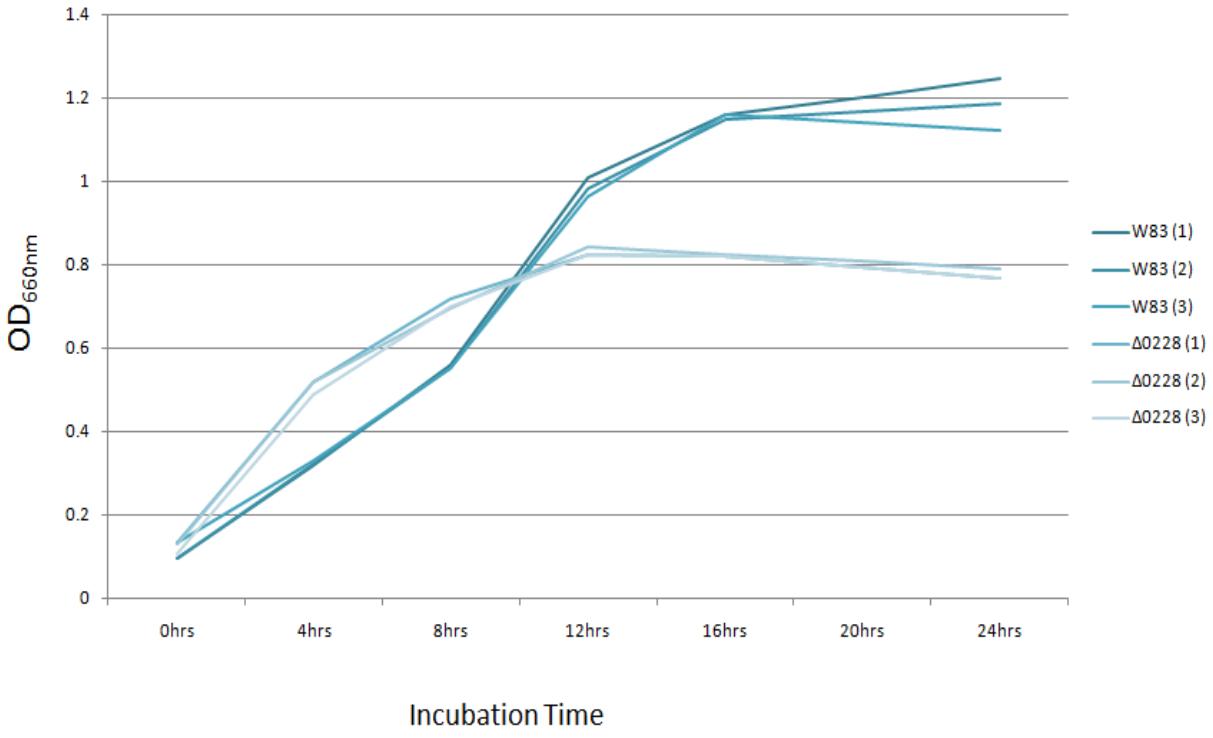

Figure 22. Growth Rate of Δ0228 Mutant Strain. This figure reveals the growth rate of the Δ0228 mutant strain compared to its wild type. The mutant strain lacks PG0228. Both strains are grown in identical conditions and at the same time. Optical densities were taken by a spectrophotometer at a wavelength of 660nm at 4hr time points. The strains were observed for 24hrs for final density measurements. **(a)** Strains were grown in triplicates and optical densities **(b)** and their averages were recorded. Optical densities of triplicates were then plotted out on a graph for better visual representation. No recordings were taken at 20hrs post dilution.

3.5. Differential Gene Expression Determined Using Microarray Analysis

The Δ0228 strain was further studied for differential gene expression using microarray analysis. To gain a better insight into whether PG0228 plays a role in gene regulation, expression profiles of the mutant were compared to wild type. Both W83 and Δ0228 were grown to an OD_{660} of 0.5 under the same conditions and harvested simultaneously. Overnight cultures were diluted to an OD_{660} measurement of 0.2 and allowed to grow to an OD measurement of 0.5. Final OD values of both strains were within 0.07 of each other before harvesting. Previous growth studies revealed the Δ0228 strain grows at the same rate as W83 until the mutant reaches early stationary phase around an OD of 0.7. Thus, both strains were used at their logarithmic phase of growth for microarray analysis. Also, their growth rates were the same thus excluding any effects of growth rate on the array results.

Differentially labeled cDNA from W83 (635nm) and Δ0228 (532nm) were combined and used to hybridize to glass slides containing probes for all genes present on the genome of *P. gingivalis* W83 strain. The quantity of each hybridized label to gene probe was detected with an Axon4200 scanner. Data from signal detection was processed for statistical significance using ArrayAssist software (Stratagene).

Each gene present on the W83 genome had 5 probes on the glass slide, thus 5 measurements were made for each *P. gingivalis* gene. Statistical analysis was taken from 4 probes and averaged. 19 genes were found significantly upregulated (Table 3), and 60 genes were found significantly downregulated (Table 4) in the Δ0228 mutant strain compared to W83. Each gene selected had an average fold change of close to 2 or higher (1.6 < ratio 635/532 <

0.56). Only genes with 4 consistent upregulated or downregulated ratios were included and averaged.

Of the 19 upregulated genes detected by microarray, 16 had an average fold change of greater than 2. 3 of these genes, PG007, PG1133, PG1185 are hypothetical proteins and therefore their function is unknown. Other upregulated genes include those encoding proteins involved in metabolism including PG0195 (rubrerythrin), PG1421, PG1813, and PG1190 (glycerate dehydrogenase): all involved in electron transport during oxidative stress.

Of the 60 downregulated genes detected by microarray, 50 had an average fold change of greater than 2. Downregulated PG1294 (ferrous iron transport protein B), PG1551 (hmuY protein), and PG1552 (TonB-dependent receptor hmuR) are all involved in iron uptake. Fifteen of these detected downregulated targets include enzymes and 28 hypothetical proteins.

Table 3. Upregulated Genes Detected in Δ0228 Strain.

Primary Target	Common Name of Primary Target	Gene Symbol	Ratio (635/532)
PG0007	hypothetical protein		**0.49**
PG0079	abortive Infection protein, putative		**0.44**
PG0152	carboxynorspermidine decarboxylase	***nspC***	**0.49**
PG0195	rubrerythrin		**0.34**
PG0548	pyruvate ferredoxin/flavodoxin oxidoreductase family protein		**0.47**
PG0651	HDIG domain-containing protein		**0.44**
PG0682	ABC transporter, permease protein, putative		**0.32**
PG1048	N-acetylmuramoyl-L-alanine amidase		**0.45**
PG1049	ABC transporter, permease protein, putative		**0.33**
PG1133	Hypothetical protein		**0.47**
PG1185	Hypothetical protein		**0.46**
PG1190	glycerate dehydrogenase	***hprA***	**0.48**
PG1239	3-oxoacyl-(acyl-carrier-protein) reductase	***fabG***	**0.37**
PG1421	ferredoxin, 4Fe-4S		**0.14**
PG1687	HIT family protein		**0.40**
PG1688	transcription elongation factor GreA	***greA***	**0.35**
PG1765	acyl carrier protein	***acpP***	**0.53**
PG1813	ferredoxin, 4Fe-4S		**0.56**
PG1956	4-hydroxybutyrate CoA-transferase	***abfT-2***	**0.51**

Table 4. Downgulated genes detected in Δ0228 strain.

Primary Target	Common Name of Primary Target	Gene Symbol	Ratio (635/532)
PG0253	Hypothetical protein		5.06
PG0258	ABC transporter, ATP-binding protein		2.32
PG0437	BexD/CtrA/VexA family polysaccharide export protein		2.22
PG0451	CBS domain-containing protein		2.01
PG0495	Hypothetical protein		3.34
PG0613	Hypothetical protein		2.59
PG0768	Hypothetical protein		4.25
PG0805	Prolipoprotein diacylglyceryl transferase	*igt*	2.83
PG0838	Integrase		2.38
PG0854	Hypothetical protein		11.57
PG0855	Hypothetical protein		3.06
PG0933	Elongation factor G		2.66
PG0972	Hypothetical protein		2.91
PG0987	Hypothetical protein		1.98
PG1021	Hypothetical protein		1.99
PG1029	Hypothetical protein		2.52
PG1036	Excinuclease ABC, A subunit	*uvrA-1*	2.45
PG1040	Transcriptional regulator, putative		8.03
PG1077	Electron transfer flavoprotein, beta subunit	*etfB-2*	1.92
PG1107	Hypothetical protein		4.45
PG1110	Hypothetical protein		1.80

Primary Target	Common Name of Primary Target	Gene Symbol	Ratio (635/532)
PG1128	Exodeoxyribonuclease VII large subunit	*xseA*	3.05
PG1138	Pigmentation and extracellular proteinase regulator	*porR*	1.60
PG1155	ADP-heptose--LPS heptosyltransferase, putative		3.09
PG1175	ABC transporter, ATP-binding protein, putative		1.92
PG1178	Hypothetical protein		7.24
PG1179	Hypothetical protein		2.27
PG1180	Hypothetical protein		5.02
PG1181	TetR family transcriptional regulator		2.45
PG1184	Alginate O-acetyltransferase, putative		1.88
PG1229	Hypothetical protein		4.07
PG1230	Hypothetical protein		2.81
PG1294	Ferrous iron transport protein B	*feoB-2*	2.12
PG1395	Rod shape-determining protein MreC		11.22
PG1473	Conjugative transposon protein TraQ		1.97
PG1484	Hypothetical protein		2.24
PG1513	Phosphoribosyltransferase, putative/phosphoglycerate mutase family protein		1.89
PG1525	Isochorismate synthase, putative		2.49
PG1528	Hypothetical protein		4.26
PG1551	HmuY protein	*hmuY*	7.29

Primary Target	Common Name of Primary Target	Gene Symbol	Ratio (635/532)
PG1552	TonB-dependent receptor HmuR	*hmuR*	7.13
PG1554	Hypothetical protein		4.12
PG1570	Rhodanese-like domain-containing protein		11.26
PG1662	Hypothetical protein		2.51
PG1666	RND family efflux transporter MFP subunit		1.82
PG1679	Hypothetical protein		2.97
PG1733	Hypothetical protein		3.78
PG1814	DNA primase	*dnaG*	2.17
PG1842	Acetyltransferase		2.47
PG1858	Flavodoxin FldA		9.15
PG1892	Hypothetical protein		2.19
PG2043	Hypothetical protein		2.51
PG2061	Dihydrofolate reductase	*folA*	8.10
PG2070	Hypothetical protein		2.55
PG2071	Hypothetical protein		2.72
PG2081	Biotin synthetase	*bioB*	6.96
PG2102	Immunoreactive 61 kDa antigen PG91		2.01
PG2103	Hypothetical protein		2.08
PG2171	D-isomer specific 2-hydroxyacid dehydrogenase family protein		3.45
PG2189	Aspartate kinase	*lysC*	2.18

Table 5. Transcription Profile of *nusA,* locus located downstream of PG0228.

Primary Target		Common Name of Primary Target	Gene Symbol	Ratio (635/532)
PG0229		**Transcription elongation factor nusA**	**nusA**	
P#	**1**	**Transcription elongation factor**	***nusA***	**0.87**
P#	**2**	**Transcription elongation factor**	***nusA***	**1.02**
P#	**3**	**Transcription elongation factor**	***nusA***	**1.02**
P#	**4**	**Transcription elongation factor**	***nusA***	**1.03**
Average		**Transcription elongation factor**	***nusA***	**0.98**

Table 6. Transcription Profile of LuxR transcriptional regulator.

Primary Target		Common Name of Primary Target	Gene Symbol	Ratio (635/532)
PG1237		LuxR Family Transcriptional Regulator	luxR	
P#	1	LuxR Family Transcriptional Regulator	*luxR*	0.73
P#	2	LuxR Family Transcriptional Regulator	*luxR*	1.09
P#	3	LuxR Family Transcriptional Regulator	*luxR*	1.02
P#	4	LuxR Family Transcriptinoal Regulator	*luxR*	1.12
Average		LuxR Family Transcriptional Regulator	*luxR*	0.99

Table 7. Transcription Profile of *luxS*

Primary Target		Common Name of Primary Target	Gene Symbol	Ratio (635/532)
PG0498		**Ribosylhomocysteinase**	**luxS**	
P#	**1**	**Ribosylhomocysteinase**	***luxS***	**1.25**
P#	**2**	**Ribosylhomocysteinase**	***luxS***	**1.34**
P#	**3**	**Ribosylhomocysteinase**	***luxS***	**1.35**
P#	**4**	**Ribosylhomocysteinase**	***luxS***	**1.35**
Average		**Ribosylhomocysteinase**	***luxS***	**1.32**

3.6. Analysis of Δ0228's Ability to Survive with Host Cells

A survival was done with Δ0228 to analyze its ability to handle changes in environment. In order to expose the strains to host environmental conditions, bacteria were introduced to HN4 epithelial cells at a 100:1 MOI. Δ0228 and W83 cultures were grown to an OD_{660nm} of about 0.5 to ensure cells were in log phase (Figure 23). It is important to note there has been no evidence of changes in epithelial invasion rate between the two strains. Thus, the number of invading bacteria into the HN4 cells is theoretically identical. Studies have shown a small percentage of W83 bacteria will invade the HN4 cell if introduced. 4×10^5 HN4 cells are infected at a 100:1 MOI in triplicates, resulting in 6 HN4 wells. In order to evaluate only the bacteria inside the epithelial cells, the HN4 cells were incubated with an antibiotic to kill extracellular bacteria. Therefore, only bacteria inside the HN4 cells are analyzed. After the 30 minute infection, the HN4 cells are lysed. The lysate containing the invading bacteria is plated at a 1:4 and 1:10 dilution on BHI + He plates. Seven-to-ten days later, viable colonies are counted. Table 8 represents the number of colonies of each strain after incubation period.

The number of resulting Δ0228 colonies after incubation period ranged from 0-6 from the 1:4 dilutions, and ranged between 0-2 from the 1:10 dilutions. The number of resulting W83 colonies was significantly higher ranging from 4-94 from the 1:4 dilutions and 0-35 from the 1:10 dilutions. 2.3 (Δ0228) and 40.7 (W83) are the average number of colonies appearing on the BHI + hemin plates from the 1:4 dilutions (Figure 25).

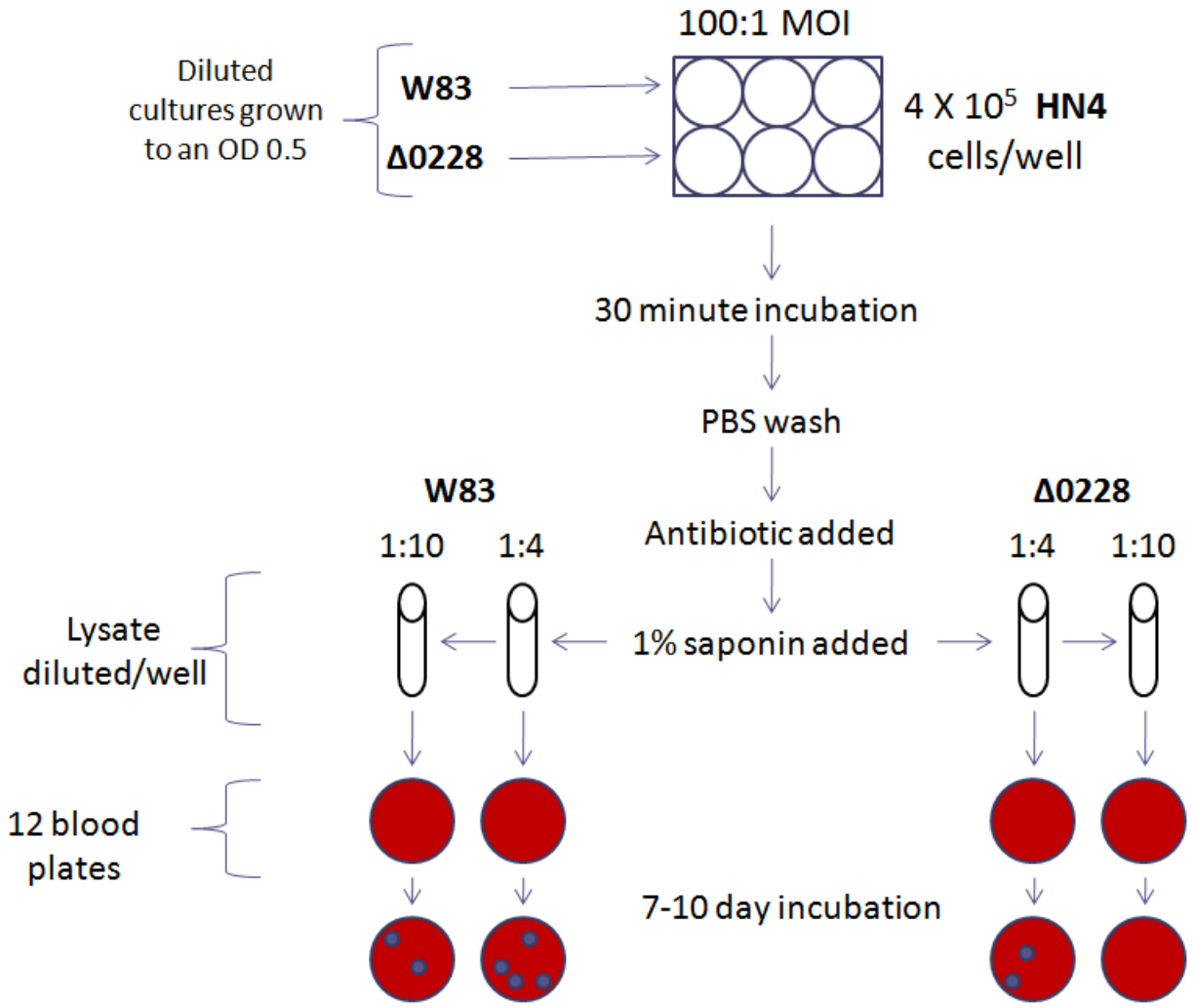

Figure 23. Survival Schematic. This figure demonstrates a simplistic protocol of the survival study done with HN4 cells.

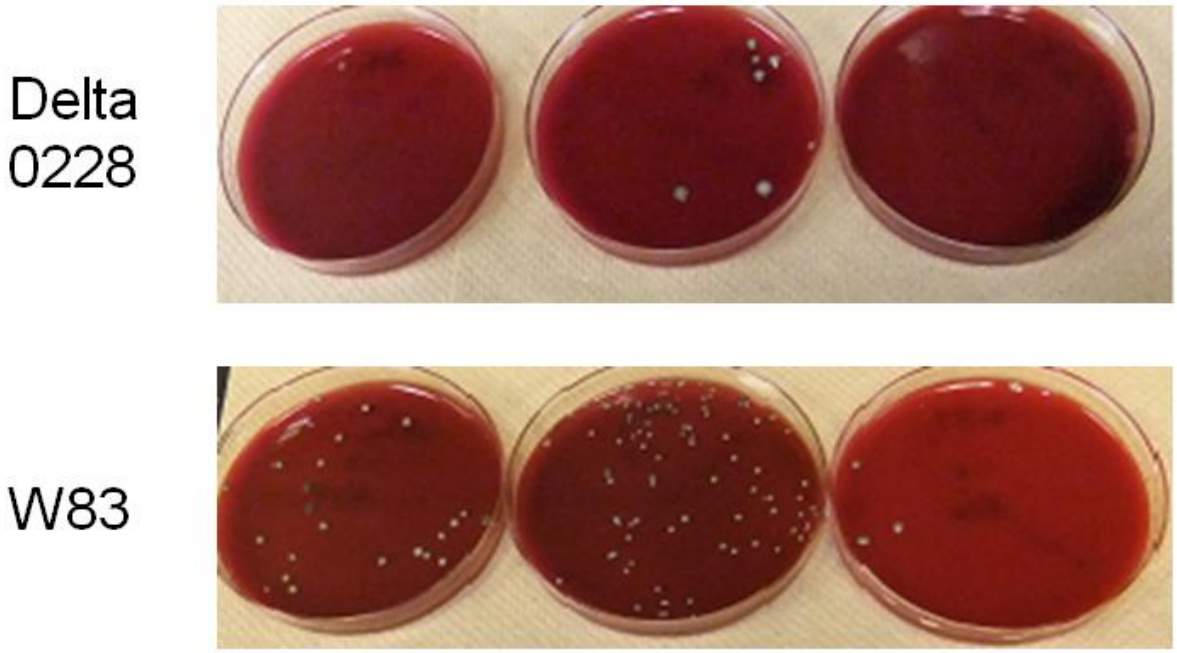

Figure 24. Photo of Δ0228 and W83 Colonies for Survival Study. A survival study was completed to analyze any changes in sensitivity to host defense mechanisms compared to W83. Photo represents the differences in viability between the two strains post epithelial invasion. The top photo is the Δ0228 strain seven days after invasion. The bottom photo is the W83 strain seven days after invasion.

Strain	Dilution	# of Colonies
Δ0228a	1:4	**1**
Δ0228b	1:4	**6**
Δ0228c	1:4	**0**
Δ0228a	1:10	**0**
Δ0228b	1:10	**2**
Δ0228c	1:10	**0**
W83a	1:4	**24**
W83b	1:4	**94**
W83c	1:4	**4**
W83a	1:10	**2**
W83b	1:10	**35**
W83c	1:10	**0**

Strain	Dilution	Range	Average # of Colonies
Δ0228	1:4	0-6	2.3
W83	1:4	4-94	40.7
Δ0228	1:10	0-2	0.67
W83	1:10	0-35	12.3

Table 8. The number of colonies found on the blood agar plates after HN4 invasion. 4 X 10^5 HN4 cells are infected at a 100:1 MOI in triplicates. Invading bacteria is plated at a 1:4 and 1:10 dilution on BHI + He plates. Seven-to-ten days later, viable colonies are counted.

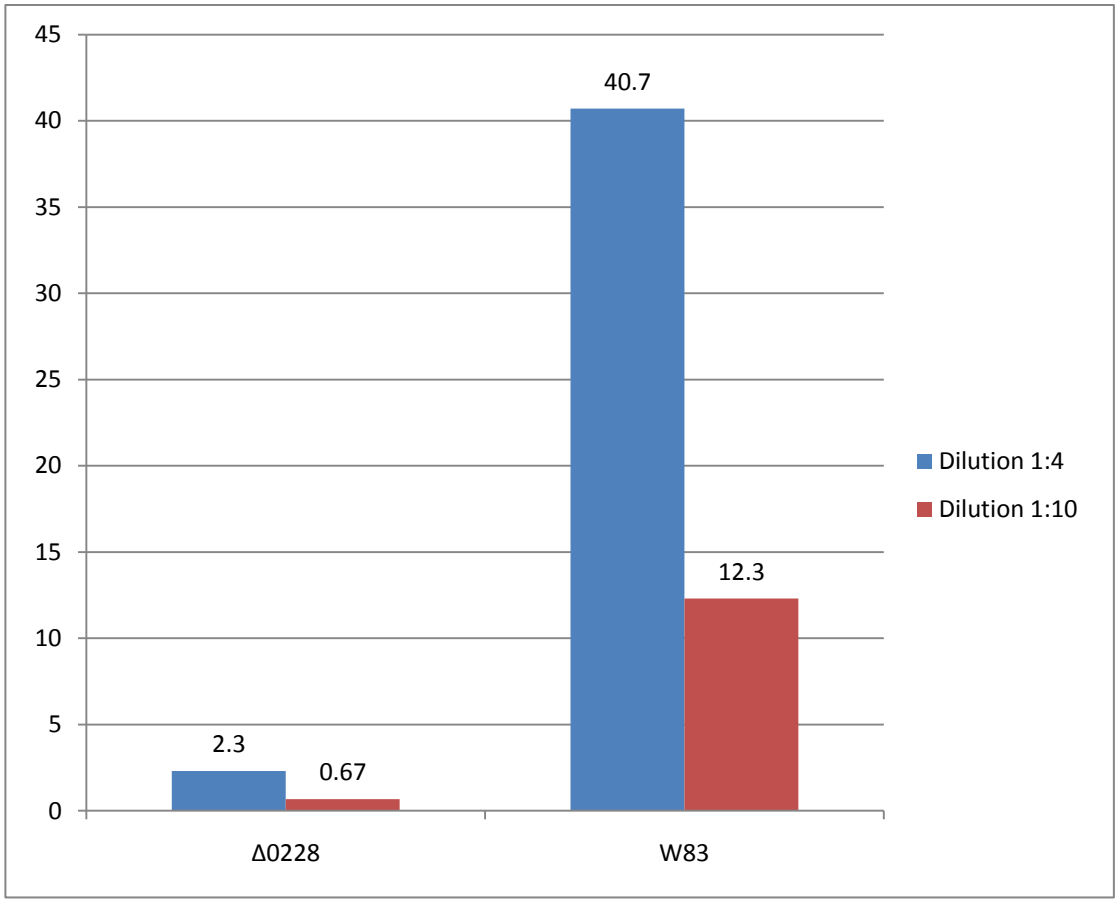

Figure 25. Survival Data. Average number of colonies appearing on the BHI + hemin plates from both 1:10 and 1:4 dilutions from Survival

Chapter 4: DISCUSSION

4.1. Δ0228 Strain

Several steps were completed to ensure that Δ0228 was engineered correctly. General PCR methods were first used to produce individual desired fragments. By amplifying specific segments of W83 genomic DNA surrounding our gene of interest, we were able to manipulate the sequencing within the gene. This amplified DNA surrounding the gene of interest still allowed for easy integration back into the W83 genome, but it gives the added advantage of deleting or adding fragments between the crossover segments.

Flanking DNA fragments were amplified using primers Mut1F and Mut1R and with Mut2F and Mut2R. Mut1R and Mut2F, for instance, were designed so that the amplification produces fragments with tails that have the same identity as the ends of the *ermF* cassette. The Mut1 and Mut2 fragments and the pre-amplified *ermF* cassette are then annealed together through fusion PCR by Mut1F and Mut2R primers. Numerous fusion PCR attempts were made before our fragment was amplified. Because the final length of our fragment was over 2 kb and we were attempting to anneal 3 segments together, troubleshooting with different annealing temperatures, extension times, and enzyme concentrations were needed until one combination amplified the DNA fragment.

It is important to verify each step of this process to make sure the DNA is indeed being amplified, it is the right length, and finally, it is the desired fragment. Figure 12 (a) confirms the individual DNA fragments are the correct length and (b) confirms the fusion PCR amplified a fragment that matches our desired length. Although it is highly unlikely these specific primers amplified a different fragment coincidently the exact same length, the fragment was sequenced to confirm correct sequencing.

Before the fragment was sequenced, it was cloned into the TOPO-TA Vector. This was done because the DNA fragment is significantly more stable when ligated to a vector for storage. Once the DNA fragment was sequenced it still needed to be integrated into the W83 genome in order to generate a mutant strain. Generating a mutant strain allows observation of many factors, including changes in phenotype and gene expression, not possible to see by looking at the fragment at the molecular level alone. The fragment was therefore electroporated into *P. gingivalis* W83 for transformation. Mutant screening was verified by PCR amplification and genomic DNA sequencing. Screening with the original Mut1F and Mut2R primers (Figure 15) on the potential mutants and W83 will produce a longer fragment in mutant by 0.5kb if integration has occurred. Even though the mutant fragment has the 456bp PG0228 removed, it has the 1kb *ermF* antibiotic resistance cassette inserted in its place. Therefore, the addition of the cassette in the mutant produces a 2.1kb fragment while W83 produces a 1.6kb fragment, as demonstrated by the agarose gel on Figures 14 and 15.

4.2. Differential Gene Expression

Microarray analysis establishes differential gene expression between Δ0228 and W83 strains, demonstrating that PG0228 plays a significant role in gene regulation in *Porphyromonas gingivalis*. It is uncertain to say, however, what the mechanism of this regulation is. Of the 2,227 loci analyzed, close to 5% of genes were found to have a fold change of near 2 or above in abundance of RNA transcripts ($1.6 < \text{ratio } 635/532 < 0.56$). Our array has 5 probes which serve as technical replicates and are used to confirm accuracy of array hybridization. For our work, only genes with 4 consistently detected regulated ratios were included and averaged. More than 100 additional genes showed an average fold change of 2 or higher from 3 of the 5 probes, but are not included in the table and their differential expression will need to be confirmed by additional array hybridization or other experimental approaches. However, the high level of regulation of those genes does suggest they are regulated, and if accounted for, the number of genes differentially expressed between the mutant and the parental strain would be approximately 15% of total genes present on the genome.

Bacterial cells for microarray analysis were taken during log phase (OD 0.5) and higher Hfq levels were recorded during stationary phase compared to log phase in other bacterial species[103]. From this, one can infer if levels of Hfq are higher during times of slow growth, their effects on gene regulation would be more prominent as well. Therefore, if analysis of differential expression during early stationary phase was done in addition to log phase we could compare the two levels of PG0228 and overall changes in regulation gaining a better insight

into PG0228's overall role. Such studies were not possible for the current time frame but are planned for the future.

According to the transcriptional profile, the transcription of the downstream gene from PG0228, *nusA*, was not altered, indicating the observed changes in mRNA levels were from global regulation of PG0228 and not due to polar effect of the mutation which would lead to altered function of *nusA* (see Table 4). If PG0228 and PG0229 (*nusA*) were co-transcribed, some of the changes observed in regulation could have been due to abrogation of the *nusA* transcription, however our results show that this was not the case and thus the changes in transcriptional profile we see are due to deletion of PG0228.

As previously stated, Hfq is considered to act as a key global regulator of gene expression and facilitate sRNA regulation on target mRNA[56;83]. This therefore, creates a cascade of gene regulation from changes in Hfq which affects sRNA which affects target mRNA. Small RNAs can downregulate target protein levels[106] and positively affect ribosomal binding to mRNA targets causing translation [35;54;101]. Furthermore, sRNAs can regulate one or multiple target genes while simultaneously being regulated by Hfq or transcription factors [54;65;97] further complicating regulation. Many sRNAs are *trans*-encoded, and thus, are not physically linked to their target mRNAs on the genome. In addition, most of these *trans*-encoded sRNAs require Hfq for optimum function[98]. It is likely the changes in transcript levels of the hypothetical proteins and others are due to inefficient *trans*-encoded sRNA function because PG0228's lack of facilitation.

It is also important to recall, Hfq can act alone to regulate gene expression by influencing polyadenylation or translation of mRNA[98]. This demonstrates Hfq's direct gene regulation and therefore some genes regulated in Δ0228 could be attributed to PG0228's direct regulation.

sRNAs play a key role in regulating their mRNA targets by influencing translation or mRNA stability. These sRNAs may be involved in numerous cellular processes including cell development, growth, differentiation, and death by turning genes on and off[1;16;46]. Of the 79 regulated genes found from microarray analysis, 31 were hypothetical proteins, and as a result, it is impossible to know their function at this time.

Among genes encoding protein of known functions were haemin-uptake encoding genes *(hmu*YR*). P. gingivalis* requires haemin for growth and as a major source of iron. High levels of haemin are found within humans, though it is bound to proteins and not freely available[52]. Gram-negative pathogenic bacteria, including *P. gingivalis*, have developed mechanisms for scavenging iron from haemin bound to proteins within their host[34]. Several studies show the heamin-uptake mechanisms are organized into operons inside *P. gingivalis* ensuring these genes are regulated by one regulator[52;84]. Two *P. gingivalis* genes detected to be downregulated (over 7-fold) in the Δ0228 strain include PG1551 (encoding HmuY) and PG1552 (encoding HmuR). Both of these proteins are involved in haemin-uptake and are co-transcribed. The genomic locus transcribing *hmu*Y and *hmu*R contains six genes (*hmu*YRSTUV), each most likely encoding proteins involved in sequestering haemin[52;107]. Downstream products of the operon, *hmu*STUV, are labeled PG1553 thru PG1556. Due to the fact PG1554

(*hmu*T) is encoded downstream of *hmu*YR and these six genes are located on an operon, it is assumed the transcripts *hmu*S is also downregulated in the Δ0228 strain.

In times when iron is abundant, HmuY and HmuR are repressed, and when iron levels are low (as in dental plaque), the level of HmuY is high[70]. Consequently, the expression of these proteins must be regulated. PG1237, the LuxR family transcriptional regulator, was found to be required for the expression of *hmu*Y and *hmu*R [107] and studies show PG0498, LuxS, also controls the expression of genes involved in haemin uptake[19;45]. However, no changes in transcription were found in *lux*R or *lux*S according to our microarray analysis (see Table 5 and 6). Both the Δ0228 and W83 were grown in the same conditions (see section 2.8.) so the low levels of *hmu*Y and *hmu*R found in Δ0228 strain could not be attributed an abundance of iron. These data would indicate the regulation of these haemin sequestering proteins is more complex and involves more players other than LuxR and LuxS. We have shown transcript levels of *hmu*YRST are lower in the Δ0228 strain however, this is not due to a downregulation of *lux*R or *lux*S, thus the change is from a lack of PG0228, not from altered levels of *lux*R or *lux*S. This suggests PG0228 plays a role in the regulation of haemin-uptake mechanisms.

Another gene upregulated in our study in the PG0228 deficient mutant encodes rubrerythrin. Rubrerythrin is a non-haem iron protein involved in the protection from reactive oxygen species (ROS) and oxidative stress[53;87]. The protein is upregulated in several anaerobic bacteria, including *P. gingivalis,* during oxidative stress[67;74;92]. It is suggested rubrerythrin acts as a catalyst reducing intracellular hydrogen peroxide levels[92]. Interestingly, our data showed rubrerythrin (PG0195) to be upregulated in the Δ0228 strain. Microarray

analysis also showed upregulation of loci PG1421 and PG1813, both of which encode ferredoxins. Ferredoxins are a group of small iron-sulfur proteins involved in electron transfer[23]. Enzymes catalyze the exchange of electrons between electron carriers such as ferredoxins therefore serving as antioxidants during oxidative stress. The transcrpt level of one such enzyme, encoded by PG0548, part of the ferredoxin oxidoreductase family, was also upregulated in the Δ0228 strain. In addition, a previous study subjecting *P. gingivalis* to 6% oxygen also showed downregulation of the *hmu* locus [51] like we have seen for Δ0228. These indicate genes encoding proteins that play a role in protection from oxidative stress were upregulated. A bacterium's resistance to oxidative stress is affected by Hfq but its mechanism is still not understood[88]. Mutants deficient in *hfq* show increased oxidation of carbon levels, lowered tolerance to reactive nitrogen species (RNS), and reactive oxygen species (ROS)([88;97]. The upregulation of rubrerythrin, ferredoxins, and ferredoxin oxidorecuctase indicates that the Δ0228 strain has deregulated oxidative stress mechanisms and further work is required to examine the role of the deregulation in growth of the bacterium with oxidative stress.

4.3. RNA Binding to PG0228

Genes, like those involved in haemin-uptake and oxidative stress, need to be quickly turned on and off to ensure the bacterium's survival. Small RNAs regulate stress responses, virulence, metabolism, and many other complex pathways[44;49;86]. However, little is known about these sRNAs in *P. gingivalis*, particularly which targets they regulate. It is suggested that less energy is expelled by the cell using sRNAs compared to synthesizing bulky regulatory

proteins in response to environmental stress[4]. Because these RNAs are small and untranslated, they are more cost effective thus allowing a fast response to external stimuli and fast recovery once the external stimulus is removed[82]. Most of these sRNAs require Hfq for optimum function, which is Hfq's most prominent function[86]. We have shown PG0228 is involved in gene regulation and has numerous similarities to Hfq. However, sRNAs are post-transcriptional regulators, thus information as regards changes in transcripts levels resulting from destabilization of the mRNA can be found by microarray analysis. Further work is required to examine the changes in P0228-deficient strain at protein level.

Hfq is a RNA chaperone, therefore, is often found bound to RNA. If it can be shown PG0228 also binds to RNA, it will strengthen the idea PG0228 is most likely an Hfq homologue. Furthermore, if the identity of these bound RNAs turns out to be known regulatory sRNAs found in *P. gingivalis*, it will further strengthen PG0228's Hfq candidacy. The protein needs to be crosslinked in vivo to any bound RNA and immunoprecipitated out. However, there is no known specific antibody to precipitate PG0228. Therefore, a new approach was needed. A tagged fusion protein approach was therefore used using basic concepts based on the ChIP assay (Promega). This added a 3' tag at the genomic level and would be expressed along with the protein. A specific resin from the company allows our specific tagged protein to be retrieved *in vivo* to study bound RNA. For the purpose of this study, the 0228-tagged fusion mutant was generated which included the 3' HaLoTag for the bound RNA study.

A reversible cross-linking combined with immunoprecipitation was done with the 0228-HaLo strain to study RNA-protein interactions *in vivo*. Cross-linking with formaldehyde allows

rapid preservation of interactions between the PG0228 protein and RNA. The cells are then lysed. A resin based ligand, the HaloLink Resin, covalently interacts with the 0228-*tagged* protein and is precipitated out. The cross-links are reversed using glycine and the RNA bound to the protein is isolated. A RNA library are then created and sent in for sequencing. We have not yet received the data from this study and therefore it is not yet included at this time.

4.4. Evaluation of Phenotypic Changes in Δ0228

As stated, no Hfq homologue has been identified in *Porphyromonas gingivalis*. However, it is highly likely *P. gingivalis* possesses an Hfq homologue due to the fact it has been encoded by nearly half of eubacteria, including pathogens and due to Hfq's importance as an overall RNA cofactor[18]. A deficiency in Hfq greatly impacts overall bacterial virulence and fitness. Luckily, several phenotypic studies can be done since deficient strains are still generally viable[18]. First deleted in *E. coli,* the *hfq* null mutant shows pleiotropic phenotypes, including decreased yields, increased cell size, osmosensitivity, and increased sensitivity of UV light[36;88;97].

Growth defects in broth or on plates are generally mild and include longer lag phase and overall lower final density in *B. abortus, E. coli, Francisella tularensis, Legionella pneumophila, Neisseria meningitides,* and *Pseudomonas aeruginosa* to name a few[18;25;57;58;75;80;85]. Although, there were no obvious growth defects found in Gram-positive bacteria, *Listeria monocytogenes* or *Staphylococcus aureus* [18]. As a result, a growth study was done on Δ0228 strain to view PG0228's effect on W83 growth.

Figure 22 is an observation of the mutant growth rate compared to W83. The final density of both strains is also compared after the 24hr incubation period. The growth study was repeated with data measured in 2hr and 5hr increments. The data from both studies mirror data points given in this study with 4hr increments and therefore were not included.

According to the results of the growth study done on Δ0228, the growth rate is comparable to W83 for the first 8-10 incubation hours during log phase. The mutant bacteria, however, enters stationary phase, indicated by the loss of slope on the graph, at an earlier time point than W83. These results match the data found in many *hfq* null mutants, again strengthening the idea that PG0228 is potentially an Hfq orthologue.

The environmental niche of *P. gingivalis* is within a biofilm consisting of several bacterial species and experiences changes including available nutrients, pH levels, temperature, and osmolarity [29;38]. In addition, virulent pathogens like *P. gingivalis* can invade and colonize within gingival epithelial cells [10;47] but virulence phenotypes of *hfq* mutants are highly noticeable in Gram-negative pathogens *B. abortus, Salmonella*, and *V. cholerae*, showing high attenuation in mouse infections[18]. For these reasons, a survival study was done to analyze the mutant's ability to handle instant changes in environment. This was done because *hfq* mutants often are not able to adjust to changes in their environment (as stated above) with an exception of *S. aureus hfq* mutants[12]. The bacteria were exposed to host cell environment to mimic conditions they encounter in the oral cavity and sub-gingival regions. Our results show there are no changes in invasion rates between the two strains of bacteria (data not shown), thus, the number of invading Δ0228 and W83 bacteria is assumed identical. To reduce the

number of potential variables, only the host invading bacteria are analyzed by removing attached and non-invading bacteria. This is done by treating the HN4 cells with antibiotic. As expected, the Δ0228 strain was not able to handle the added stresses it encountered including increased oxidation levels, changes in iron availability, and changes in acid levels. This is evidenced by the significantly lower number of colonies after the incubation period following the host invasion (Table 8). This result again reiterates the fact that, much like Hfq, PG0228 is instrumental during high stress conditions, including host invasion, when genes need to be turned on and off quickly in order for the bacterium to survive.

There are multiple other studies to be done such as the above-mentioned oxidative stress survival test or other tests that can be predicted based on the changes in transcriptional profile. Another guide will be results of differentially abundant proteins when comparing the parental and PG0228 mutant strains. Such studies are planned for the future.

4.5. Alternate Hypothesis

Although we hypothesize that PG0228 functions like Hfq, PG0228 does also have some sequence homology with the ribosome maturation factor, RimP. The *in vivo* maturation of the 50s and 30s ribosomal subunits requires auxiliary proteins that are not part of the mature ribosomes [69]. Originally found in *E. coli*, the RimP protein (formerly YhbC or P15a) is essential for the maturation of the 30S ribosomal subunit. Coincidently, both PG0228 and *rimP* loci are found upstream from *nusA*. However, *rimP* is co-transcribed with *nusA* and *infB* in *E. coli[69]*. According to our microarray results, there was no gene regulation of the downstream *nusA* in the Δ0228 strain. This indicates PG0228 is not co-transcribed with its downstream *nusA* in

W83, and therefore it is unlikely PG0228 is *rimP*. However, PG0228 characteristics are similar to both Hfq and RimP. It is not impossible PG0228 has both functions since both are structurally similar and bind RNA. Future studies are needed to determine the effect of PG0228 on ribosome maturation in *P. gingivalis*.

4.6. Future Studies

Mutants depleted of *hfq* have shown regulation in 5-20% of total genes present on the genome depending on the bacterial species [61]. Δ0228 presents high regulation in 15% of genes present on the W83 genome. PG0228 and *hfq* deficient strains are both viable, present a shorter log phase, and have lower final cell density (excluding *Listeria monocytogenes* and *Staphylococcus aureus)*. Furthermore, strains deficient in PG0228 and hfq are less likely to adapt to changes in host environment. Without the global regulator, genes are less efficiently turned on or off, resulting in slow bacterial reaction. This gives the host a better chance to rid themselves of the pathogen. Immunoprecipitation studies show the identities of Hfq-bound RNAs. We hypothesize the results of our completed immunoprecipitation will also show bound RNA.

In addition to the RNA sequencing results from the immunoprecipitation, data for protein analysis and transcriptomic mRNA are still being processed and have not been returned. We believe this information will shine a bright light on gene regulation by PG0228 at both the transcription and post-transcription level.

Although we believe PG0228 is an Hfq homologue, several additional studies need to be completed. An analysis of differential expression during early stationary phase should be

completed to compare the two levels of PG0228 and overall changes in regulation. The survival study also needs to be repeated to give better insight into host defense. Plus, more phenotypic changes need to be measured to compare to other Hfq mutants. However, studies thus far have demonstrated PG0228 is an excellent Hfq candidate, and we hypothesize further studies will show PG0228 is an Hfq homologue. Finally, additional work involving determination of the role of PG0228 in ribosome maturation will shed light on its possible dual role in both processes. It is possible that both functions are merged in one protein in *P. gingivalis* which contains a much smaller genome and associated with that coding capacity compared with *E. coli* that can allow itself to code for two proteins.

LITERATURE CITED

(1) Aguda BD, Kim Y, Piper-Hunter MG, Friedman A, Marsh CB: MicroRNA regulation of a cancer network: consequences of the feedback loops involving miR-17-92, E2F, and Myc. Proc Natl Acad Sci U S A 2008; 105(50):19678-19683.

(2) Ali AT, Iwata A, Nishimura A, Ueda S, Ishihama A: Growth phase-dependent variation in protein composition of the Escherichia coli nucleoid. J Bacteriol 1999; 181(20):6361-6370.

(3) Altschul SF, Gish W, Miller W, Myers EW, Lipman DJ: Basic local alignment search tool. J Mol Biol 1990; 215(3):403-410.

(4) Altuvia S, Wagner EG: Switching on and off with RNA. Proc Natl Acad Sci U S A 2000; 97(18):9824-9826.

(5) Altuvia S, Zhang A, Argaman L, Tiwari A, Storz G: The Escherichia coli OxyS regulatory RNA represses fhlA translation by blocking ribosome binding. EMBO J 1998; 17(20):6069-6075.

(6) Armitage GC, Robertson PB: The biology, prevention, diagnosis and treatment of periodontal diseases: scientific advances in the United States. J Am Dent Assoc 2009; 140 Suppl 1:36S-43S.

(7) Bartel DP: MicroRNAs: genomics, biogenesis, mechanism, and function. Cell 2004; 116(2):281-297.

(8) Bascones-Martinez A, Matesanz-Perez P, Escribano-Bermejo M, Gonzalez-Moles MA, Bascones-Ilundain J, Meurman JH: Periodontal disease and diabetes-Review of the Literature. Med Oral Patol Oral Cir Bucal 2011.

(9) Becker Y: Trends in research and development of antiviral substances. Isr J Med Sci 1975; 11(11):1135-1167.

(10) Belton CM, Izutsu KT, Goodwin PC, Park Y, Lamont RJ: Fluorescence image analysis of the association between Porphyromonas gingivalis and gingival epithelial cells. Cell Microbiol 1999; 1(3):215-223.

(11) Bodet C, Chandad F, Grenier D: [Pathogenic potential of Porphyromonas gingivalis, Treponema denticola and Tannerella forsythia, the red bacterial complex associated with periodontitis]. Pathol Biol (Paris) 2007; 55(3-4):154-162.

(12) Bohn C, Rigoulay C, Bouloc P: No detectable effect of RNA-binding protein Hfq absence in Staphylococcus aureus. BMC Microbiol 2007; 7:10.

(13) Bortolaia C, Sbordone L: [Biofilms of the oral cavity. Formation, development and involvement in the onset of diseases related to bacterial plaque increase]. Minerva Stomatol 2002; 51(5):187-192.

(14) Bozzola M, Locatelli F, Gambarana D, Moretta A, Valtorta A, Giorgiani G, Cisternino M, Severi F: Effect of corticoid therapy on growth hormone secretion. Horm Res 1991; 36(5-6):183-186.

(15) Bratthall D, Petersen PE, Stjernsward JR, Brown LJ: Oral and Craniofacial Diseases and Disorders. 2006.

(16) Bumgarner SL, Dowell RD, Grisafi P, Gifford DK, Fink GR: Toggle involving cis-interfering noncoding RNAs controls variegated gene expression in yeast. Proc Natl Acad Sci U S A 2009; 106(43):18321-18326.

(17) Butland G, Peregrin-Alvarez JM, Li J, Yang W, Yang X, Canadien V, Starostine A, Richards D, Beattie B, Krogan N, Davey M, Parkinson J, Greenblatt J, Emili A: Interaction network containing conserved and essential protein complexes in Escherichia coli. Nature 2005; 433(7025):531-537.

(18) Chao Y, Vogel J: The role of Hfq in bacterial pathogens. Curr Opin Microbiol 2010; 13(1):24-33.

(19) Chung WO, Park Y, Lamont RJ, McNab R, Barbieri B, Demuth DR: Signaling system in Porphyromonas gingivalis based on a LuxS protein. J Bacteriol 2001; 183(13):3903-3909.

(20) Colombo AV, da Silva CM, Haffajee A, Colombo AP: Identification of intracellular oral species within human crevicular epithelial cells from subjects with chronic periodontitis by fluorescence in situ hybridization. J Periodontal Res 2007; 42(3):236-243.

(21) de Haseth PL, Uhlenbeck OC: Interaction of Escherichia coli host factor protein with oligoriboadenylates. Biochemistry 1980; 19(26):6138-6146.

(22) Duran-Pinedo AE, Nishikawa K, Duncan MJ: The RprY response regulator of Porphyromonas gingivalis. Mol Microbiol 2007; 64(4):1061-1074.

(23) Elsen S, Efthymiou G, Peteinatos P, Diallinas G, Kyritsis P, Moulis JM: A bacteria-specific 2[4Fe-4S] ferredoxin is essential in Pseudomonas aeruginosa. BMC Microbiol 2010; 10:271.

(24) Ezzo PJ, Cutler CW: Microorganisms as risk indicators for periodontal disease. Periodontol 2000 2003; 32:24-35.

(25) Fantappie L, Metruccio MM, Seib KL, Oriente F, Cartocci E, Ferlicca F, Giuliani MM, Scarlato V, Delany I: The RNA chaperone Hfq is involved in stress response and virulence in Neisseria meningitidis and is a pleiotropic regulator of protein expression. Infect Immun 2009; 77(5):1842-1853.

(26) Figueroa-Bossi N, Lemire S, Maloriol D, Balbontin R, Casadesus J, Bossi L: Loss of Hfq activates the sigmaE-dependent envelope stress response in Salmonella enterica. Mol Microbiol 2006; 62(3):838-852.

(27) Fletcher HM, Macrina FL: Molecular survey of clindamycin and tetracycline resistance determinants in Bacteroides species. Antimicrob Agents Chemother 1991; 35(11):2415-2418.

(28) Ford PJ, Raphael SL, Cullinan MP, Jenkins AJ, West MJ, Seymour GJ: Why should a doctor be interested in oral disease? Expert Rev Cardiovasc Ther 2010; 8(10):1483-1493.

(29) Forng RY, Champagne C, Simpson W, Genco CA: Environmental cues and gene expression in Porphyromonas gingivalis and Actinobacillus actinomycetemcomitans. Oral Dis 2000; 6(6):351-365.

(30) Fox CH: New considerations in the prevalence of periodontal disease. Curr Opin Dent 1992; 2:5-11.

(31) Franze de Fernandez MT, Eoyang L, August JT: Factor fraction required for the synthesis of bacteriophage Qbeta-RNA. Nature 1968; 219(5154):588-590.

(32) Franze de Fernandez MT, Hayward WS, August JT: Bacterial proteins required for replication of phage Q ribonucleic acid. Pruification and properties of host factor I, a ribonucleic acid-binding protein. J Biol Chem 1972; 247(3):824-831.

(33) Garlet GP: Destructive and protective roles of cytokines in periodontitis: a re-appraisal from host defense and tissue destruction viewpoints. J Dent Res 2010; 89(12):1349-1363.

(34) Genco CA, Dixon DW: Emerging strategies in microbial haem capture. Mol Microbiol 2001; 39(1):1-11.

(35) Gottesman S: The small RNA regulators of Escherichia coli: roles and mechanisms*. Annu Rev Microbiol 2004; 58:303-328.

(36) Gottesman S: Micros for microbes: non-coding regulatory RNAs in bacteria. Trends Genet 2005; 21(7):399-404.

(37) Guisbert E, Rhodius VA, Ahuja N, Witkin E, Gross CA: Hfq modulates the sigmaE-mediated envelope stress response and the sigma32-mediated cytoplasmic stress response in Escherichia coli. J Bacteriol 2007; 189(5):1963-1973.

(38) Haffajee AD, Socransky SS, Goodson JM: Subgingival temperature (I). Relation to baseline clinical parameters. J Clin Periodontol 1992; 19(6):401-408.

(39) Hajnsdorf E, Regnier P: Host factor Hfq of Escherichia coli stimulates elongation of poly(A) tails by poly(A) polymerase I. Proc Natl Acad Sci U S A 2000; 97(4):1501-1505.

(40) Haraszthy VI, Zambon JJ, Trevisan M, Zeid M, Genco RJ: Identification of periodontal pathogens in atheromatous plaques. J Periodontol 2000; 71(10):1554-1560.

(41) Hasegawa N: [Effect of high mobility group box 1 (HMGB1) in cultured human periodontal ligament cells]. Kokubyo Gakkai Zasshi 2008; 75(3):155-161.

(42) Hengge-Aronis R: Signal transduction and regulatory mechanisms involved in control of the sigma(S) (RpoS) subunit of RNA polymerase. Microbiol Mol Biol Rev 2002; 66(3):373-95, table.

(43) Hosogi Y, Duncan MJ: Gene expression in Porphyromonas gingivalis after contact with human epithelial cells. Infect Immun 2005; 73(4):2327-2335.

(44) Hussein R, Lim HN: Disruption of small RNA signaling caused by competition for Hfq. Proc Natl Acad Sci U S A 2011; 108(3):1110-1115.

(45) James CE, Hasegawa Y, Park Y, Yeung V, Tribble GD, Kuboniwa M, Demuth DR, Lamont RJ: LuxS involvement in the regulation of genes coding for hemin and iron acquisition systems in Porphyromonas gingivalis. Infect Immun 2006; 74(7):3834-3844.

(46) Johnston RJ, Jr., Chang S, Etchberger JF, Ortiz CO, Hobert O: MicroRNAs acting in a double-negative feedback loop to control a neuronal cell fate decision. Proc Natl Acad Sci U S A 2005; 102(35):12449-12454.

(47) Lamont RJ, Chan A, Belton CM, Izutsu KT, Vasel D, Weinberg A: Porphyromonas gingivalis invasion of gingival epithelial cells. Infect Immun 1995; 63(10):3878-3885.

(48) Le DJ, Boni IV, Regnier P, Hajnsdorf E: Hfq affects mRNA levels independently of degradation. BMC Mol Biol 2010; 11:17.

(49) Lease RA, Woodson SA: Cycling of the Sm-like protein Hfq on the DsrA small regulatory RNA. J Mol Biol 2004; 344(5):1211-1223.

(50) Lewis JP: Metal uptake in host-pathogen interactions: role of iron in Porphyromonas gingivalis interactions with host organisms. Periodontol 2000 2010; 52(1):94-116.

(51) Lewis JP, Iyer D, naya-Bergman C: Adaptation of Porphyromonas gingivalis to microaerophilic conditions involves increased consumption of formate and reduced utilization of lactate. Microbiology 2009; 155(Pt 11):3758-3774.

(52) Lewis JP, Plata K, Yu F, Rosato A, Anaya C: Transcriptional organization, regulation and role of the Porphyromonas gingivalis W83 hmu haemin-uptake locus. Microbiology 2006; 152(Pt 11):3367-3382.

(53) Li H, Jubelirer S, Garcia Costas AM, Frigaard NU, Bryant DA: Multiple antioxidant proteins protect Chlorobaculum tepidum against oxygen and reactive oxygen species. Arch Microbiol 2009; 191(11):853-867.

(54) Liu D, Chang X, Liu Z, Chen L, Wang R: Bistability and Oscillations in Gene Regulation Mediated by Small Noncoding RNAs. PLoS One 2011; 6(3):e17029.

(55) Marsh PD: The significance of maintaining the stability of the natural microflora of the mouth. Br Dent J 1991; 171(6):174-177.

(56) Masse E, Escorcia FE, Gottesman S: Coupled degradation of a small regulatory RNA and its mRNA targets in Escherichia coli. Genes Dev 2003; 17(19):2374-2383.

(57) McNealy TL, Forsbach-Birk V, Shi C, Marre R: The Hfq homolog in Legionella pneumophila demonstrates regulation by LetA and RpoS and interacts with the global regulator CsrA. J Bacteriol 2005; 187(4):1527-1532.

(58) Meibom KL, Forslund AL, Kuoppa K, Alkhuder K, Dubail I, Dupuis M, Forsberg A, Charbit A: Hfq, a novel pleiotropic regulator of virulence-associated genes in Francisella tularensis. Infect Immun 2009; 77(5):1866-1880.

(59) Mikulecky PJ, Kaw MK, Brescia CC, Takach JC, Sledjeski DD, Feig AL: Escherichia coli Hfq has distinct interaction surfaces for DsrA, rpoS and poly(A) RNAs. Nat Struct Mol Biol 2004; 11(12):1206-1214.

(60) Mineoka T, Awano S, Rikimaru T, Kurata H, Yoshida A, Ansai T, Takehara T: Site-specific development of periodontal disease is associated with increased levels of Porphyromonas gingivalis, Treponema denticola, and Tannerella forsythia in subgingival plaque. J Periodontol 2008; 79(4):670-676.

(61) Moller T, Franch T, Hojrup P, Keene DR, Bachinger HP, Brennan RG, Valentin-Hansen P: Hfq: a bacterial Sm-like protein that mediates RNA-RNA interaction. Mol Cell 2002; 9(1):23-30.

(62) Moller T, Franch T, Udesen C, Gerdes K, Valentin-Hansen P: Spot 42 RNA mediates discoordinate expression of the E. coli galactose operon. Genes Dev 2002; 16(13):1696-1706.

(63) Moore WE, Moore LH, Ranney RR, Smibert RM, Burmeister JA, Schenkein HA: The microflora of periodontal sites showing active destructive progression. J Clin Periodontol 1991; 18(10):729-739.

(64) Morita T, Maki K, Aiba H: RNase E-based ribonucleoprotein complexes: mechanical basis of mRNA destabilization mediated by bacterial noncoding RNAs. Genes Dev 2005; 19(18):2176-2186.

(65) Muffler A, Traulsen DD, Fischer D, Lange R, Hengge-Aronis R: The RNA-binding protein HF-I plays a global regulatory role which is largely, but not exclusively, due to its role in expression of the sigmaS subunit of RNA polymerase in Escherichia coli. J Bacteriol 1997; 179(1):297-300.

(66) Mustapha IZ, Debrey S, Oladubu M, Ugarte R: Markers of systemic bacterial exposure in periodontal disease and cardiovascular disease risk: a systematic review and meta-analysis. J Periodontol 2007; 78(12):2289-2302.

(67) Mydel P, Takahashi Y, Yumoto H, Sztukowska M, Kubica M, Gibson FC, III, Kurtz DM, Jr., Travis J, Collins LV, Nguyen KA, Genco CA, Potempa J: Roles of the host oxidative immune response and bacterial antioxidant rubrerythrin during Porphyromonas gingivalis infection. PLoS Pathog 2006; 2(7):e76.

(68) Nelson KE, Fleischmann RD, DeBoy RT, Paulsen IT, Fouts DE, Eisen JA, Daugherty SC, Dodson RJ, Durkin AS, Gwinn M, Haft DH, Kolonay JF, Nelson WC, Mason T, Tallon L, Gray J, Granger D, Tettelin H, Dong H, Galvin JL, Duncan MJ, Dewhirst FE, Fraser CM: Complete genome sequence of the oral pathogenic Bacterium porphyromonas gingivalis strain W83. J Bacteriol 2003; 185(18):5591-5601.

(69) Nord S, Bylund GO, Lovgren JM, Wikstrom PM: The RimP protein is important for maturation of the 30S ribosomal subunit. J Mol Biol 2009; 386(3):742-753.

(70) Olczak T, Wojtowicz H, Ciuraszkiewicz J, Olczak M: Species specificity, surface exposure, protein expression, immunogenicity, and participation in biofilm formation of Porphyromonas gingivalis HmuY. BMC Microbiol 2010; 10:134.

(71) Parahitiyawa NB, Scully C, Leung WK, Yam WC, Jin LJ, Samaranayake LP: Exploring the oral bacterial flora: current status and future directions. Oral Dis 2010; 16(2):136-145.

(72) Pichon C, Felden B: Small RNA gene identification and mRNA target predictions in bacteria. Bioinformatics 2008; 24(24):2807-2813.

(73) Regnier P, Hajnsdorf E: Poly(A)-assisted RNA decay and modulators of RNA stability. Prog Mol Biol Transl Sci 2009; 85:137-185.

(74) Riebe O, Fischer RJ, Wampler DA, Kurtz DM, Jr., Bahl H: Pathway for H2O2 and O2 detoxification in Clostridium acetobutylicum. Microbiology 2009; 155(Pt 1):16-24.

(75) Robertson GT, Roop RM, Jr.: The Brucella abortus host factor I (HF-I) protein contributes to stress resistance during stationary phase and is a major determinant of virulence in mice. Mol Microbiol 1999; 34(4):690-700.

(76) Rudney JD, Chen R: The vital status of human buccal epithelial cells and the bacteria associated with them. Arch Oral Biol 2006; 51(4):291-298.

(77) Sacco G, Carmagnola D, Abati S, Luglio PF, Ottolenghi L, Villa A, Maida C, Campus G: Periodontal disease and preterm birth relationship: a review of the literature. Minerva Stomatol 2008; 57(5):233-250.

(78) Schumacher MA, Pearson RF, Moller T, Valentin-Hansen P, Brennan RG: Structures of the pleiotropic translational regulator Hfq and an Hfq-RNA complex: a bacterial Sm-like protein. EMBO J 2002; 21(13):3546-3556.

(79) Senear AW, Steitz JA: Site-specific interaction of Qbeta host factor and ribosomal protein S1 with Qbeta and R17 bacteriophage RNAs. J Biol Chem 1976; 251(7):1902-1912.

(80) Shakhnovich EA, Davis BM, Waldor MK: Hfq negatively regulates type III secretion in EHEC and several other pathogens. Mol Microbiol 2009; 74(2):347-363.

(81) Shapiro L, Franze de Fernandez MT, August JT: Resolution of two factors required in the Q-beta-RNA polymerase reaction. Nature 1968; 220(5166):478-480.

(82) Shimoni Y, Friedlander G, Hetzroni G, Niv G, Altuvia S, Biham O, Margalit H: Regulation of gene expression by small non-coding RNAs: a quantitative view. Mol Syst Biol 2007; 3:138.

(83) Sledjeski DD, Whitman C, Zhang A: Hfq is necessary for regulation by the untranslated RNA DsrA. J Bacteriol 2001; 183(6):1997-2005.

(84) Smalley JW, Byrne DP, Birss AJ, Wojtowicz H, Sroka A, Potempa J, Olczak T: Correction: HmuY Haemophore and Gingipain Proteases Constitute a Unique Syntrophic System of Haem Acquisition by Porphyromonas gingivalis. PLoS One 2011; 6(3).

(85) Sonnleitner E, Hagens S, Rosenau F, Wilhelm S, Habel A, Jager KE, Blasi U: Reduced virulence of a hfq mutant of Pseudomonas aeruginosa O1. Microb Pathog 2003; 35(5):217-228.

(86) Soper T, Mandin P, Majdalani N, Gottesman S, Woodson SA: Positive regulation by small RNAs and the role of Hfq. Proc Natl Acad Sci U S A 2010; 107(21):9602-9607.

(87) Strand KR, Sun C, Li T, Jenney FE, Jr., Schut GJ, Adams MW: Oxidative stress protection and the repair response to hydrogen peroxide in the hyperthermophilic archaeon Pyrococcus furiosus and in related species. Arch Microbiol 2010; 192(6):447-459.

(88) Su Z, Nakano M, Koga T, Lian X, Hamamoto A, Shimohata T, Harada Y, Mawatari K, Harada N, Akutagawa M, Nakaya Y, Takahashi A: Hfq regulates anti-oxidative ability in Vibrio parahaemolyticus. J Gen Appl Microbiol 2010; 56(3):181-186.

(89) Sukhodolets MV, Garges S: Interaction of Escherichia coli RNA polymerase with the ribosomal protein S1 and the Sm-like ATPase Hfq. Biochemistry 2003; 42(26):8022-8034.

(90) Sun X, Zhulin I, Wartell RM: Predicted structure and phyletic distribution of the RNA-binding protein Hfq. Nucleic Acids Res 2002; 30(17):3662-3671.

(91) Szewczyk E, Nayak T, Oakley CE, Edgerton H, Xiong Y, Taheri-Talesh N, Osmani SA, Oakley BR: Fusion PCR and gene targeting in Aspergillus nidulans. Nat Protoc 2006; 1(6):3111-3120.

(92) Sztukowska M, Bugno M, Potempa J, Travis J, Kurtz DM, Jr.: Role of rubrerythrin in the oxidative stress response of Porphyromonas gingivalis. Mol Microbiol 2002; 44(2):479-488.

(93) Takada A, Wachi M, Kaidow A, Takamura M, Nagai K: DNA binding properties of the hfq gene product of Escherichia coli. Biochem Biophys Res Commun 1997; 236(3):576-579.

(94) Thompson KM, Rhodius VA, Gottesman S: SigmaE regulates and is regulated by a small RNA in Escherichia coli. J Bacteriol 2007; 189(11):4243-4256.

(95) Toro I, Basquin J, Teo-Dreher H, Suck D: Archaeal Sm proteins form heptameric and hexameric complexes: crystal structures of the Sm1 and Sm2 proteins from the hyperthermophile Archaeoglobus fulgidus. J Mol Biol 2002; 320(1):129-142.

(96) Tsui HC, Feng G, Winkler ME: Transcription of the mutL repair, miaA tRNA modification, hfq pleiotropic regulator, and hflA region protease genes of Escherichia coli K-12 from clustered Esigma32-specific promoters during heat shock. J Bacteriol 1996; 178(19):5719-5731.

(97) Tsui HC, Leung HC, Winkler ME: Characterization of broadly pleiotropic phenotypes caused by an hfq insertion mutation in Escherichia coli K-12. Mol Microbiol 1994; 13(1):35-49.

(98) Valentin-Hansen P, Eriksen M, Udesen C: The bacterial Sm-like protein Hfq: a key player in RNA transactions. Mol Microbiol 2004; 51(6):1525-1533.

(99) Vanterpool E, Aruni AW, Roy F, Fletcher HM: regT can modulate gingipain activity and response to oxidative stress in Porphyromonas gingivalis. Microbiology 2010; 156(Pt 10):3065-3072.

(100) Vanterpool E, Roy F, Fletcher HM: The vimE gene downstream of vimA is independently expressed and is involved in modulating proteolytic activity in Porphyromonas gingivalis W83. Infect Immun 2004; 72(10):5555-5564.

(101) Vasudevan S, Tong Y, Steitz JA: Switching from repression to activation: microRNAs can up-regulate translation. Science 2007; 318(5858):1931-1934.

(102) Vecerek B, Moll I, Blasi U: Translational autocontrol of the Escherichia coli hfq RNA chaperone gene. RNA 2005; 11(6):976-984.

(103) Vytvytska O, Jakobsen JS, Balcunaite G, Andersen JS, Baccarini M, von GA: Host factor I, Hfq, binds to Escherichia coli ompA mRNA in a growth rate-dependent fashion and regulates its stability. Proc Natl Acad Sci U S A 1998; 95(24):14118-14123.

(104) Wassarman KM: Small RNAs in bacteria: diverse regulators of gene expression in response to environmental changes. Cell 2002; 109(2):141-144.

(105) White DJ: Dental calculus: recent insights into occurrence, formation, prevention, removal and oral health effects of supragingival and subgingival deposits. Eur J Oral Sci 1997; 105(5 Pt 2):508-522.

(106) Wightman B, Ha I, Ruvkun G: Posttranscriptional regulation of the heterochronic gene lin-14 by lin-4 mediates temporal pattern formation in C. elegans. Cell 1993; 75(5):855-862.

(107) Wu J, Lin X, Xie H: Regulation of hemin binding proteins by a novel transcriptional activator in Porphyromonas gingivalis. J Bacteriol 2009; 191(1):115-122.

(108) Wu T, Trevisan M, Genco RJ, Dorn JP, Falkner KL, Sempos CT: Periodontal disease and risk of cerebrovascular disease: the first national health and nutrition examination survey and its follow-up study. Arch Intern Med 2000; 160(18):2749-2755.

(109) Yilmaz O: The chronicles of Porphyromonas gingivalis: the microbium, the human oral epithelium and their interplay. Microbiology 2008; 154(Pt 10):2897-2903.

(110) Yilmaz O, Yao L, Maeda K, Rose TM, Lewis EL, Duman M, Lamont RJ, Ojcius DM: ATP scavenging by the intracellular pathogen Porphyromonas gingivalis inhibits P2X7-mediated host-cell apoptosis. Cell Microbiol 2008; 10(4):863-875.

(111) Zhang A, Wassarman KM, Ortega J, Steven AC, Storz G: The Sm-like Hfq protein increases OxyS RNA interaction with target mRNAs. Mol Cell 2002; 9(1):11-22.

VITA

Courtney Danielle Schlenker was born on April 18th, 1986, in Cincinnati, Ohio. She graduated high school from Wapakoneta High School in 2004. Courtney then attended the University of Toledo where she graduated with a Bachelor's of Science in Biology in December 2007. Following her graduation from this program, she will attend the VCU School of Dentistry as part of the class of 2015.